Technische Universität Dresden

Faculty of Environmental Sciences

The effects of tree crown plasticity on the structure and dynamics of near-natural beech forests – an individual-based modeling approach

Dissertation submitted in fulfillment of the requirements for the degree Doctor rerum silvaticarum (Dr. rer. silv.)

Submitted by

Markus Engel, M.Sc. Forest Sciences

born 27.05.1990 in Dresden

1. Reviewer: Prof. Dr. Uta Berger, Technische Universität Dresden, Faculty of Environmental Sciences, Institute of Forest Growth and Forest Computer Sciences

2. Reviewer: Prof. Dr. Goddert von Oheimb, Technische Universität Dresden, Faculty of Environmental Sciences, Institute of General Ecology and Environmental Protection

3. Reviewer: Prof. Dr. Winfried Kurth, Georg-August-Universität Göttingen, Department of Ecoinformatics, Biometrics & Forest Growth

Date of the oral examination: ....

Statement of conformity

I hereby confirm the accordance of this copy with the original dissertation titled:

"The effects of tree crown plasticity on the structure and dynamics of near-natural beech forests – an individual-based modeling approach"

....
Location, Date

....
Signature

Statement of authorship

I hereby assure that I have produced the present work without inadmissible help from third parties and without aids other than those stated; ideas taken directly or indirectly from external sources are identified as such.

When selecting and evaluating the material and also when producing the manuscript, I have received support from the following persons: Prof. Dr. Uta Berger, Prof. Dr. Goddert von Oheimb, Prof. Dr. Heinz Röhle, Prof. Dr. Hans Pretzsch, Dr. Andreas Fichtner, Dr. Matthias Kunz, Louis Georgi, and Friedrich Reich.

No further persons were involved in the intellectual production of the present work. In particular, I have not received help from a commercial doctoral adviser. No third parties have received monetary benefits from me, either directly or indirectly, for work relating to the content of the presented dissertation.

The work has not previously been presented in the same or a similar format to another examination body in Germany or abroad, nor has it - unless it is a cumulative dissertation - been published. 5. If this concerns a cumulative dissertation in accordance with §10 Section 2, I assure compliance with the conditions specified there.

I confirm that I acknowledge the doctoral regulations of the Faculty of Environmental Sciences of the Technische Universität Dresden.

....
Location, Date

....
Signature

Acknowledgements

Contents

List of Figures

List of Tables

1 Introduction

Beech (*Fagus sylvatica L.*) is a naturally occurring forest tree species in Europe (Leuschner & Ellenberg, 2017). It is found in various forest types that can be characterized as the most important forest communities in central Europe (Peterken, 1996). Despite their potential prevalence, today near-natural beech forests are scattered relics mostly of small size (Leibundgut, 1993; Smejkal *et al.*, 1997; Tabaku, 2000). Extensive beech forests are exceptional, for example the beech forests of the Uholka–Shyrokyi Luh in the Ukrainian Carpathians (Commarmot *et al.*, 2005; Hobi *et al.*, 2015a; Sabatini *et al.*, 2017). Consequently, relict beech forests have been listed as a UNESCO world natural heritage (Vološčuk, 2014). The terms "natural", "virgin" or "old-growth" indicate that the particular forest has not been subject to conventional thinning and logging activities. However, low-intensity interference by humans even in the large Ukrainian forests cannot be excluded (Hobi *et al.*, 2015a), so that the term "near-natural" is used throughout this thesis. In order to sustainably provide ecosystem services from beech forests to the community, management is oriented towards specific guidelines that specify the manner of human intervention.

Yet todays forest management practices mainly rest on experiences gathered from unnatural forests as a consequence of intensive logging activities in the middle and new ages (Leibundgut, 1993). However, we need to retrieve our silvicultural understanding from near-natural forests (Mayer, 1978), as the absence of human interference is thought to preserve the inherent ecosystem processes, while thinning and logging under a specific forest management alters these processes to a variable extent dependent on the severance of human intervention. One example is the change of the light regime on the forest floor caused by the removal of canopy trees (Annighöfer, 2018).

First studies in near-natural forests are available from the beginning of the 20th century (Cermak, 1910; Frölich, 1925; Markgraf, 1931). Since then,

our understanding about processes and dynamics in near-natural forests has been considerably enhanced. Organisms living within forests have been studied and close relationships between them have been revealed. Further, forest organisms have been found to develop and adapt to the environment rendering the forest itself highly dynamic. The sum of all those intricate relationships and characteristics enabled the delineation of forests as so-called ecosystem, which itself has specific characteristics and underlies a certain development through time.

We may nowadays understand forests as complex adaptive systems that develop and adapt to a changing environment and in which their constituents interact with one another, which leads to the emergence of structures and patterns (Puettmann *et al.*, 2013). But still, the revelation of complex biogeochemical cycles and energy fluxes as well as organismic interaction networks over several trophic levels leaves our understanding of natural processes incomplete. This underpins the need for more studies of near-natural forests. However, such studies are rare, because of the limited access to beech forest reserves as study objects and the considerable measurement effort that is needed to obtain long-term data. Thus, we need to relocate our activities partly away from empirical research into fields developed more recently, such as forest modeling. Modeling forests support us in testing hypotheses and deepening our understanding about processes and dynamics in near-natural forests that cannot be answered elsewhere. For example, to test the hypothesis that patterns from near-natural beech forests reappear after century-long management, might require the observation of a forest development plot over more than 100 years. As a consequence of unforeseeable developments during those 100 years, we might not be able to verify this hypothesis. However, knowledge can be gained faster, if we construct a specific forest model that reflects the conceptual understanding needed for answering research questions and testing hypothesis. Knowledge derived

from computer simulation experiments may then serve as basis for the development of sustainable forest management practices. As forest patterns and structures emerge from the interactions of its constituents, of which trees are essential (Puettmann *et al.*, 2013), we can investigate those tree interactions and their impact on those patterns by means of simulation experiments. The trees can be conceived as individuals or agents in the forest ecosystem whose interactions give rise to specific patterns. Analyzing those patterns is related to the field of pattern-oriented modeling which attempts to understand the underlying processes and structure of such patterns observed in complex systems using a bottom-up approach (Grimm *et al.*, 2005).

As trees are bound to a certain location, their only movement is growth in dimension above and below ground. Growing trees use available resources in their close environment, such as water or sunlight. However, those resources are limited and sometimes already depleted by a neighbor tree, which restricts tree growth. Trees may share resources, compete for them or even communicate with one another. That is termed tree interaction. As trees can be biologically very different, their interactions are driven by species-specific traits (Kunstler *et al.*, 2012). As the struggle for sunlight is crucial for tree growth, some trees, such as beech, have developed remarkable capabilities to use the least amount of sunlight. Besides their tolerance of very low light levels, they developed the ability to adapt their crown shape to their individual neighborhood (Longuetaud *et al.*, 2013). This trait is particularly important for the species beech, but we still lack a sound understanding of this trait in beech forest dynamics (Schröter *et al.*, 2012; Metz *et al.*, 2013; Juchheim *et al.*, 2017b). It can be assumed that the ability to adapt crown shapes positively affects the trees' competitiveness for sunlight and in turn their growth and neighborhood interaction. Furthermore, this change in tree interactions likely affects emergent forest patterns.

This study, therefore, aimed at the development of a forest model with

particular focus on the species beech in order to investigate tree interactions and their effect on the emergence of structures and patterns in near-natural beech forests. In particular, it was investigated which effects the plasticity of tree crowns has on beech forest structure and how this impact is influenced by management through selective thinning.

2. State of the art

2.1 Forests as Complex Adaptive Systems

A natural system is a conglomeration of interrelated system elements, such as species, and it is delineated from its environment by spatiotemporal boundaries. It can be characterized by specific functions and processes that lead to particular structures and patterns, such as the distribution of tree species in a forest. Forests are specified as an ecosystem with complex and adaptive interactions of its elements (Mitleton-Kelly *et al.*, 1997). Complex adaptive systems (CAS) are studied in a broad range of fields involving ecology, economy, sociology, and computer sciences (Holland, 2006). To study CAS, being cells, societies, ecosystems or artificial intelligence systems, means to reveal the interplay between system elements and processes that operate over different spatiotemporal scales and organizational complexity levels (Levin, 2002).

Ecosystems are "prototypical examples" of CAS, because system properties on the macro-scale, such as nutrient fluxes, emerge from the interaction of system components and feed back on those again (Levin, 1998). The spatiotemporal interactions of system elements over different organizational levels are non-linear and lead to complex system behaviors (Holland, 2006). Forest ecosystems as CAS can be characterized by (Puettmann *et al.*, 2013):

1. Composition of components (e.g., trees, fungi) and processes (e.g., photosynthesis, nutrient cycling)

2. Interaction of components and processes with each other and the system environment

3. Non-linear relationships and structures caused by those interactions (e.g., tree mortality that leads to a heterogeneous forest structure)

4. Structures and relationships are a combination of randomness and determination (e.g., seed dispersion)

5. Both positive and negative feedback mechanisms that may stabilize or destabilize the system (e.g., positive tree interactions under harsh environmental conditions promote tree survival and stabilization of the community)

6. Openness to its environment in terms of energy and matter fluxes (e.g., water resources at the landscape-scale)

7. Development being sensitive to initial conditions and memory of disturbances (e.g., disturbance alters soil microbial communities)

8. Nested adaptive sub-systems giving rise to emergent system properties (e.g., mycorrhizal networks influence tree recruitment and establishment)

Living organisms in a forest ecosystem, such as trees, constitute crucial system components that can be designated as agents or individuals (Railsback, 2001), whose interactions trigger the emergence of patterns and structures. Studying those interactions will provide us with a deeper understanding of how the forest system operates, which might have implications for management treating forests as CAS (Messier *et al.*, 2014). Placing this study within the framework of CAS is essential in order to base emergent system properties observed in near-natural forests, such as tree distributions, on tree interactions.

Computer models are used to deepen our understanding of CAS (Holland, 2006) by converging the conceptual thinking about a system into a mathematical model and then into a computer program that allows studying the system's behavior (Ringler *et al.*, 2016; Kim & Maroulis, 2018; Nair & Reed-Tsochas, 2019). This study likewise used computer simulation experiments for studying near-natural beech forests as CAS by focusing on trees and their interactions.

2.2 Tree interactions in near-natural beech forests

2.2.1 Plant interaction theory

Plants grow in an environment that provides a limited amount of resources, such as nutrients or water. These can be accessed by the plant through various mechanism, for example by soil water extraction, which is constrained by the range and distribution of plant roots. The amount of resources that one individual plant utilizes are no longer available for another. Hence, resources at a particular location in the environment are depleted by a specific plant. Plant interactions are, therefore, concerned with the struggle for a limited amount of resources. Plant interactions are often described in terms of competition and facilitation. Competition occurs when different plants interact such that one exerts a negative effect on the growth or survival of the other, whereas facilitation takes place when at least one plant is being positively affected by the presence of another. These forms of interactions have been investigated in numerous studies (Holmgren *et al.*, 1997; Callaway & Walker, 1997; Schwinning & Weiner, 1998; Weiner *et al.*, 2001; Stoll & Weiner, 2000; Weiner & Damgaard, 2006; Berger *et al.*, 2008; Bronstein, 2009; Chu *et al.*, 2010). Both, competition and facilitation are seen as major processes for structuring plant communities (Berger *et al.*, 2008; McIntire & Fajardo, 2011).

Competition can be further distinguished in symmetric (Schwinning &

6

Fox, 1995) and asymmetric (Schwinning & Weiner, 1998) forms. While symmetric competition divides the resources among individuals proportional to their size, asymmetric competition leads to an unproportional resource gain for an individual. For example, soil water resources between two neighboring plants can be divided proportional to their size (symmetric competition), which could be described by their root biomass (Cahill & Casper, 2000).

2.2.2 Aboveground competition

The aboveground competition for Photosynthetic Active Radiation (PAR) in forests is described as asymmetric (Brunner *et al.*, 1998), which is also valid for beech forests (Metz *et al.*, 2013; del Rio *et al.*, 2014). PAR is the spectral range of solar radiation that plants can absorb and use for assimilation. Asymmetric means that PAR resources between two neighboring trees is not divided symmetric to their size, but the greater tree individual receives unproportional more PAR resources. This is caused by PAR interception and absorption of the bigger tree individual.

Beech trees compete for crown space and adapt their crown shape according to the available space, to the neighborhood crown pressure (Muth & Bazzaz, 2003), and the available PAR (Petriţan *et al.*, 2009). This mechanism is known as crown plasticity, which results from the aboveground competition for PAR in that trees position their leaf organs to the greatest possible gain of PAR. Release events in the forest canopy caused by the death of trees lead to an extension of tree crowns into canopy gaps (Muth & Bazzaz, 2002; Fichtner *et al.*, 2013). If the gap is sufficiently small, closure is reached after several years depending on the vitality of the trees that surround the gap edges. Canopy gaps remain if their size is beyond the average shoot growth potential of the canopy trees. Trees position their crowns away from neighborhood pressure and shading (Muth & Bazzaz, 2003). Rugani *et al.* (2013) showed that near-natural beech forest canopies are charac-

terized by a highly dynamic gap creation and gap closure process due to the crown plasticity of beech. Crown plasticity facilitates the expansion of tree crowns into canopy gaps and, in turn, enhances individual tree growth (Juchheim *et al.*, 2017a), which demonstrates the importance of plastic tree crowns as a driver of forest dynamics (Fichtner *et al.*, 2013; Rugani *et al.*, 2013; Glatthorn *et al.*, 2017). This mechanism has already been studied for mixed species forests (Longuetaud *et al.*, 2013; Jucker *et al.*, 2015) and for forests of *Pinus sylvestris* L. (Uria-Diez & Pommerening, 2017), but not in its effects on beech stand dynamics.

2.2.2 Belowground competition

Belowground competition in plant communities has been found to be symmetric (Cahill & Casper, 2000) or asymmetric (Rajaniemi, 2003; Facelli & Facelli, 2002). Likewise, both symmetric (Rewald & Leuschner, 2009a) and asymmetric (Rewald & Leuschner, 2009a,b; Lei *et al.*, 2012) competition has been found for forest tree species. Beyer *et al.* (2013) found asymmetric intra- and interspecific competition for beech and ash (*Fraxinus excelsior* L.). Asymmetric belowground competition can also be found in forests of oak (*Quercus robur* L.) and beech (Leuschner *et al.*, 2001).

From an hydrological perspective, the spatiotemporal water uptake by
The interactions below ground are far more difficult to describe (Rewald & Leuschner, 2009a; Coomes & Grubb, 2000; Lang *et al.*, 2010; Lei *et al.*, 2012; Jacob *et al.*, 2013), because of their complexity and measurement difficulties. The ease with which aboveground competition can be described is based on the possibility to gain high-resolution 3D data of the tree shape (Metz *et al.*, 2013) and to actually measure the available PAR for a tree (Emborg, 1998). Yet we cannot simply scan root morphological structures below ground or describe detailed 3D root structures and distributions without destructive sampling methods, such as root excavation.

From an hydrological perspective, the spatiotemporal water uptake by

tree roots can be modeled and quantified (Volkmann *et al.*, 2016). Further, we are able to locate the soil water sources in the soil by means of stable isotope analysis (Gralher *et al.*, 2018; Brinkmann *et al.*, 2018), which allows us to quantify belowground competition for soil water resources. However, this has not been achieved yet for beech near-natural forests and those studies are characterized by high sampling efforts over several years. Additionally, phenomenons as hydraulic lifts and soil water redistribution (Hafner *et al.*, 2017), which can be seen as facilitative interactions, complicate our attempts to quantify interactions below ground.

2.2.3 Facilitation

Central to the understanding of facilitation between plants is the Stress-Gradient-hypothesis (SGH), which developed from the work of Hunter & Aarssen (1988) and assumes that positive interactions are more prevalent in stressful habitats where competition loses its importance (Bertness & Callaway, 1994; Brooker *et al.*, 2008; Maestre *et al.*, 2009). Various studies showed that the SGH is not only valid for interspecific interactions but also on the intraspecific level (Chu *et al.*, 2008, 2009; Eränen & Kozlov, 2008; McIntire & Fajardo, 2011). The SGH has been confirmed by numerous studies (Callaway *et al.*, 2007; Pugnaire *et al.*, 2011; Soliveres *et al.*, 2011; He *et al.*, 2013; Pretzsch *et al.*, 2013; Michalet *et al.*, 2014). On the contrary, facilitation was absent in other investigations (Tielbörger & Kadmon, 2000; Maestre *et al.*, 2005, 2009).

Facilitative interactions have also been found outside stressful environments (Holmgren & Scheffer, 2010; Holmgren *et al.*, 2012). McIntire & Fajardo (2013) extend the importance of facilitative interactions beyond the SGH across multiple scales. To capture the complexity of species interactions along stress gradients, the SGH framework has been extended by the inclusion of the strength of pair-wide interactions, the characteristics of

stress-factors as well as the life-history of interacting species (Maestre *et al.*, 2009).

2.2.4 Facilitation in forests

One example for facilitation in forests is belowground overyielding; a form of facilitation which refers to enhanced root biomass and soil exploitation in species mixtures compared to monospecific stands (Fölster *et al.*, 1991; Jacob *et al.*, 2013), Further, the phenomenon of the hydraulic lift that can be observed in mixed oak forests in drought periods can be assigned to belowground facilitation (Dawson *et al.*, 1993; Caldwell *et al.*, 1998; Pretzsch *et al.*, 2012). Due to deep tap roots that allows oak to deplete water resources from deeper soil layers, soil water is redistributed to more shallower soil layers that benefit neighboring trees.

Species mixtures of spruce (*Picea abies* L.) and beech may lower competition and enhance available resources by complementary resource depletion through different root morphologies which cause trees to deplete soil resources from different depths (Pretzsch & Schütze, 2009). Complementary effects are also reported from forests of fir (*Abies alba* L.) and spruce, but are absent in other forests, which indicates a redundancy in the species-specific resource use (Vilà *et al.*, 2013). Pretzsch *et al.* (2013) and Pretzsch *et al.* (2010) found facilitation and overyielding on poor forest sites, whereas rich sites were characterized by competition and underyielding, which again support the SGH. The mixture of tree species may lead to new interactions that enhance the physiological efficiency and structural adaption which may transform also into an aboveground overyielding effect (Amoroso & Turnblom, 2006; Erskine *et al.*, 2006; Pretzsch & Schütze, 2009), which could be detected by higher stem volumes per hectare.

2.2.5 The competition-facilitation continuum and its controversy

According to Forrester *et al.* (2014a), competition and facilitation are the net product of multiple dynamic interactions on different scales. All interactions evolve within a continuum ranging from competition to facilitation (Lin *et al.*, 2012), while the relative importance of those interactions determines the net outcome for the individual plant. This continuum is affected by temporal and spatial changes and characterized by a dynamic nature across all scales (Bertness & Callaway, 1994; Tielbörger & Kadmon, 2000; Kunstler *et al.*, 2011; Pugnaire *et al.*, 2011; Lin *et al.*, 2012; Forrester *et al.*, 2014a).

Yet plants do not interact exclusively in a competitive or facilitative way. For example, while aboveground competition for PAR leads to a growth reduction, plants can, at the same time, benefit from the presence of neighbors by micro-climate melioration and transfer of photosynthates through rhizomes, root graft, exudates, or mycorrhizal networks (Simard *et al.*, 2012, 2013). The net outcome of such complex interactions is hard to predict. It depends not only on the abiotic settings (limitation of resources or level of non-resource stressors), but also on the functional traits of the species involved, which in turn may change through ontogeny (Kunstler *et al.*, 2016).

Trees are able to stimulate microbial activities in their rhizosphere by sending chemical signals, and the microbial community is able to feedback on their hosts again (Prescott & Grayston, 2013), which improves the belowground resource gain for the tree host and its associated microbial assemblage. Gorzelak *et al.* (2015) even specifies this communication as tree–talk altering the potential of trees to influence the diversity and community composition in this microbial network. Plant hosts as well as soil microbes are able to select high-quality partners by preferential allocation of resources (Fellbaum *et al.*, 2014; Werner & Kiers, 2015). For this reason, the species composition of ectomycorrhizal networks, for example, varies with tree identity (Lang *et al.*, 2011; Goldmann *et al.*, 2015), but also with soil parameters

and understory vegetation (Wubet *et al.*, 2012), respectively.

Mykorrhiza networks are seen as vital for forest ecosystem functioning (Simard *et al.*, 2012; Itoo & Reshi, 2013) as they play a significant role for stress amelioration (Itoo & Reshi, 2013) and nutrient cycling (Ekblad *et al.*, 2013). Klein *et al.* (2016) observed a substantial bidirectional tree-to-tree carbon transfer among mature trees of four different species (*Picea abies* (L.) H. Karst., *Fagus sylvatica* L., *Pinus sylvestris* L., *Larix decidua* MILL.). The authors suggested that this occurred most likely through common ecto-mycorrhiza networks; far-reaching fungal networks uniting different species of particular functional groups. In the study of Klein *et al.* (2016), all trees were dominant, healthy, and tall individuals, which were growing without obvious carbon limitations. In complex forest stands with a heterogeneous mixture of tree dimensions, source-sink gradients of carbon exist between individual trees. Hereby, large-diameter trees are assumed to uphold the topology of microbial networks and function as "hubs" similar to homonymous connection points in modern information networks (Beiler *et al.*, 2015). The network concept, thus, considers trees no longer as isolated individuals that compete or facilitate but as meta-organisms or holobionts (Hacquard & Schadt, 2015).

Despite all progress in studying microbial networks in the field, empirical results are controversial and hinder the development of a general theory about the importance of these networks for plant ecology (Hoeksema, 2015). For example, some studies revealed that single plants including tree saplings benefit from microbial activities (Simard *et al.*, 2012), while others document no benefit (Kytöviita *et al.*, 2003) or even an amplification of plant competition (Merrild *et al.*, 2013). Although mycorrhizal networks evidently facilitate the establishment of seedlings in forests (Booth & Hoeksema, 2010), seedling genetics and life history might outweigh this potential under drought (Bingham & Simard, 2013).

The net outcome of tree interactions in near-natural beech forests is, thus, very complex and not yet resolved. Facilitative effects have been observed between small- and large-diameter trees probably caused by mycorrhizal networks (Beiler *et al.*, 2015; Fichtner *et al.*, 2015). These effects could even increase the resilience of forests against environmental changes which would be in agreement with the hypothesis that forests with a long ecological continuity are better adapted to environmental changes than others (von Oheimb *et al.*, 2014). The existence of beech-microbial mutualism is shown by the study of Cesarz *et al.* (2013). Beech selectively allocates carbon to specific mycorrhizal species at the root tip level (Valtanen *et al.*, 2014) and mycorrhizal species feedback by influencing nutrient uptake, transfer, and storage (Seven & Polle, 2014). However, empirical studies were not able to capture the importance of these belowground interactions for stand dynamics so far.

As this study is concerned with near-natural beech forests, tree interactions can be summarized in a schematic way (Fig. 1). First, beech trees compete for crown space above ground and adapt their crown shapes to the available space. Second, trees compete asymmetrically for available PAR. Third, trees interact with their microbial assemblage. Fourth, trees compete below ground for resources, although the mode of competition or facilitation appears to be highly dynamic and hard to conceive.
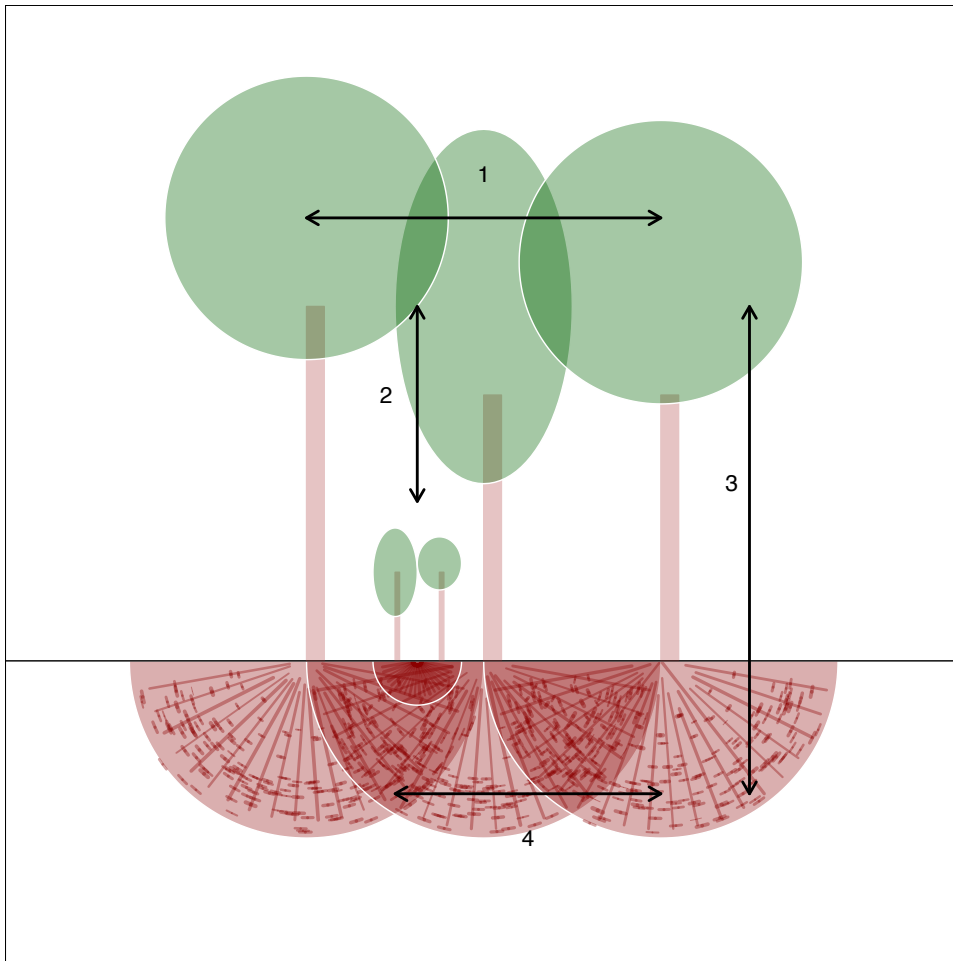
Figure 1: Schematic drawing of tree interactions in a beech forest. Red half-spheres denote the rooting zones of the trees. Arrows denote tree interactions. Trees compete above ground for available crown space (1) and compete asymmetrically for available PAR (2). Trees further interact with their microbial assemblage (3) and compete or facilitate below ground (4).

2.3 Patterns and processes in near-natural beech forests

The following overview on the current knowledge of beech forest research focuses on European forests. Investigations from northern Iran (Sefidi *et al.*, 2011; Akhavan *et al.*, 2012) are not considered, although these forests may share similarities with their European counterparts. The overview focuses

specifically on the spatial and temporal dynamics, on tree interactions, and the emergent structures and patterns.

Near-natural beech forests are characterized by a mosaic pattern of different successional stages (Watt, 1925; Lemée, 1987; Koop & Hilgen, 1987; Emborg, 1998; von Oheimb *et al.*, 2005; Piovesan *et al.*, 2010; Hobi *et al.*, 2015a; Paluch *et al.*, 2015), while trees within those patches share similarities in terms of age, size, and social status. This pattern of small-scale heterogeneity needs a significant amount of time to evolve, e.g., decades to centuries (Heiri *et al.*, 2009). While standing wood volumes can vary according to climate and historic human disturbance (Leibundgut, 1993; Smejkal *et al.*, 1997; Tabaku, 2000; von Oheimb *et al.*, 2005; Dolnik *et al.*, 2008; Hobi *et al.*, 2015a), the diameter distribution is mostly highly differentiated even at small spatial scales (Leibundgut, 1993; Korpel, 1995). The diameter distribution has been found to be reverse-J-shaped (Meyer *et al.*, 2003; Heiri *et al.*, 2009; Bílek *et al.*, 2009; Pach & Podlaski, 2015) or bimodal (Koop & Hilgen, 1987; Emborg, 1998; von Oheimb *et al.*, 2005; Piovesan *et al.*, 2005, 2010; Šebková *et al.*, 2011; Kucbel *et al.*, 2012; Pach & Podlaski, 2015), with high abundances of natural regeneration and a significant number of old large-diameter trees (von Oheimb *et al.*, 2005; Hobi *et al.*, 2015a). The latter are believed to be important for tree community assembly (Fichtner *et al.*, 2015). These old large-diameter beech trees are almost unaffected by competition (Dolnik *et al.*, 2008; Fichtner *et al.*, 2015).

Near-natural beech forests show large amounts of standing or lying dead wood, although varying in volume per hectare (von Oheimb *et al.*, 2005; Dolnik *et al.*, 2008; Hobi *et al.*, 2015a). Hobi *et al.* (2015a) found the vertical structure of these forests to be multi-layered and the age range of canopy trees to extend 300 years. Trotsiuk *et al.* (2012) found an uneven-aged forest structure in all four investigated plots. The oldest beech tree in this study was 451 years, although the authors suggest an estimated maximum age of

550 years. Piovesan *et al.* (2010) could confirm a maximum tree age of 503 years.

Near-natural beech forests show distinct gap patterns. The interplay between death of single canopy trees or even larger disturbances, such as windthrow events cause the forest canopy to be interspersed with mostly small gaps, while gaps greater than small groups of trees are very rare (Drößer & Lüpke, 2005; Zeibig *et al.*, 2005; Nagel & Diaci, 2006; Trotsiuk *et al.*, 2012; Rugani *et al.*, 2013; Hobi *et al.*, 2015a,b; Feldmann *et al.*, 2018).

Beech regeneration can establish in those gaps or may experience a significant growth increase caused by the release from the asymmetric competition for PAR with large canopy trees (Madsen & Hahn, 2008; Bílek *et al.*, 2009, 2014; Trotsiuk *et al.*, 2012; Feldmann *et al.*, 2018). The remaining gap can be closed by surrounding canopy trees through crown plasticity (Schröter *et al.*, 2012; Bulušek *et al.*, 2016) or can be filled in with younger beech trees (Trotsiuk *et al.*, 2012; Feldmann *et al.*, 2018).

Beech adapts its crown shape according to its neighborhood and extends its crown into free canopy space (Dieler & Pretzsch, 2013; Juchheim *et al.*, 2017b). This crown plasticity leads to large crown displacements defined as the horizontal distance between the stem foot point and the crown centroid (Schröter *et al.*, 2012; Bulušek *et al.*, 2016). Further, this mechanism causes crown centroids to be more regularly distributed than stem foot points (Schröter *et al.*, 2012; Bulušek *et al.*, 2016). Stem foot points can show a wide range of patterns from regular to aggregated depending on the occurrence of different developmental stages in a specific plot under scrutiny (Bílek *et al.*, 2011).

Canopy gaps contribute to the available PAR in the understory depending on the location, gap size and tree species in the forest canopy (Canham *et al.*, 1990). The available PAR in beech forest gaps increases with gap size (Modrý *et al.*, 2004; Gálhidy *et al.*, 2006; Hahn *et al.*, 2007; Bílek *et al.*,

16

2014; Čater *et al.*, 2014). Further, gaps allow the beech understory to receive an increase in precipitation and mean air temperatures (Ritter & Vesterdal, 2006), although the gap itself is characterized by considerable micro-site variations depending on the gap orientation and shape (Ritter *et al.*, 2005; Gálhidy *et al.*, 2006; Čater *et al.*, 2014; Čater & Kobler, 2017). Relative light intensities under closed beech forest canopies can decrease to 1-3 % of the available PAR above the canopy, but these small amounts of PAR suffice for beech seedling growth (Emborg, 1998; Modrý *et al.*, 2004). Beech is a shade-tolerant tree species that grows best with 100 % of relative light intensities, but their growth rates differ little to those under 30 % (Wagner *et al.*, 2010). The growth reaction to different light intensities follows a degressive curve and is influenced by an ontogenetic trend (Ammer *et al.*, 2008; Wagner *et al.*, 2010).

Near-natural beech forest are characterized by a distinct relationship between the number of living trees and tree size, represented by the quadratic mean tree diameter (Pretzsch, 2006; Pretzsch & Mette, 2008; Schütz & Zingg, 2010), which can be referred to as Reineke's stand density rule (Reineke, 1933). These rule is, however, not fixed as the maximum size-density relationship for beech varies with climate and site conditions (Condés *et al.*, 2017). Considering the relationship between the average plant biomass and stand density, Yoda *et al.* (1963) developed the -3/2 power law for even-aged plant populations, assuming that a plant's growth complies with isometric scaling. Enquist *et al.* (1998) postulated a scaling slope exponent of -4/3 instead, based on the theoretical fractal-like resource distribution. Peters *et al.* (2019) showed that the different slope exponents of Reineke (1933), Yoda *et al.* (1963), and Enquist *et al.* (1998) can be explained by the maximum maintainable biomass per ground area, which complies with Condés *et al.* (2017), different competition modes, and species-specific allometric relations.

It is important to note that the outlined characteristics of near-natural forests can be found even on small spatial scales of less than 1 ha (Piovesan *et al.*, 2005; Alessandrini *et al.*, 2011).

So far, patterns and processes in beech forest have been outlined, which serve as the basis for model development.

2.4 Forest growth modeling

A model is an abstraction of a real-world phenomenon that attempts to describe the relationships of a system (Weiskittel *et al.*, 2011). In case of forest ecosystems, we can model these CAS over different spatial and temporal scales as well as organizational complexity levels (Pretzsch, 2001). The decision for the model's spatiotemporal dimension and complexity is driven by the scientists knowledge and purpose. System processes, such as photosynthesis, and structures are differently aggregated dependent on the scale and purpose of the model. As described by Pretzsch (2001), ecophysiological models are the less aggregated and most detailed, while focusing on cells and organs to organisms. These models are followed by single-tree models and whole forest stand models. The highest level of aggregation is assigned to forest succession models and ecosystem models, which are able to model forest growth at the landscape level over great temporal scales, such as centuries.

2.4.1 Development and types of forest growth models

Earliest developments of forest growth models include forest yield tables specifically designed for different species and management guidelines (Wiedemann, 1936; Assmann & Franz, 1963) with the purpose of forest taxation and sustainable wood harvesting. Single-tree models for management purposes, such as stand prognosis, have been developed with different approaches; tree position-independent (Wykoff *et al.*, 1982; Hasenauer, 1994; Monserud

18

& Sterba, 1996), tree-position dependent (Ek & Monserud, 1974; Mitchell, 1975; Nagel, 1999), and site- and position-dependent (Pretzsch, 1992). Forest succession models have been developed in order to study the consequences of environmental changes from small stands (Botkin *et al.*, 1972; Shugart & West, 1977) to ecosystem levels (Box & Meentenmeyer, 1991).

Distinction between forest models can also be made by empirical and mechanistic models (Taylor *et al.*, 2009), although Weiskittel *et al.* (2011) argues that this differentiation is misleading, because all models share some level of empiricism, which is the dependence on actual data derived from field studies. Weiskittel *et al.* (2011) proposes a set of different categories for forest growth models: statistical models, process models, hybrid models, and gap models. Statistical models mainly focus on the prediction of forest stand growth by characterizing the forest by its statistical variability of estimated parameters, where parameter estimation is based on field data. Examples for statistical models include the mentioned yield tables. Process models represent physiological processes, such as PAR interception through forest canopies or photosynthesis (Brunner *et al.*, 1998; Landsberg *et al.*, 2003). Hybrid models combine statistical and process models for enhancing system understanding and prediction (Piccolroaz *et al.*, 2016). Gap models are used to study ecological processes and forest succession in the long-term (Bugmann, 2001). The term gap specifies a gap in the canopy of a forest, in which alterations of the environmental conditions favor the establishment of tree seedlings and subsequent forest regeneration. Another type of models, called individual-based, is covered in the separate section 2.6, because of its close relation to this study.

Not all developed models have been successful in answering the research questions for which they were designed. Grimm *et al.* (1996) found the most successful models the ones which oriented their structure and purpose to patterns observed in nature. A pattern is a clearly distinguishable structure in

nature itself or in data derived from it (Grimm *et al.*, 1996). If we choose a model structure that principally allows the reproduction of patterns, the model becomes more realistic in that it contains key structural elements of the real system under scrutiny (Wiegand *et al.*, 2003). This modeling approach is called pattern-oriented modeling (Grimm *et al.*, 2005). An example is the model of Jeltsch *et al.* (1999), which was designed to reproduce spatial tree distribution patterns in a savanna ecosystem.

Irrespective of the purpose and model type chosen to answer research questions and to study forest systems behavior, the created models must be subject to a model validation (Weiskittel *et al.*, 2011). As this topic is differently covered in literature, this study focused on the theoretical framework of Schmolke *et al.* (2010). Further information is provided in section 2.6.

2.4.2 Structure of forest stand growth models

The structure of position-dependent forest growth simulators is briefly described, as it is linked with the development of the model in this study. If a forest model is position-dependent, then trees are characterized by a specific location that influences its growth (Weiskittel *et al.*, 2011). In order to predict tree growth and stand development, forest simulators such as BWINPro (Nagel, 1999) or SILVA (Pretzsch *et al.*, 2002) calculate tree growth, tree competition, tree mortality as well as tree regeneration.

Tree growth focuses on the spatiotemporal development of the tree's organs, be it above or below ground. The manner of growth is dependent on the model formulation, which includes specific parts of a tree. Usually, forest models calculate tree growth as their stem diameter growth, their height growth as well as their crown dimensions growth (Pretzsch *et al.*, 2002), although the latter can also be described as dependent from tree height and tree diameter (Nagel, 1999). Because of the constraints upon deriving infor-

mation about root distributions and root morphologies outlined above, root growth can be described as dependent from aboveground variables easily measured, such as tree diameter, or completely excluded. Root growth models, however, advanced recently even to 3D spatiotemporal models (Dupuy *et al.*, 2010), but have not been merged with forest growth models so far. Model formulations about diameter and height growth can be based on regression models that use measured increments and a vector of additionally independent variables, such as environmental conditions or tree competition to predict tree growth.

Tree competition in position-dependent forest growth models is often described by distance-dependent indices or can also be quantified if processes, such as PAR interception through the forest canopy, are included. Distance-dependent competition indices grasp the available resources for a tree individual in an abstract relative measure, that depends on the relative location of a focal tree to its neighbors (Weiskittel *et al.*, 2011). For example, the Heygi-Index (Hegyi, 1974) considers neighboring trees around the subject tree within a fixed radius as potential competitors and calculates the index as the sum of the ratios between the sizes of each competitor and the subject tree weighted by the inter-tree distance. This approach assumes that the trees' influence on accessible resources within a circular zone around its location is dependent on its size and diminished by the influences of neighboring trees. A large variety of other competition indices has been developed and its uses are model-specific (Weiskittel *et al.*, 2011). Position-dependent indices often do not distinguish between above- and belowground competition, they rather assume that those processes are linked and related to each other in that a large tree which dominates aboveground competition will also do so below ground (Weiskittel *et al.*, 2011). As the underlying causes of belowground interactions are still unclear, this is a rather coarse assumption. An example for another approach is the model

PLATHO (Gayler *et al.*, 2006) which simulates the growth of individual trees considering their phenological development, photosynthesis, water and nutrient uptake, respiration, biomass allocation as well as senescence. Thus, this model is of a process nature. Competition is quantified above ground as the available amount of PAR that a tree receives, while the model considers belowground competition separately. Belowground competition is calculated between neighboring individual trees by the overlap of their rooting zones represented by discs, which impacts the tree's resource capture capacity.

Tree mortality is the occurrence of tree death observed at various spatial and temporal scales. Tree death is caused by internal (e.g., decreasing pace of cell division with tree age) and external (e.g., diseases, fire) factors. While the internal physiological causes of tree death are still poorly understood (Weiskittel *et al.*, 2011), the external forces leading to tree death can be readily observed. As those external forces occur on sudden occasions and disturb the forest ecosystem functioning, they are termed disturbance events. Generally, the types of regular and irregular mortality are distinguished for modeling purposes. While regular mortality depends on tree competition and stand density, irregular mortality depends on external forces, such as wind storms Weiskittel *et al.* (2011). Which kind of mortality a forest growth model includes is again dependent on their purpose. For example, the single tree-based simulator SILVA calculates the survival probability of single trees as a function of tree dimension and competition. The survival probability is based on a logit-function and was parameterized on empirical mortality data derived from long-term monitoring plots. In a next step, the calculated probability is compared to a random number of the same interval as the probability. A particular tree dies, if the survival probability is greater then a random number drawn with equal probability (Pretzsch *et al.*, 2002).

Tree regeneration is the renewal of trees in a forest by means of seed production, seed dispersion, seed germination, seedling establishment, and

tree recruitment. All those processes are highly stochastic (Weiskittel *et al.*, 2011) and driven by various tree-internal and external factors. For example, seed production for the species beech considerably depends on precipitation sums and mean air temperatures during three years prior to seed dispersal (Gruber, 2003). The seed dispersal itself is driven by the seed size and weight in that beech is a barochor species that lets dispersal be driven by parent tree crown size and gravity (Wagner *et al.*, 2010). Seed dispersal distances are, therefore, mostly restricted to an area close to the parent tree, although some seeds are further carried away by animals (Wagner *et al.*, 2010). Beech nuts can germinate if they receive enough PAR, moisture in spring and escape fungal infections and devouring by animals. The seedlings establishes if benign conditions continue and the tree is recruited when it reaches a certain size (Weiskittel *et al.*, 2011). However, forest growth models with a management purpose such as BWINPro (Nagel, 1999) reduce the complexity of the mentioned processes by simply calculating establishment probabilities for particular species, calculating the new tree location on the basis of stand density and tree competition, and finally adding the recruited tree with fixed size to a tree list.

2.5 Modeling beech forest growth with cellular automaton models

Many developed forest growth models focused on rather short time horizons such as SILVA (Pretzsch *et al.*, 2002) or studied long-term dynamics of large forests in terms of their species composition such as with succession models (Taylor *et al.*, 2009). However, only few focused on patterns observed in monospecific stands (Rademacher *et al.*, 2004). So far, two grid-based or cellular automaton models have been specifically developed for the species beech (Wissel, 1992; Rademacher *et al.*, 2004). These models simulate forest growth on patches that are the result of dividing the simulation area by a

grid of varying spatial resolution. Thereby, dynamics of single patches may or may not be influenced by neighboring ones. The grid-based approach was chosen to enable the reproduction of the mosaic cycles in beech forests as significant pattern. Every patch is characterized by variables such as the tree number, tree size, or tree age. The model according to Wissel (1992) models the effect of solar radiation on beech trees and cyclic succession. Rademacher et al. (2004) developed the 3D rule-based model BEech FOREst (BEFORE) that simulates large-scale spatiotemporal dynamics of Central European beech forests. Rules-based means that model formulations contain if-then rules that describe the effects of tree growth, mortality and wind storms on the forest structure. This model is partly individual-based as it describes trees in the two upper height classes of a grid cell individually by their age and crown projection area. However, all models mentioned so far allow no further studies on the effects of crown plasticity on beech forest structure and dynamics.

2.6 Modeling beech forests using individual-based models

Individual-based models (IBMs) describe autonomous individual organisms and have been used in various disciplines from ecology (Grimm, 1999) to others dealing with complex systems, such as social sciences (Gilbert & Troitzsch, 2005), economics (Tesfatsion, 2002), geography (Parker et al., 2003), and political sciences (Huckfeldt et al., 2004). IBMs allow us to investigate the emergence of system-level characteristics from the adaptive behavior and interaction of the individuals involved (Railsback, 2001), which makes them ideal for studying complex adaptive system (CAS), such as forests.

The model development, analysis, and application of IBMs may be oriented to Schmolke et al. (2010), where consequent steps are provided. First, the model is conceptually formulated upon research questions or a problem

formulation, which is then implemented into concrete formulations and algorithms. The developed model is parameterized and calibrated with adequate data in a further step. Second, the developed model is used for first simulations, while the sensitivity of model outcomes to parameter specifications is analyzed and model results are verified by comparison to empirical data. If a pattern-oriented approach is chosen then model structure and analysis are oriented towards those patterns. In a next step, the model is validated with independent empirical data, which was not used for parameterization or calibration before. Third, the model can be applied and recommendations for environmental decision can be formulated. These subsequent steps are termed a modeling cycle (Schmolke *et al.*, 2010), which emphasizes the possibility to rework the model development if new knowledge for example from the sensitivity analysis or model evaluation can contribute to an enhanced modeling of the formulated problem. In this sense, the modeling cycle is not closed and finite, but open to new inputs in all stages.

Individual-based forest models, such as LES, include the plasticity of tree crowns (Liénard & Strigul, 2016) and allow studying their effect on tree growth and forest structure. However, the LES model was not designed for beech forests. Crown plasticity has been modeled on an individual basis for mangrove forests in the model mesoFON (Grueters *et al.*, 2014) and for *Hevea brasiliensis* (Willd.) plantations (Vincent & Harja, 2008). Beech crown dynamics were accurately modeled for single trees but not for complete stands, nor from an individual-based perspective (Beyer *et al.*, 2014, 2015, 2017). Therefore, no model exists so far that enables the investigation of the effects of crown plasticity on beech forest structure and dynamics, although this particular species trait alters the forest light regime, tree competition, and gap dynamics, which is essential for the emergence of forest structure.

3. Research questions and hypotheses

To sum up the findings outlined, aboveground competition for PAR in beech forests can be well described, whereas interactions below ground are not only very complex but also hard to describe in their effect on stand dynamics. Thus, the net outcome of aboveground competition, belowground competition and possibly belowground facilitation is yet beyond our understanding. Field investigations in beech forests demonstrate that crown plasticity considerably influences tree competition for PAR, but its effect on stand dynamics, forest structure and emergent patterns is yet unclear. Further, beech forest stands have been managed by selective thinning for centuries, but the management impact on crown plasticity effects on forest structure is not resolved.

This leads to following research questions:

1. Does a model focus on aboveground competition for PAR suffices to model beech forests and to reproduce the patterns we observe in near-natural beech forests without any specific descriptions of belowground processes?

2. What effects has tree crown plasticity on the structure and dynamics in near-natural beech forests?

3. What effects has forest management through selective thinning on the structure and dynamics in near-natural beech forests?

To answer these questions, a new individual-based model called BEEch Plasticity (BEEP) was developed that focuses on the aboveground competition for PAR and explicitly describes tree crown plasticity. The following hypotheses derived from the research questions (1 – 3) above are examined through simulation experiments with the BEEP model. Five hypotheses are derived from the first research question.

The detailed phenomenological description of aboveground competition for PAR and crown space suffices to reproduce:

1.1 a multi-layered vertical forest structure.

1.2 a small-scale heterogeneous forest structure that consists of several developmental stages in close proximity to each other.

1.3 a typical diameter distributions of a reversed J or bimodal shape with a high number of tree regeneration and old large-diameter trees.

1.4 large age ranges of canopy trees of more than 100 years.

1.5 varying tree stem foot and crown centroid positions from regular to aggregated patterns, while a regular pattern can be observed in the long run.

Four hypotheses are derived from the second research question.

2.1 Tree crown plasticity causes crown centroids to be more regularly distributed as the stem foot positions of beech trees.

2.2 Tree crown plasticity decreases the aboveground competition for crown space and PAR.

2.3 Tree crown plasticity enhances the horizontal and vertical forest structure.

2.4 Tree crown plasticity enables more developmental stages to coexist and contributes to a small-scale heterogeneous forest structure in the long run.

Four hypotheses are derived from the third research question.

3.1 Thinning decreases the vertical and horizontal forest structure.

3.2 Thinning decreases the aboveground competition for crown space and PAR.

3.3 Thinning causes the forest structure to be less heterogeneous on a small-scale.

3.4 Thinning leads to more aggregated patterns of stem foot positions and crown centroids.

4. Data material

4.1 Data for model development

4.1.1 Forest reserve Schattiner Zuschlag

Data for model development was derived from unmanaged beech forest reserves which have already been subject to repeated inventory. Central forest reserve used for model parameterization and calibration is the forest "Schattiner Zuschlag" with an area of 48 ha in North Germany (53° 46′ 41 N, 10° 47′ 53 E). The data was kindly provided by the forest district Stadtwald Lübeck to which this reserve belongs. Forest management ceased in this forest 1950, which allowed natural processes to coin the forest structure. Although it is certainly not an old-growth or virgin forest, recent investigations revealed a considerable degree of near-naturalness in the forest structure (Dolnik *et al.*, 2008). Another beech forest reserve with longer phases of natural development of several hundreds of years is the Serrahn beech forest located in Western Mecklenburg-Pommerania in the North of Germany (53° 20′ 35 N, 13′ 12'13 E), but repeated inventory data is currently not available for this forest.

The forest vegetation in the Schattiner Zuschlag is dominated by meso- and eutroph beech forests (Galio-Fagetum EU habitat code 9130) growing in a suboceanic climate with mean annual temperature of 5.3 °C and annual precipitation of 580–871 mm (Gauer & Aldinger, 2005). Side conditions are moderately moist to moist on recent moraine soils from the Weichselian

glaciation. Soil types can be characterized as luvisols and cambisols. The dominant tree species is beech (*Fagus sylvatica* L.) interspersed with horn-beam (*Carpinus betulus* L.), oak (*Quercus robur* L.), ash (*Fraxinus excelsior* L.), and larch (*Larix decidua* Mill.).

While the Schattiner Zuschlag is not managed, other forests within the forest district Stadtwald Lübeck are managed according to Forest Steward-ship Council (FSC) principles with low-thinning intervention aimed at the protection of natural disturbance regimes (Sturm, 1993; Westphal *et al.*, 2004). For beech forests, this means only single-tree removal of trees with a target diameter greater than 65 cm. This type of thinning intervention is applied in this study in a separate simulation experiment with selective thinning.

Forest inventory has been carried out by systematic sampling methods on a 90 x 65 m grid (Dolnik *et al.*, 2008) in the years 1992, 2003, and 2013. Plot areas of 100, 200, and 500 m^2 varied with tree diameter. Trees within sampling plots were recorded in terms of their species, age, height, and diameter at breast height (1.3 m above ground). For parameterizing and calibrating the BEEP model, only sampling plots located in pure beech stands were recognized.
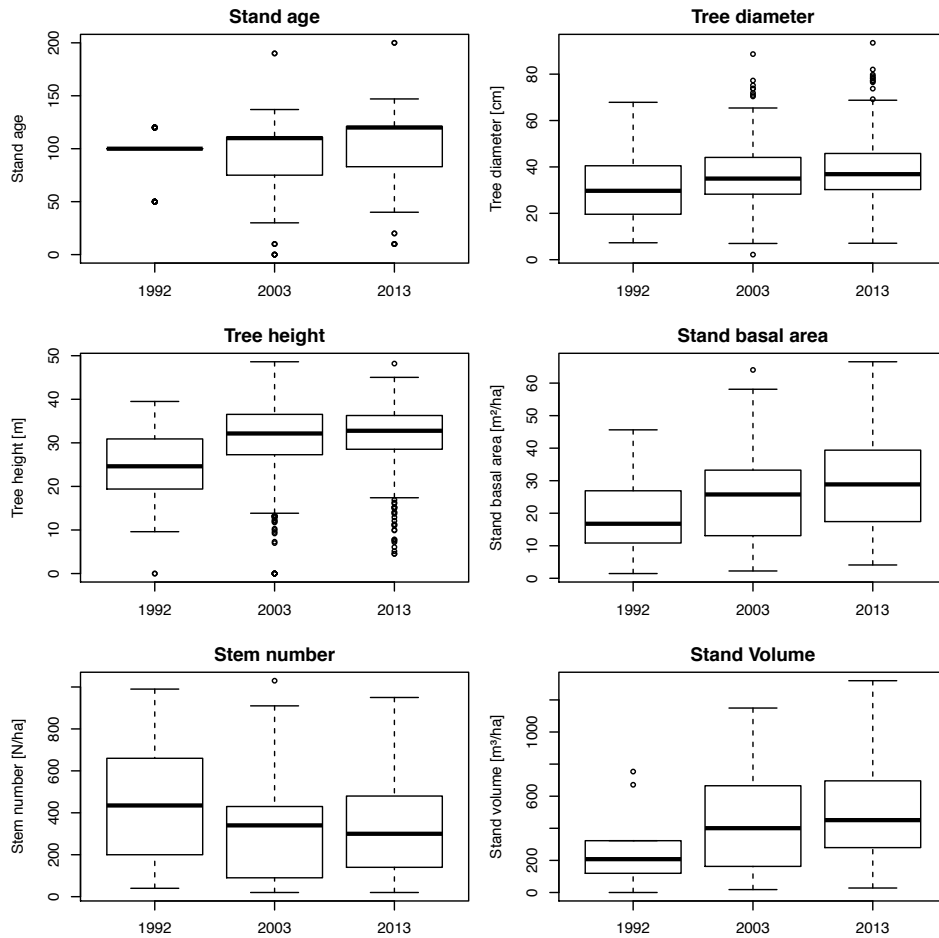
Figure 2: Forest stand data for pure beech stands from three inventories in the reserve Schattiner Zuschlag. The data was kindly provided by the forest district Stadtwald Lübeck.

Fig. 2 provides stand data from three inventories in 1993, 2003, and 2013 that have been used for model development. Stand ages vary greatly from 10 to 200 years, which indicates that the data set provides information from all age classes. The biggest tree diameter was 93.5 cm, while the tallest tree was 48.6 m high. Stand basal areas and stand volumes increased from 1993 to 2013 and reached maximum values of 66.6 m^2 per hectare and 1319.7 m^3 per hectare, respectively. These stocking levels can only be reached by long-term undisturbed development, which is an indicator for the near-naturalness of

the forest (Dolnik *et al.*, 2008).
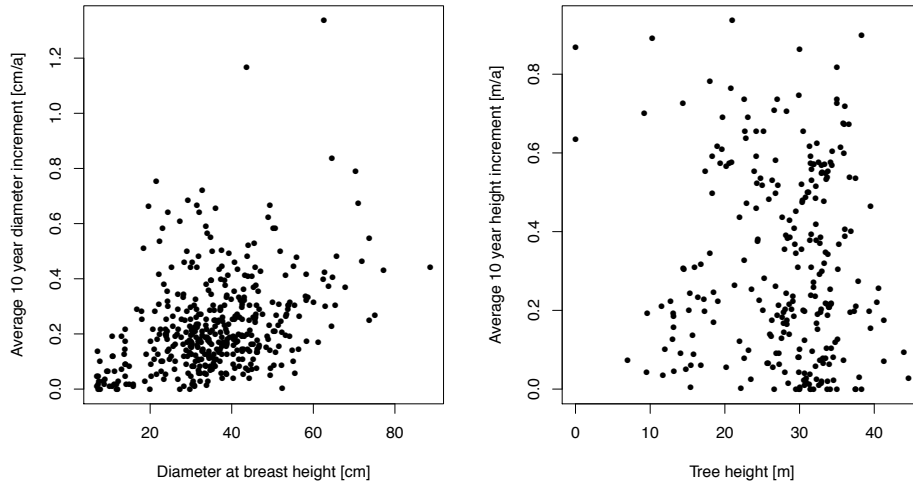
Figure 3: 10 year average height and diameter increments for beech from forest inventory in the Schattiner Zuschlag. Inventory data was provided by the forest district Stadtwald Lübeck.

As inventories were accomplished in 1992, 2003, and 2013, tree height and diameter increments could be calculated, although not all plots of 2003 and 2013 were already measured in 1992. Fig. 3 shows the 10 year average height and diameter increments per year over the tree height and diameter. Both, diameter and height increments show a large variation that is probably caused by individual tree differences in competition and site conditions.
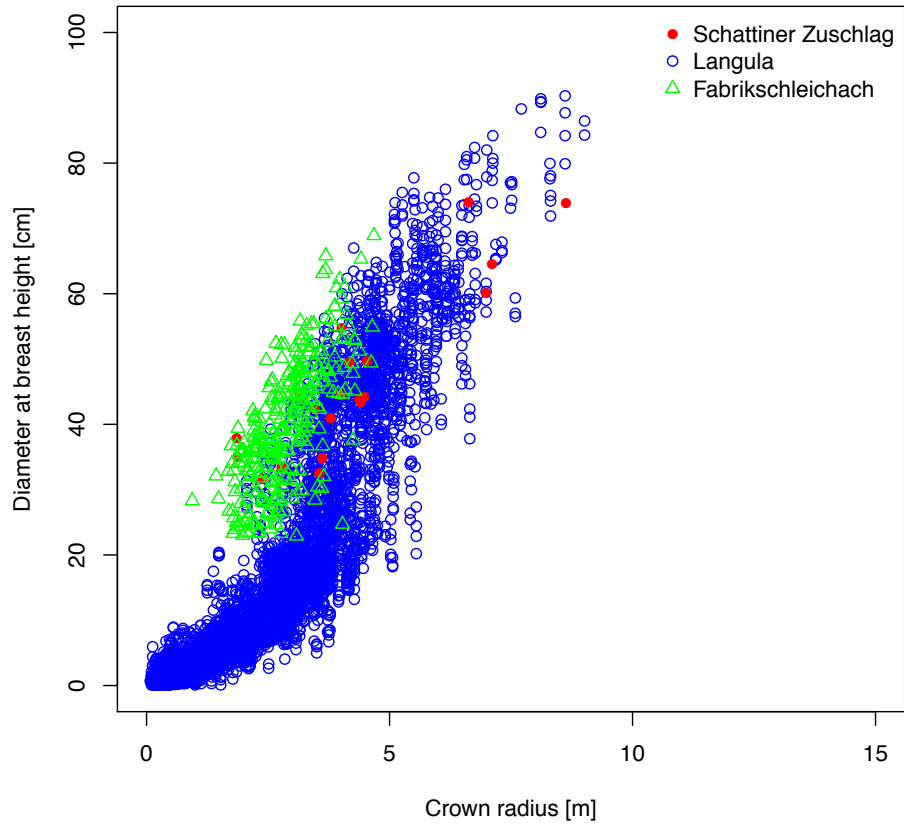
Figure 4: Beech tree diameters over crown radii from the sites Schattiner Zuschlag in North-Germany, Langula and Fabrikschleichach in Central Germany. Data was provided by the forest district Stadtwald Lübeck, Prof. Hans Pretzsch, Chair of Forest growth and Yield Sciences Technische Universität München, and Prof. Heinz Röhle, former Chair of Forest Growth of the Technische Universität Dresden.

Additional to tree diameter and height, crown onset heights and crown radii were measured for 20 dominant beech trees randomly selected in pure beech plots. Tree diameters over averaged crown radii measured in eight directions (N, NE, E, SE, S, SW, W, NW) are provided in Fig. 4.

4.1.2 Long-term experiments Fabrikschleichach and Langula

Crown data from near-natural beech forests was additionally derived from two long-term experiments located in Central Germany. For the experiment Fabrikschleichach, the data was kindly provided by Prof. Hans Pretzsch, Chair of Forest Growth and Yield Sciences of the Technische Universität München. In case of the experiment Langula, the data was kindly provided by Prof. Heinz Röhle, former Chair of Forest Growth of the Technische Universität Dresden.

The experiment Fabrikschleichach (49° 55′ 07 N, 10° 34′ 16 E) is surveyed since 1870 and was originally established as growth and yield experiment with low-thinning applications where one plot was left untreated (Pretzsch, 2003, 2005). Soil types can be characterized as cambisols over marl and red sandstone. Annual precipitation is 820 mm, while annual mean temperature is 7.5 °C. Stand ages range from 38 to 179 years, while dominant tree heights range from 22 to 33 m. A total of 161 trees in 1980 and 140 trees in 2000 were subject to crown sampling in the untreated control stand where crown radii in eight directions (N, NE, E, SE, S, SW, W, NW) were measured.

The selective thinning experiment Langula (51° 08′ 59 N, 10° 25′ 03 E) is characterized by three plots established in 1956 (Gerold & Biehl, 1992). The applied selective thinning is an intense forest management practice where single beech trees are removed if they reach a target diameter of 70 cm. Beech regeneration can establish in the remaining canopy gap. Soil types can be characterized as ranker and cambisol over shell limestone with layers of loess loam of varying thickness. Annual precipitations range from 600 to 800 mm, while annual mean temperatures range from 6.5 to 7.5 °C. Tree ages range from 17 to 204 years, while dominant tree heights reach 40 m. Crown radii were measured in eight directions (N, NE, E, SE, S, SW, W, NW) from trees of all size classes: 252 trees in 1996, 696 trees in 1997, 664 trees in 2002, 536 trees in 2006, and 506 trees in 2010. The experiment Langula was chosen

to obtain crown data from a selective thinning experiment, which was aspired also for this simulation study. As beech crown adaption differs between tree neighborhoods, the crown data contributes to the possible reaction range of beech crowns from all size classes, which is a valuable resource for model development.

Measured tree diameter over average crown radii from the sites Schattiner Zuschlag, Langula, and Farbikschleichach are presented in Fig. 4. The tree diameters show similar relationships with crown radii for tree diameters greater than 20 cm. Crown radii for trees smaller than this value have only been measured at Langula and show different relationships with tree diameters. This indicates changing crown efficiencies for different size classes, which means that trees with equal diameters can have substantial different crown radii.

For example, Fig. 4 shows trees with 30 cm tree diameter, while their crown radii range from 3 to 6 m. The changed crown efficiency for beech trees with diameters less than 20 cm at Langula is based on the space occupancy abilities of beech (Pretzsch & Schütze, 2005), which occupies available crown space if sufficient PAR is provided through thinning, but does not manifest this crown growth into diameter growth immediately. Rather, diameter growth lacks behind crown growth if neighborhood trees are suddenly removed by selective thinning.

4.2 Data for model validation

4.2.1 Data for validating crown morphology

Model validation is accomplished with data not used for model development. As the BEEP model describes the plasticity of beech tree crowns and crown growth, the validation should orient itself to high-resolution data from near-natural beech forests that allows comparison between observed crown growth with model predictions. For this purpose, laserscanning data of tree crowns

(Georgi *et al.*, 2018) is preferable compared to ground-based measurements of crown radii and lengths, because of the exact three-dimensional crown shape that can be obtained through this approach.

Laserscanning was implemented in the reserve Schattiner Zuschlag on three circular plots within pure beech stands in winter 2016/2017 (data unpublished). The plots had an approximate radius of 20 m. Single scans were registered and single-tree 3D point clouds extracted for further analysis. A total of 102 beech trees could be scanned and extracted for analysis of crown structures and shapes. The laserscanning data was kindly provided by Louis Georgi and Friedrich Reich, Institute of General Ecology and Environmental Protection of the Technische Universität Dresden.

Figure 5: Scanned forest plot in the forest reserve Schattiner Zuschlag. Laserscanning data was provided by Louis Georgi and Friedrich Reich, Institute of General Ecology and Environmental Protection of the Technische Universität Dresden.

The scanned tree individuals are taller than 20 m and characterized by a dominant social class. Tree crowns are constrained by their neighbors, the canopy is completely closed. Unfortunately, only one scan could be accomplished, although multiple scans are needed for validating model predictions on crown growth. Hence, validation for the BEEP model could not

35

be achieved for crown growth characteristics, but only for crown shapes and structures predicted by the BEEP model. Fig. 5 provides the 3D point cloud data on single trees of one scanned plot.

4.2.2 Data for validating forest radiation calculations

Data for validating the radiation calculations in the BEEP model was derived from literature (Emborg, 1998; Ritter *et al.*, 2005; Gálhidy *et al.*, 2006; Hahn *et al.*, 2007; Bílek *et al.*, 2014). Three studies (Emborg, 1998; Ritter *et al.*, 2005; Hahn *et al.*, 2007) were all implemented in the beech-dominated near-natural forest Suserup Skov in Denmark (55° 22′ N, 11′ 34' E). The study of Gálhidy *et al.* (2006) is located in a beech forest in the Börzsöny Mountains in northern Hungary (47° 9′ N, 18′ 9' E). The study of Bílek *et al.* (2014) is located in a near-natural beech forest in the Voděradské bučiny National Nature reserve in Central Bohemia (49° 58′ N, 14′ 48' E). All studies provide data on ground-based light measurements under closed canopies and in canopy gaps of varying sizes as percentage of above canopy light (PACL). The PACL measurements of all studies over gap sizes are provided in Fig. 6. PACL values linearly increase with gap size.
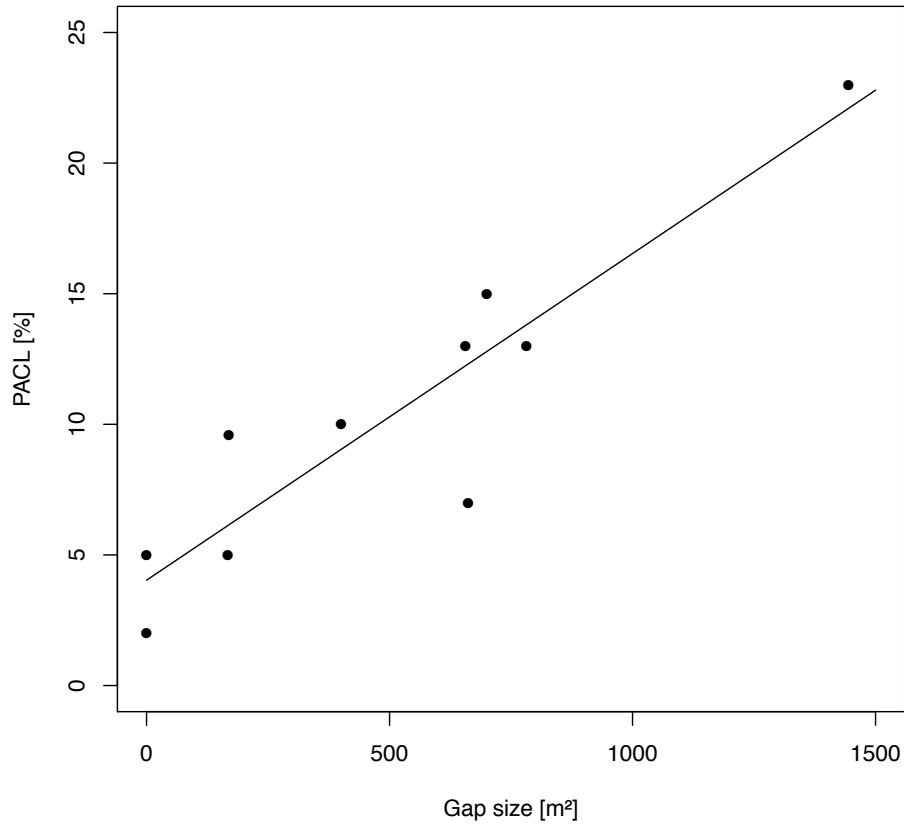
Figure 6: Measured percentages of above canopy light (PACL) over gap size (Emborg, 1998; Ritter *et al.*, 2005; Gálhidy *et al.*, 2006; Hahn *et al.*, 2007; Bílek *et al.*, 2014). The relationship between the PACL and the gap size can be characterized by a linear model with R^2 of 0.82.

4.3 Data for comparing simulated and observed spatial structures

As this study is concerned with spatial structures in near-natural beech forests, such as tree distributions, model simulation results are compared to studies that characterize tree spatial distributions (regular, random, or aggregated) by means of spatial indices, such as the Clark-Evans index (Clark

& Evans, 1954), which is described in detail in section 5.3.

The study of Schröter *et al.* (2012) is located in the Serrahn beech forest in Western Mecklenburg-Pommerania in the North of Germany (53° 20′ 35 N, 13° 12′ 13 E). This forest has not been managed for more than 300 years (von Oheimb *et al.*, 2005). Soil types are dystric cambisols, podzoluvisols, and luvisols developed over loamy sand from recent moraines of the Weichsel glacial period. The terrain can be characterized by an undulating micro-relief. Mean annual precipitation is 590 mm, whereas mean annual temperature is 7.8 °C (von Oheimb *et al.*, 2005). A total of 235 trees was censused in a 2.8 ha sample plot in 2002. Additional to measurements of tree diameter at breast height and tree height, stem positions of all trees with a minimum diameter of 7 cm were mapped. Average tree height was 38 m, while stem volume was 605 m^3/ha. In 2009, crown radii of all trees in the upper canopy layer were measured in eight directions (N, NE, E, SE, S, SW, W, NW). This enabled the creation of crown maps that delineate 2D crown shapes using measured crown radii. Further, horizontal distances between the stem foot position and the center of gravity of the crowns could be calculated as crown displacement.The data allowed the calculation of the Clark-Evans-index as well as other indices that describe forest structure, such as the CSI, SCI, and SI. Index calculations are described in detail in section 5.3. The Serrahn beech forest plot is characterized by a canopy interspersed with gaps in which natural regeneration could establish. The remaining large canopy trees have already extended their crowns into canopy gaps, which led to enhanced average crown displacements.

The study of Bulušek *et al.* (2016) provides Clark-Evans indices for stem foot positions and crown gravity centers from various permanent research plots from near-natural beech forests located in the Sudetes of the Czech Republic and Poland. Due to the large elevation gradient that the study encompasses, data for comparison was only used from mid-altitude beech

forests with elevations from 415 to 635 m and age ranges from 95 to 175 years, which enhances comparability to the BEEP model, which was parameterized on data derived from low-altitude beech forests of the Schattiner Zuschlag in North-Germany. Plots used for model comparison are K35 in the Karkonosza National Park (50° 50′ 5 N, 15° 38′ 37 E) with 0.25 ha size as well as B8 (50° 30′ 10 N, 16° 12′ 21 E), B5 (50° 34′ 42 N, 16° 15′ 34 E) and B1 (50° 34′ 24 N, 16° 15′ 42 E) with 0.24 ha size in the Broumovsko Protected Landscape Area. The inventory conducted on the permanent research plots contained trees with a minimum diameter at breast height of 4 cm. Average tree heights ranged from 20.6 to 26.8 m, while stem volume ranged from 556 to 942 m^3/ha. All plots are located on slopes with inclinations ranging from 15 to 46°.

The study of Bílek *et al.* (2011) provides Clark-Evans indices for stem foot positions from a near-natural beech forest located in the Voděrady National Nature Reserve (49° 58′ N, 14° 48′ E). Data sampling was accomplished on two permanent research plots of 1 ha established in 2005. These forest stands had not been managed through shelterwood cutting, as the surrounding forest stands. All trees with a minimum diameter of 3 cm were censused and stem positions measured. According to Bílek *et al.* (2011), the age of the canopy trees ranges from 155 – 189 years. Average tree heights were 26.4 and 30.5 m, while stem volume was 505 and 707 m^3/ha, respectively.

In terms of environmental conditions, the studies of Bílek *et al.* (2011) and Bulušek *et al.* (2016) are less comparable to the Schattiner Zuschlag than the study of Schröter *et al.* (2012), which influences comparisons between observed and simulated spatial forest structures.

5. BEEP Development and Description

5.1 Model Development

In order to answer the research questions of section 3, it is necessary to model aboveground competition for PAR and explicitly describe beech crown plasticity. This requires a conceptual design that comprises the following core elements of a model:

1. The model should focus on individual trees to study tree interactions.

2. The model should be set into a three-dimensional world to accurately simulate tree growth behavior.

3. Every tree is an individual that must have a location, a height, a diameter, and a crown.

4. The tree crown must be plastic in a way that allows it to change its shape.

5. Trees should adapt their growth to different levels of PAR they receive.

6. The model should contain a radiation model that calculates the radiative transfer of PAR through the forest canopy.

7. As the aim is to study long-term effects on forest structure and dynamics (more than 100 years), the model should contain procedures that describe tree mortality and tree regeneration.

These conceptual points were translated into a model design which is already part of the modeling cycle (Schmolke *et al.*, 2010). The developed model structure is constructed in a way that enables the reproduction of patterns from near-natural beech forests (Wiegand *et al.*, 2003). The model structure contains submodel routines for tree height, diameter, and crown growth as well as routines for tree mortality and regeneration. The following

40

subsections briefly outline the chosen submodel routines along with their conceptual derivation, whereas a detailed description is given in section 5.2

5.1.1 Radiation modeling

Radiation drives individual tree growth (Balandier *et al.*, 2007), tree competition and forest dynamics (Pacala *et al.*, 1996) as well as the morphogenesis of stems, branches, leaves, and root systems (Balandier *et al.*, 2006; Galen *et al.*, 2007; Niinemets, 2010). Forest-growth models that are process-based describe tree growth as dependent on the amount of PAR a tree receives (Forrester *et al.*, 2014b). Consequently, various radiation models have been developed, successfully implemented and tested (Ligot *et al.*, 2014). According to Ligot *et al.* (2014) model calculations in radiation models can be coarsely divided into three main parts:

1. Calculation of the distribution and magnitude of light (PAR) above the forest canopy

2. Calculation of the transfer of light (PAR) through the forest canopy, called radiative transfer

3. Calculation of light (PAR) reflection and scattering in order to enhance the description of light trajectories through the canopy

While the first part can be accomplished by applying standard astronomical laws (Brock, 1981), the second part depends on the geometric crown structure and mathematical formulations used to describe PAR transmittance, absorption, and interception. The third part is very complex and often skipped from model calculations (Ligot *et al.*, 2014). A very critical part to examine is the geometric crown structure. The stand canopy can be composed of one or several horizontal layers, which is adequate for describing ecological processes at stand level (Forrester *et al.*, 2014b), whereas three-dimensional crown shapes are adequate for studying forest dynamics

41

and stand structure (Chave, 1999; Paquette *et al.*, 2008). These 3D shapes can be also composed of several simpler forms to allow the description of degenerated shapes (DaSilva *et al.*, 2012) and even crown plasticity (Liénard & Strigul, 2016). The most detailed crown representations provide area surface models that describe leaves, branches, and stems as realistic as possible (Leroy *et al.*, 2009).

In terms of the mathematical formulations used to describe PAR attenuation, two approaches can be described: the turbid medium and the porous envelope (Ligot *et al.*, 2014). The turbid medium approach calculates PAR attenuation according to Beer's Law that describes the attenuation of a monochromatic ray within a turbid medium, that is, a medium composed of small elements which are randomly scattered and which show a homogeneous transperancy. As forest canopies can be characterized as turbid mediums that is influenced by the density and spatial distribution of leaves and branches, Beer's law has been applied to forest canopies with several correction coefficients as adaption. Commonly, the fraction of transmitted light (PAR) coming from an zenith-angle η and an azimuth-angle γ through the forest canopy $\tau(\eta, \gamma)$ can be calculated from the extinction coefficient k, the clumping factor Ω, the leaf area density LAD as proxy for the canopy element density, and the path length l of a ray through the canopy (η, γ) (Ligot *et al.*, 2014):

$$\tau(\eta, \gamma) = e^{-k*\Omega*LAD*l(\eta,\gamma)} \tag{1}$$

The porous envelope approach assumes that $\tau(\eta, \gamma)$ is simply dependent on the probability p of a ray to be intercepted by the crown foliage which is dependent on ray direction and path length l (Biovin, 2011):

$$\tau(\eta, \gamma) = p \tag{2}$$

The probability p can be interpreted as the fraction of the visible sky through a canopy (Canham *et al.*, 1999). This approach is less mechanistic than the

previous and requires less calibration effort (Ligot *et al.*, 2014).

The approach chosen for radiation modeling in the BEEP model is based on recommendations from Ligot *et al.* (2014), where simulation of forest dynamics should depend on a 3D crown model that either uses a turbid medium or porous envelope approach. As the parameter p of the porous envelope depends on field data derived from photographing isolated crowns (DaSilva *et al.*, 2012), which was unavailable for this study, but data on *LAD* could be accessed from the literature, the turbid medium approach was chosen. Calculations on PAR scattering and reflectance are complex and sufficient field data was unavailable. Thus, those calculations were excluded from radiation modeling.

This resulted in the application of a ray-tracing algorithm adopted from Brunner *et al.* (1998) with 3D crown shapes and calculations of PAR attenuation using the turbid medium approach.

5.1.2 Tree height growth modeling

Height growth modeling is complicated due to high variability in measured increments within stands and a close connection to environmental factors, such as precipitation (Weiskittel *et al.*, 2011). In general, three approaches can be distinguished (Weiskittel *et al.*, 2011). First, the potential or maximum possible height increment is calculated and multiplied by a modifier (Pretzsch *et al.*, 2002). Second, the realized height increment is directly predicted (Hasenauer & Monserud, 1997). The third approach is used for example in forest gap models (Bugmann, 2001), where height growth is indirectly modeled through height-to-diameter equations, while calculating diameter increment first. The second approach using direct height growth prediction needs sufficient data on growth-restricting variables, such as tree competition, or climate factors, such as precipitation. As inventory data from the Schattiner Zuschlag provided only limited height measurements

that could be related to tree competition or environmental factors, the first approach was chosen for the BEEP model. An additional reason to opt for approach 1 is that height growth in the BEEP model is related to crown growth. The latter is modeled in three dimensions and highly dependent to available PAR. Neither PAR data within the forest Schattiner Zuschlag nor detailed crown data was measured, which excludes a direct estimation of the realized height increment.

Potential height growth can be calculated age-dependent (Burkhart *et al.*, 1987) or age-independent (Hann & Ritchie, 1988). The earlier calculates dominant heights for the start and end of a period for homogeneous stands (Weiskittel *et al.*, 2011), while the latter describes age as a function of tree height and/ or site index and uses this to solve a dominant-height growth equation that is used to predict the potential height increment (Weiskittel *et al.*, 2011). Due to the BEEP model orientation towards heterogeneous stands, the age-independent variant was chosen. The formulations used in BEEP are adopted from Pretzsch *et al.* (2002). Details on the calculations are provided in section 5.4. Height growth is modeled depending only on available PAR in the BEEP model, as detailed measurements on environmental factors, such as soil moisture (Wagner, 1999), are not available for the measured height increments presented in section 4.1.1. Thus, height growth is modeled assuming average constant environmental conditions for climate and soil conditions and only PAR attenuation as process is included.

5.1.3 Tree crown growth modeling

The inventories from the sites Schattiner Zuschlag, Langula, and Farbikschle-ichach (see section 4.1) provide crown radii measurements that might be used for estimating tree diameters, but they are not sufficient for constructing a three-dimensional crown plasticity model. For this purpose, crown growth in a certain direction must be related to individual-tree variables, such as age,

height and received PAR. This cannot be achieved by using the presented crown data. The development of the crown growth submodel, which is at the heart of the BEEP model, was initialized by observations and conceptual thinking.

Observations of real beech trees span a wide range of possible crown shapes from plagiotroph-growing saplings in the understory over slender trees in contested neighborhoods to free-growing individuals with wide crowns that almost resemble a hemisphere (Fig. 7).
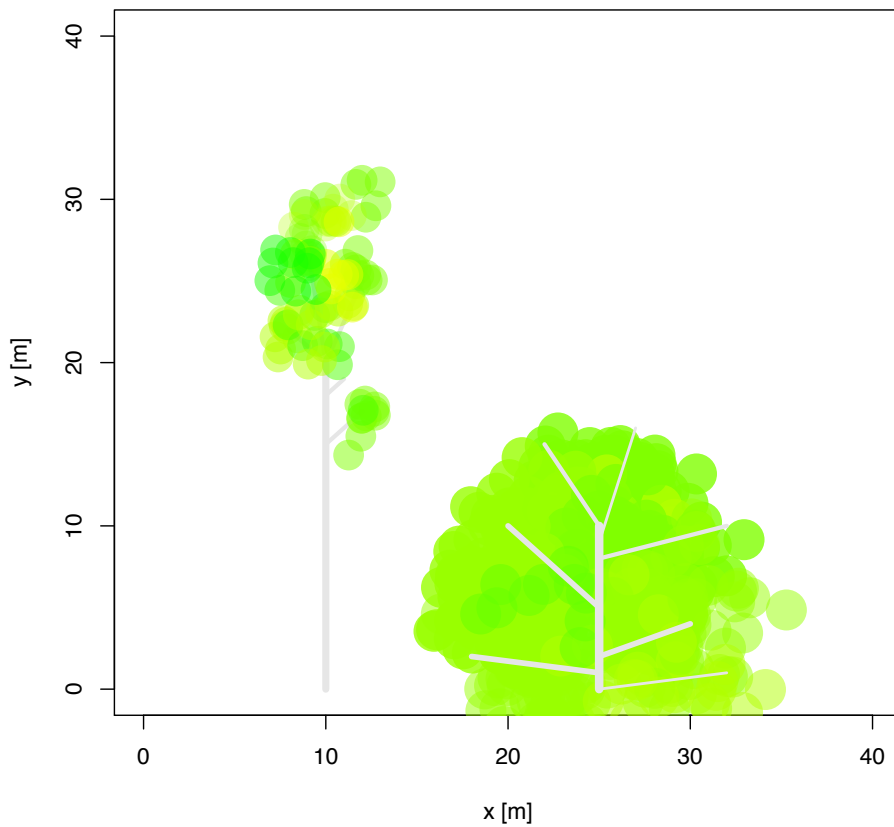
Figure 7: Tree crown shapes for beech growing in different environments. The tree on the left shows a schematic tree crown grown in contested neighborhoods within a closed forest, the tree on the right shows a crown developed under free-growing conditions.

A reasonable crown model should be able to reproduce all those structures, but the model focus for BEEP lies rather on closed beech forest environments with gap dynamics. Comparing beech crowns in forests underpins the observation that similar crown shapes can evolve with different branching patterns. For this reason, the model focus was placed on the crown shape and the location of the tree leaves as photosynthetic organs of the tree. If crown plasticity is modeled, however, there is information needed on how much a crown can grow in a certain direction in a certain amount of time. This information can be derived from the height growth of an individual tree, as height growth can be accurately described from inventory data (see above) and crown growth can be conceived as a special case of shoot or height growth.

That means, the shoot growth within a crown is dependent on the growth reaction of the whole tree. Under ideal conditions (free-growing), beech tree crowns can resemble a hemisphere, which leads to the conclusion that shoot growth under ideal conditions at any position in the crown approximately equals the height growth of the particular tree. Otherwise, the tree crown would have developed another shape. Thus, it seemed reasonable to derive crown growth from the height growth information which is readily available. This dependence, however, needed to be impacted by the available PAR, as beech trees change their crown shape and branching patterns accordingly (Beaudet & Messier, 1998; Messier & Nikinmaa, 2000).

For describing crown growth, a distinction is made between the light and the shade crown of a tree. Beech trees alter their leaves and photosynthetic activity dependent on the PAR within its crown. This impacts the tree crown shape and leads to the development of adapted leaf organs. In the upper crown part, leaves receive more PAR, which leads to the term light crown. The lower more shaded part is called shade crown accordingly. The location of both parts is assumed to be relative to the height of the greatest

crown width (Pretzsch, 2001). The approach used in this model describes the crown surface development of the light crown above the point with the highest crown width (Fig. 8). The shaded part of a tree crown is not modeled, as the position of leaves in those areas is more heterogeneous and the influence on tree assimilation is relatively low (Pretzsch, 2001).

The crown surface is spanned with a set of crown vectors (Fig. 8), which tips are crown points. These crown points describe the crown surface.
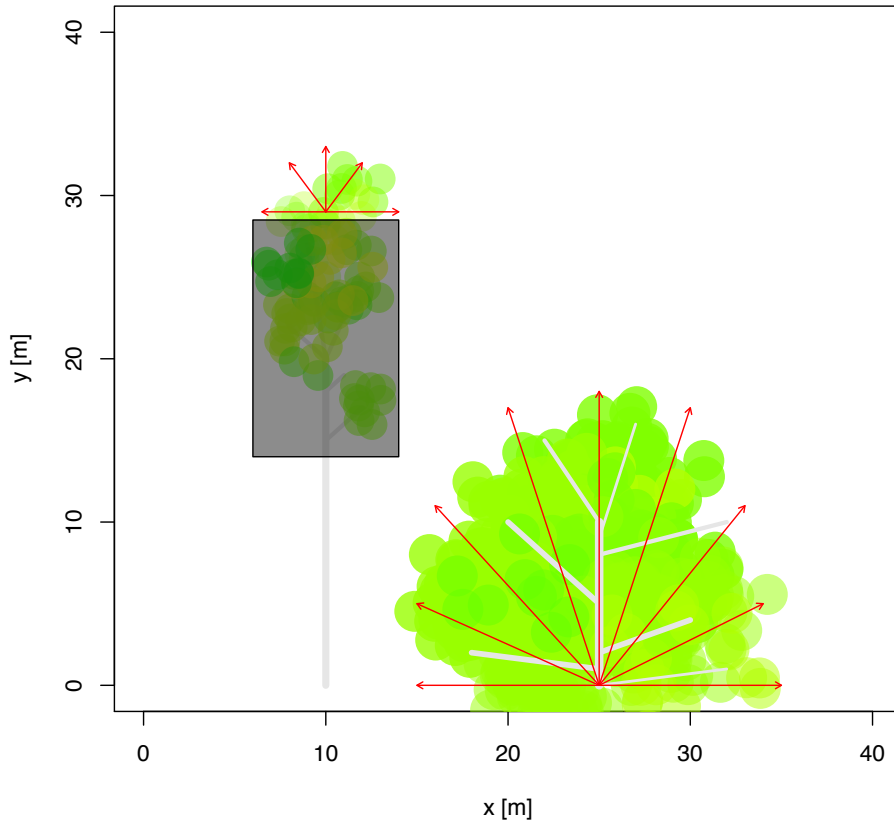
Figure 8: Tree crown shapes grown under different environmental conditions. Red arrows indicate the crown vectors that span the crown surface above the point of the greatest crown width. Trees in contested neighborhoods are characterized by a significant shaded crown part (grey rectangle), which is not modeled.

This design is used to describe the crown growth phenomenologically, that is, the behavior of the modeled crowns is based upon the understanding derived from observations and the concept outlined. The approach to base crown growth on crown vectors and the crown surface description with crown points is similar to Vincent & Harja (2008). According to Godin *et al.* (2000), the BEEP model uses a geometric representation of tree crowns. This approach was chosen to avoid more detailed descriptions of plant architecture, for which no data was available, such as modular representations of stems, branches and leaves (Godin *et al.*, 2000). Another possible approach could have been the discretization of modeling space into 3D voxels for representation (Godin *et al.*, 2000), but this would have undermined information from continuous height and crown growth.

5.1.4 Tree diameter growth modeling

Tree diameter growth at breast height (1.3 m above ground) can be directly predicted or gained by multiplying the potential increment with a modifier that includes constraining variables, such as competition, similar to height growth modeling (Weiskittel *et al.*, 2011). Potential diameter increment equations with multiplicative modifiers are used for example in the model SILVA (Pretzsch, 2001). Data from inventories in the Schattiner Zuschlag provide considerably varying increment data (see section 4.1.1), which can only be related to tree age, height, and tree location, but not with crown dynamics. As tree diameter increment is highly correlated with crown size for beech trees (Fichtner *et al.*, 2013), neglecting crown dynamics in diameter increment predictions would lead to bias. Therefore, diameter growth was described as directly dependent on crown size, namely the crown projection area, because the data material obtained from the site Schattiner Zuschlag, Langula, and Frabrikschleichach allows the construction of a nonlinear regression model that predicts tree diameter from the trees' crown

projection area. Through this approach, diameter growth can be related to crown dynamics and consequently to tree competition for crown space and PAR. The resulting submodel routine predicts the tree diameter in a static way, that means, each time the crown projection area increases, the tree diameter increases as well. However, the tree diameter cannot shrink if crown size decreases due to losses in crown space due to competition or disturbance.

5.1.5 Tree mortality modeling

Tree mortality in the BEEP model can be distinguished between regular and irregular (Weiskittel *et al.*, 2011). The regular competition-dependent mortality is achieved through crown modeling. If an individual tree is devoid of any available PAR or crown space, then the tree is termed dead. In contrast, modeling irregular mortality is more complex. Tree mortality is characterized by a strong temporal and spatial variability (Franklin *et al.*, 1987; Weiskittel *et al.*, 2011) which is still poorly understood (Dietze & Moorcroft, 2011) and hinders the construction of generally applicable mortality models (Hawkes *et al.*, 2000). There exist mechanistic (Wang *et al.*, 2010) and empirical (Weiskittel *et al.*, 2011) mortality models. The former predicts tree mortality from physiological processes, the latter builds a relationship between the likelihood of tree death and variables that can be internal or external to the tree, such as the availability of soil water. While explicit mechanistic mortality models for beech do not exist, there are numerous empirical models from Switzerland (Dobbertin & Brang, 2001; Wunder *et al.*, 2008), Germany (Nothdurft, 2013; Boeck *et al.*, 2014) or Austria (Hasenauer, 1994; Monserud & Sterba, 1999). However, there was no long-term mortality data available from beech stands at Schattiner Zuschlag, so that no empirical mortality model for the site itself could be developed and parameterized. Existing empirical mortality models predict tree mortality

from (1) tree size, vitality and competition within a forest stand (Monserud & Sterba, 1999), (2) from tree size and growth (Holzwarth *et al.*, 2013), and (3) from tree age and environmental variables (Neuner *et al.*, 2015). Tree vitality or tree growth is commonly assessed based on the diameter or basal area increment (Hülsmann *et al.*, 2016), assuming that decreasing increments sign tree death, although the reasons for decreasing increments are diverse ranging from defoliation following insect attacks, forest fire, flooding to drought.

As outlined above, the BEEP model does not include environmental processes, except PAR attenuation in the forest canopy. Thus, irregular tree mortality cannot be based upon environmental stress, such as soil water limits. While height growth is described as a function of tree size and age, diameter growth is directly related to crown growth. Predicting tree mortality probability on tree diameter or basal area increment (Hülsmann *et al.*, 2016), therefore, would lead to false conclusions, because if a tree cannot increase its crown projection area due to limiting crown space, it does not grow in diameter. However, absent growth in crown projection area does not imply tree death, as the modeled tree in the BEEP model can also temporarily be contested by its tree neighbors. Thus, using diameter or basal area increment as explanatory variable is inadequate, which excludes the application of many developed empirical mortality models (Hülsmann *et al.*, 2016). Further, other empirical mortality models are parameterized for specific data sets and applications to forest stands outside the parameterization range should be always treated with care (Hülsmann *et al.*, 2016). Therefore, the BEEP model needed a new mortality description for irregular mortality.

Disturbance events, such as windthrow, are discrete in time and impact forest structure and forest ecosystem processes (Seidl *et al.*, 2011). Discrete disturbance events can be described according to their frequency, return

interval and predictability, but also by their impact severity (Seidl *et al.*, 2011). On a greater scale, such as landscape, mortality can be described in terms of a disturbance regime (White & Jentsch, 2001). Climate impacts such as drought or storms can be predicted from existing meteorological time series data (Seidl *et al.*, 2011), which are nevertheless characterized by high uncertainty and a random nature (Stillmann *et al.*, 2017). Further, forest fires and insect outbreaks are likewise difficult to predict, because of their dependence on weather conditions (Nelson *et al.*, 2013). Hobi *et al.* (2015b) showed that gap patterns in primeval beech forests in the Ukraine revealed mostly small-scale mortality events, where single or groups of trees died, whereas large-scale disturbances were rare. These findings led to the description of random irregular tree mortality by which single or groups of trees die. It is assumed that the probability of a tree to be affected by storms or insects increases with tree age and size. To avoid dependence on tree age alone, which can be misleading if young beech saplings grow in the understory for more than 100 years (Hobi *et al.*, 2015a), tree mortality probability is related to tree height. The discrete event, at which height a tree is affected, is described by the ratio between the current tree height and its potential maximum, which is drawn from a normal distribution. Further, trees in the BEEP model do not vanish immediately if they are termed dead. Rather, they are undergoing a senescence process in which parts of their crown are randomly deleted, which leads to a gradual tree death that allows also a gradual gap creation in the modeled forest. Further details are provided in section 5.2.9.

5.1.6 Tree regeneration modeling

Beech is a tree species that flowers and masts in rhythms of 2 to 3 years dependent on weather conditions prior to a mast year (Gruber, 2003). As the BEEP model does not account for climate-dependency of tree growth,

a synchronous mast rhythm of seed production of 3 years is assumed. Seed dispersal is driven by crown size, as beech is a barochor species that drops seeds because of its seed mass and gravity (Wagner *et al.*, 2010). The larger the crown size, the greater distances from a parent tree can a seed achieve. Is is assumed that seeds are randomly dispersed from the parent tree in terms of distance and direction. As field studies showed (Wagner *et al.*, 2010), dispersal distances of beech seeds from a parent tree reach up to 20 m, although greater distances are possible, for example by dispersal through mammals. Tree establishment in the BEEP model is dependent on PAR alone, although site conditions such as soil moisture are important (Wagner *et al.*, 2010), but not accounted for in the BEEP model. Further details are provided in section 5.2.7.

5.2 BEEP Model Description

The description of the individual-based BEEP model follows the ODD protocol (Grimm *et al.*, 2010). All model simulation and analysis was carried out with R 3.4.0 (R Development Core Team, 2017) using further the latest versions of the packages geometry (Habel *et al.*, 2015), plyr (Wickham, 2011), mgcv (Wood, 2017), and rgl (Adler & Murdoch, 2018). Parameter values included in the ODD protocol are the result of model parameterization and calibration described in section 5.4 and 5.5.

5.2.1 Purpose

The BEEP model was developed for the description of near-natural forests of European beech (*Fagus sylvatica* L.). The model explicitly considers tree crown plasticity as a response to available PAR and neighboring tree crowns. The model is used to explore the mutual link between PAR competition, crown displacement, tree growth, and mortality. Particular emphasis is placed on the importance of crown plasticity for structural patterns, such as

the vertical heterogeneity in tree heights and horizontal distribution patterns of stem locations and crown centroids.

5.2.2 Entities, state variables, and scales

The BEEP model has only one entity, namely individual beech trees. They are described by a set of simple state variables characterizing the location for the tree and the dimension of the stem:

- x, y [m, m] coordinates of the stem foot point

- dbh [cm] stem diameter at breast height

- h [m] tree height

Further state variables specify the crown dimensions:

- O [m] - height of the crown onset point (the x, y – coordinates are equal to the stem foot point of the tree). The crown onset point is the origin of the crown vectors shown in Fig. 8 and Fig. 9.

- x, y, z [m, m, m] - coordinates of the points spanning the crown surface. Vectors connecting the onset point with the various points on the crown surface are referred to as crown vectors.

Considering the photosynthetic active radiation (PAR) as environmental factor, the

- PACL [%] - percentage of above canopy light received is the last state variable of the trees regulating their height growth.

One time step represents one year in order to track the slightest changes in crown growth, shape, and competition. Space is described in three dimensions. The typical size of a simulated plot is 0.5 ha as a results of the findings of Tabaku (2000) on the sizes of forest development phases in beech forests. The simulation area can be, nevertheless, varied by the experimenter.
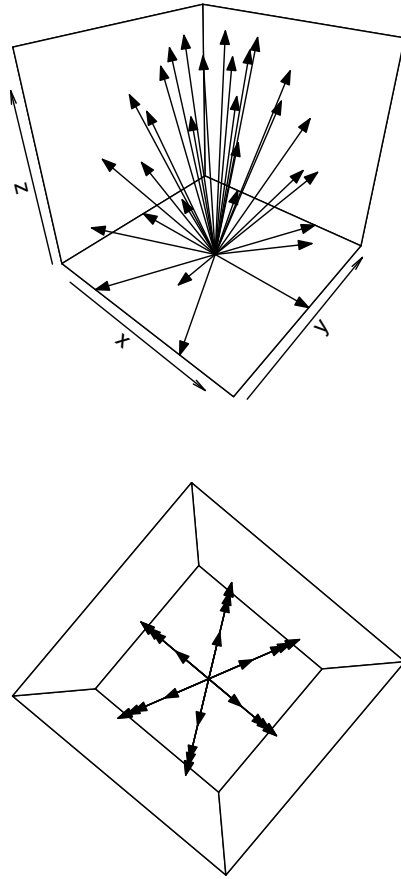
Figure 9: Initialized tree sapling with initial crown radius of 0.05 m. The crown points are systematically placed in six horizontal directions and five layers. Arrows indicate crown vectors emanating from the crown onset point.

5.2.3 Process overview and scheduling

The model describes five processes, namely *regeneration, radiation, mortality*, as well as *height and crown growth*. The flowchart in Fig. 10 shows the sequence of their execution.
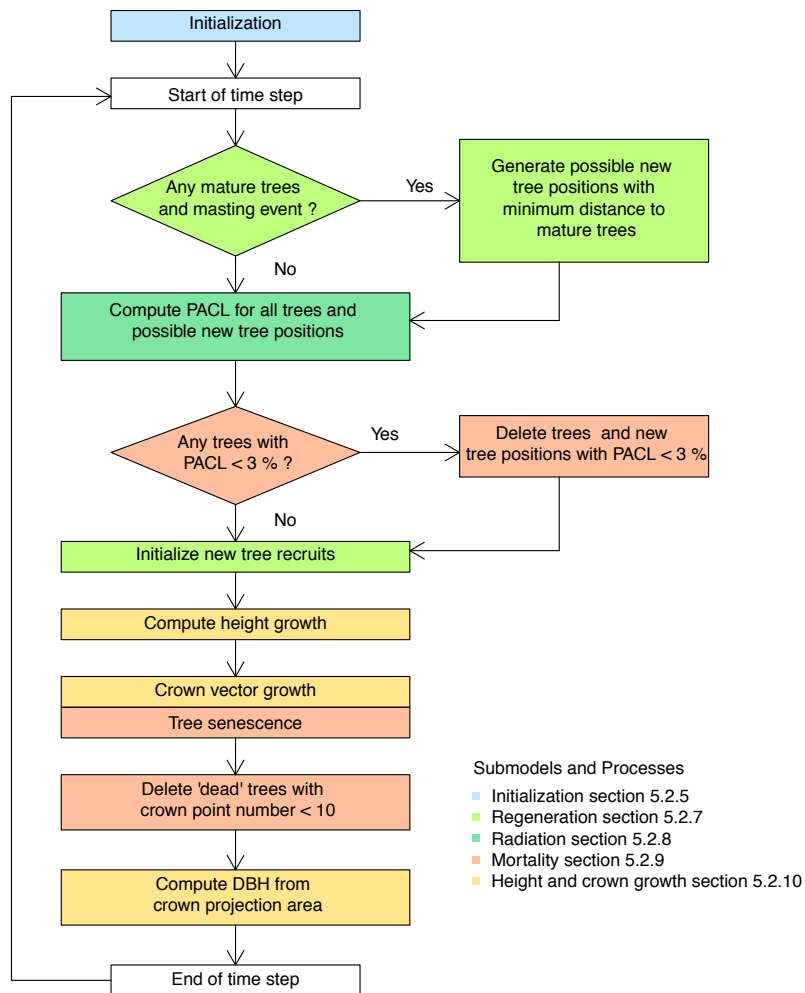
Figure 10: Flowchart of the model processes in its execution order. PACL is the percentage of above canopy light, DBH is the diameter at breast height [cm].

Regeneration assumes a masting rhythm of three time steps. The new tree recruits are established if the PAR availability - described as PACL threshold - is sufficient.

Radiation describes the availability of photosynthetic active radiation (PAR) within the forest stand. This occurs in two steps: (1) the total PAR

above the canopy is decomposed into direct and diffuse PAR and their spatial distributions are simulated over the upper hemisphere. (2) The transmission of direct and diffuse radiation through the canopy (PACL) is calculated as percentage of above canopy light according to the Lambert-Beer-Bouguer law with leaf area density as the driving variable. The total PAR in Step (1) is executed only once during the initialization of a simulation experiment. The transmission in Step (2) is calculated for each tree in each simulation step considering light competition by neighboring trees.

Mortality refers to the death of a tree, which occurs if its crown cannot be maintained. This can occur either as a result of competition for crown space (regular mortality), or as a consequence of random losses of crown points due to tree senescence (irregular mortality). All trees are initialized with a certain threshold mortality index, which informs about the tree height at which its senescence begins. This index is the relation of the current tree height to its maximum tree height. As the tree reaches its individual threshold, e.g. 95 % of its maximum height, a random number of its crown points is deleted. This process is repeated the following time steps, until the crown point number falls below a threshold (see section 2.2.9).

Height and crown growth describes (1) the increase of the tree height as a function of PACL, and (2) the extension of the crown surface by increasing the crown vectors (Fig. 14). The length of the crown vector extension depends on the realized height growth and the available space in the canopy defined by competing neighboring trees. This can result in crown shape distortion. Stem diameter is derived from the crown projection area.

Sections 5.2.7 — 5.2.10 provide detailed information about the implementation of the related submodels.

5.2.4 Design Concepts

Basic principles: Height and crown growth base on the classical concept of

optimal growth reduced by the photosynthetic active radiation (PAR). The attenuation of PAR in the canopy is calculated according to the Lambert-Beer-Bouguer law using leaf area density as main factor.

Emergence: The size distributions of tree dimensions (tree height and diameter at breast height) as well as the spatial patterns of tree stem foot points and crown centroids emerge from the neighborhood interactions and the ecological processes described by the model.

Adaptation: Trees adapt their crown to the neighborhood constellation. Due to this plasticity, they optimize their use of the available canopy space.

Objectives: Not relevant

Learning: Not relevant

Prediction: Not relevant

Sensing: Trees sense neighboring crowns. For this, all crown points of a focal tree check for crown points of neighbors in a vision cone. The vision cone is a cone with an opening angle of 60 ° and a height of 10 m set with its tip upon a crown point (see Fig. 15 for further details).

Interaction: Trees interact (a) indirectly via the reduction of the available PAR beneath their canopy (PAR competition), and (b) directly by hindering the growth of crown vectors of neighbor trees (space competition).

Stochasticity: The stem foot positions of the tree (x- and y-coordinates) and individual tree variables determine the height and crown vector growth. In particular: three parameters defining the maximum size of the trees, namely maximum height (MaxH), maximum pace of height increment (MaxHp), and potential diameter increment (potD) are random. The mortality index that determines tree senescence is random as well.

Collectives: Not relevant.

Observation: Stem foot position, crown centroid, diameter at breast height, tree height, and crown projection area are registered for all trees of the forest stand at each time step. Edge effects were reduced by truncating a

boundary of 10 m from the edges and excluded the simulated individuals from analysis.

5.2.5 Initialization

At the start of the simulation, a number of 3000 small tree saplings are randomly distributed over the simulated area of 0.5 ha. The initial sapling number is derived from planting recommendations for beech trees of 6000 individuals per hectare (Muck *et al.*, 2009). The simulation area of 0.5 ha is derived from sizes of beech forest developmental phases, which rarely exceed 0.5 ha and fluctuate in their median values from 0.1 to 0.3 ha according to Tabaku (2000). The simulation is initiated with tree saplings to create a more realistic forest canopy development, although beginning with mature trees is possible as well. The x and y coordinates of the stem foot point are drawn from a uniform distribution. These values fix the simulation area, so that new tree recruits cannot establish outside this area. The initial values of the state variables and model parameters are assigned to the trees (see Table 1 for details). A tree sapling is characterized by a height of 0.05 m, a diameter of breast height of 0 cm, and an initial crown radius of 0.05 m. Initial sapling sizes are derived from observations from beech seeding experiments (Ammer & Kateb, 2007). At the beginning, every tree is characterized by a PACL of 100 % and a mortality index ranging between 0.8 and 0.98 (see details in section 5.2.9). Table 1 provides an overview on the model parameters.

Table 1: Estimated and calibrated parameter ranges. * Parameter ranges are randomly set by drawing values from a normal distribution with the given mean (Mean) and standard deviation (Sd) at the initialization of every tree. Parameters a – c were estimated according to (Beyer *et al.*, 2017), parameters d – f fitted according to (Ammer, 2000). MaxD is the maximum diameter at breast height, which was parameterized along with parameter i from crown-diameter relationships (see section 4.1.1). potD is the parameter altering crown efficiency.

Parameter	Parameter value	Equation	Source
a	0.0040	3	estimated
b	0.3817	3	estimated
c	10.6620	3	estimated
d	1.01267	9	fitted
e	-6.88919	9	fitted
f	1.60155	9	fitted
g	0.0091	10	estimated
h	-0.0091	10	estimated
MaxH	Mean=48, Sd=0.1*	7/8	Calibrated
MaxHp	Mean=0.017, Sd=0.00022*	7/8	Calibrated
i	0.0026	12	Parameterized
MaxD	150	12	Parameterized
potD	Mean=0.7, Sd=0.1*	12	Calibrated

As tree growth is described phenomenologically, the maximum tree height (MaxH) and the maximum pace of height increment (MaxHp) are randomly chosen and are not part of a detailed process-based submodel. Parameter values are drawn from a normal distribution (see Table 1) to create initial differences in height and crown growth.

5.2.6 Input Data

The distribution of diffuse and direct radiation at the position of the town Lübeck (N 53 ° 52.1738′, E 10 ° 41.2547′), North-Germany, is calculated in advance and loaded in the initialization process. Details of the calculation are given in Brunner *et al.* (1998) and Brock (1981) and in section 5.2.8.

5.2.7 Regeneration

Trees become adult with an age of 60 years (Gruber, 2003). Trees are assumed to mast synchronously every 3 time steps if they have already reached an adult state and a minimum height of 20 m (Gruber, 2003). The minimum height of 20 m is assumed to avoid tree masting of small trees in the understory, which might have already reached an age of 60 years. In a masting year, every mature canopy tree produces three saplings. This sapling number is sufficient to accumulate regeneration numbers of 6000 individuals as in the initialization. For example, 300 parent canopy trees (see Fig. 2 in section 4.1.1) produce 6300 saplings over a period of 20 time steps through this masting rhythm.

The saplings are distributed in a ballistic way: (1) a dispersal angle is randomly chosen between 0 ° and 360 °, (2) a dispersal distance is chosen from a Poisson distribution using the average crown radius λ of the parent tree as expected value. Tree positions with a PACL below 3 % are deleted. If the PACL at any particular location is greater than 3 %, a new tree is initialized according to section 5.2.5 but with its tree position already calculated. The sapling number is set as the parameter Regenerate in the sensitivity analysis.

5.2.8 Radiation

The growth of the trees depends on the received percentage of above canopy light (PACL). The model calculates light interception and transfer through

the forest stand with the ray-tracing algorithm according to Brunner *et al.* (1998). In this approach, photosynthetic active radiation (PAR) attenuation in the modeled canopy is calculated according to Bouguer's law with leaf area density as the driving variable. By tracing sample rays distributed over a hemisphere, the model calculates the spatial distribution of direct and diffuse PAR in the forest stand resulting in the PACL of a particular tree. To apply this, the model initializes the exact position of 8192 sample rays over a hemisphere, and calculates the direct and diffuse radiation for every ray above the canopy. The ray number was chosen according to the results of the sensitivity analysis by Brunner *et al.* (1998). The ray distribution is almost even, while the average angular resolution is 0.01 ° in the altitude direction and 0.04 ° in the azimuthal direction. This setting does not change during the simulation. The sum of diffuse and direct radiation for every ray is specified as the above-canopy-light (ACL). This ACL is calculated from the exact sun positions during the period from March to October for the town Lübeck in North-Germany. This distribution of total PAR is provided as a file and loaded into the model before initialization.

As this radiation model was developed for rotation-symmetric crown shapes (Brunner *et al.*, 1998), it had to be adapted to asymmetric crown shapes. Stems and branches are not considered as obstructions to irradiance. Further, leaf area density is assumed to be constant and equally distributed within the individual tree crown, thus, the clumping factor Ω is excluded (Ligot *et al.*, 2014). Leaf area density (LAD) is estimated for every tree according to the results of Beyer *et al.* (2017) depending on tree height (H) with

$$LAD = a * H^2 + b * H + c \tag{3}$$

Firstly, the model identifies all trees taller than the focal tree. The height difference between the focal tree and identified competing neighbors was included as CanopyPACL in the sensitivity analysis. After all competing

61

trees have been identified, the model calculates which rays from the given distribution are obstructed by a tree crown. The obstructed ray passes through the crown of a neighbor tree, while its path length [m] (PATH) through the crown is estimated as:

$$PATH = CL * \cos(\phi) \tag{4}$$

where CL is the crown length [m] being the difference between tree height H and the height of the crown onset point O, and ϕ is the zenith angle of the particular ray. The resulting percentage of above canopy light for the particular ray ($PACL_{ray}$) is calculated as:

$$PACL_{ray} = e^{-0.5*LAD*PATH} \tag{5}$$

The sum of all $PACL_{ray}$ values of all obstructed rays and the ACL values of all unobstructed rays gives the PACL of the focal tree.

The simulated plot of 0.5 ha is assumed to be embedded in a closed forest, which does not allow rays to pass through the forest canopy beyond the borders of the simulated plot. This particularly affects the PACL calculation of edge trees, because PAR competition is exacerbated towards the plot edges. Those edge trees are excluded from further analysis.

5.2.9 Mortality

Individual trees die, if they cannot maintain a minimum number of 10 crown points. The minimum number of 10 equals the number of crown points that can be gained at every time step (see section 5.2.10 below). Any tree with a point number less than 10 is automatically deleted. This deterministic approach is chosen to establish a proxy for a minimum growth that the tree must be able to maintain. The exact number of 10 points is further considered a result of the regular crown point arrangement (Fig. 9). The number of crown points can fall below this threshold due to neighbor crown

62

competition. Every crown point of a particular tree detects neighbor crown points in an upright vision cone with an opening angle of 60 ° and a height of 10 m. These crown points of a particular tree are deleted if they detect more than two neighbor crown points. If the crown point number of the tree falls below 10 as a result of this competition for crown space, the individual tree is deleted (details in section 5.2.10). Furthermore, trees cannot only die from competition for canopy space, but also from irregular mortality. This was accomplished with a mortality index M that signals when tree senescence begins, which means a loss of crown points. This mortality index is assigned at the beginning:

$$M = \frac{H}{MaxH} \tag{6}$$

The mortality index is drawn from a normal distribution (Fig. 11), while maximum mortality indices are set to 0.98, because of the asymptotic tree height growth, which could lead to no death during the simulation. The resulting indices range from 0.75 to 0.98. In other words, a tree is affected by irregular mortality between 75 and 98 % of its maximum possible height.
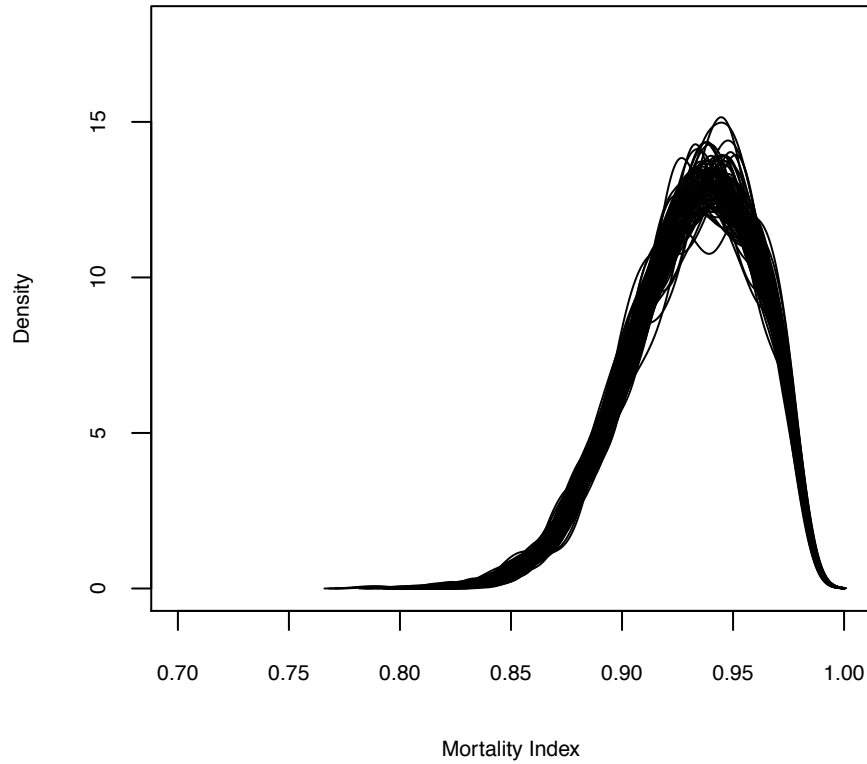
Figure 11: Mortality index distributions for 100,000 trees drawn from a normal distribution.

When a tree reaches its mortality index M, a random number of its crown points are deleted in the following time steps. These crown points can have any location in the individual tree crown. This procedure continues until the threshold of 10 crown points (see above) cannot be maintained, and the individual tree is deleted. Thus, the decline of the tree spreads over several time steps and its crown gradually shrinks, which allows a gradual canopy opening and increase of PACL values in the forest understory. The ratio between current and maximum tree height was set as parameter Mortindex.

5.2.10 Height and crown growth

A tree grows by extending its crown surface relative to its vertical stem axis. This is described in two steps: (1) the calculation of the potential height growth based on the theoretical age of the tree (Pretzsch, 2001), which will be (2) modified to the realized height growth by light competition.

The theoretical age of the tree TA depends on the current tree height H:

$$TA = \frac{-\ln\left(1 - \sqrt{\frac{H}{MaxH}}\right)}{MaxHp} \tag{7}$$

where MaxH gives the maximum height a tree can reach and MaxHp modifies the pace of height increment. The theoretical age defines that particular age the tree should have under optimum growing conditions.

The potential height growth PI is then derived from the theoretical age TA and the current tree height H (Pretzsch, 2001) by

$$PI = MaxH * (1 - e^{-MaxHp*(TA+1)})^2 - H \tag{8}$$

Based on this information, the extension of all crown vectors can be calculated as described in the following, as the potential height increment PI equals the maximum possible extension of all crown vectors.

The potential growth PI is modified by the relative growth response RG to the available $PACL$ (Burschel & Schmaltz, 1965a,b; Gemmel *et al.*, 1996; Ammer, 2000; Kunstler *et al.*, 2005) and a shoot reduction factor SR. RG is calculated as:

$$RG = d * (1 - e^{-e*PACL})^f \tag{9}$$

where d, e, and f are coefficients fitted according to Ammer (2000). Considering the shade tolerance of beech saplings, tree growth is possible if PACL is greater or equal than 3 % (Emborg, 1998; Modrý *et al.*, 2004). This value

was set as parameter minPACL in the sensitivity analysis. RG ranges between 0 and 1 (Fig. 12). The relative growth response is calculated on the tree level.
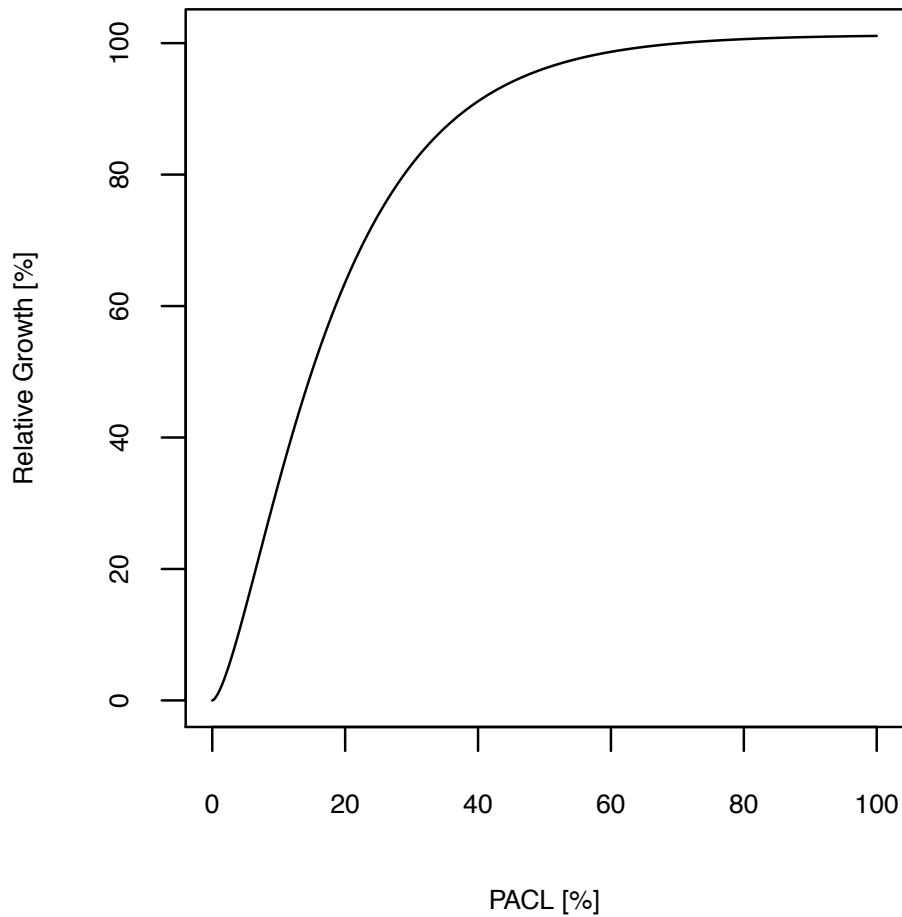
Figure 12: Relationship between the relative growth response and available Percentage of Above Canopy Light (PACL).

In a next step, the growth of the crown vectors is calculated. Beech trees are assumed to reduce the growth of crown vectors according to the position of the crown vectors to the individual stem axis, if the available PACL is less than 100 %. This leads to slender crown shapes of trees in the understory. The reduction is achieved by the shoot reduction factor SR ranging from 0.1

to 1. The minimum value of 0.1 secures that a crown vector cannot shrink. The growth is linearly reduced according to the angle between crown vector and the stem axis following the equation:

$$SR = (g * PACL + h) * \alpha + 1 \tag{10}$$

where α is the angle between the stem axis and the particular crown vector, g and h are parameters specified in Table 1. The parameters were estimated to enable a linear reduction according to the angle between crown vector and stem axis. The lower the available PACL, the more slender the tree crown becomes. On the contrary, if the PACL is 100 %, no reduction is imposed. The tree crown then develops to a hemispherical shape. (Fig. 13) shows the different crown shapes that result from the shoot reduction factor. The tree on the left side grew 50 time steps with PACL of 100 % and no competition. The tree on the right side grew 50 time steps with a PACL of 20 %. The resulting tree shape is not only slender but significantly smaller. Both trees in this example received no competition from neighboring tree crowns.
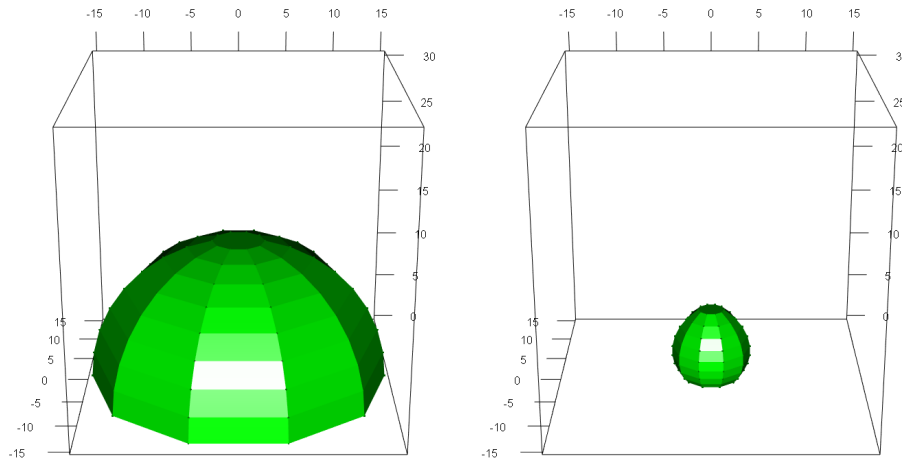
Figure 13: Crown shapes for trees grown 50 years under PACL values of 100 % (left) and 20 % (right).

The realized increment I of the particular crown vector is then:

$$I = PI * RG * SR \tag{11}$$

All crown vectors are extended at once according to their crown vector increment. This leads to a crown surface expansion and an increase in tree height (Fig. 14).
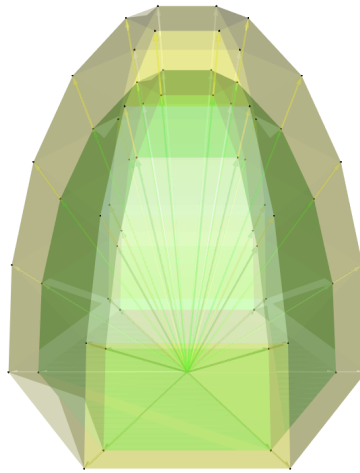
Figure 14: Crown growth accomplished by extending all crown vectors (arrows) at once according to their crown vector increment. The crown surface expands, displayed here from green to yellow. The crown vector growth leads automatically to a new tree height, which is defined as the maximum z-coordinate of the crown points at the vector tips.

The new tree height H is the maximum z-coordinate of all crown points, which have been relocated by crown vector growth.

Neighbor crowns hinder the crown vector growth. Thus, before extending a crown vector, the particular crown point "senses" neighbor crown points in an upright vision cone with a height of 10 m and an opening angle of 60 ° (see Fig. 9). This value was fixed to 60 ° to achieve maximum crown point detection and to avoid artificial canopy gaps due to large opening angles. This value was set as parameter VisionCone in the sensitivity analysis.

Crown points of the focal tree crown are excluded from detection. The particular crown point is deleted if more than two points are detected, which enables the contact between neighboring tree crowns, but prevents further crown intersection. The point number is a result of the regular crown point arrangement (see (Fig. 14))
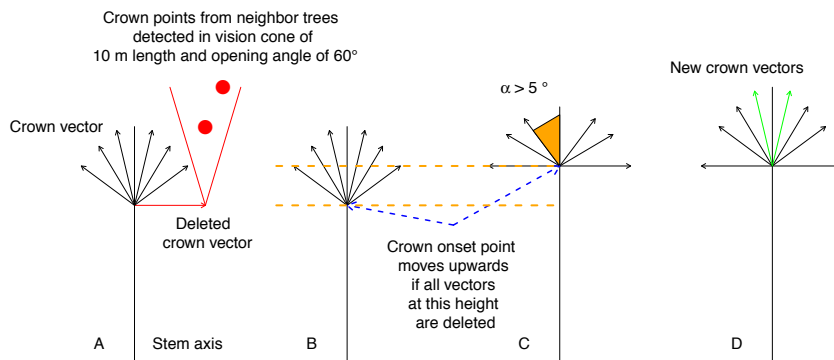
Figure 15: Schematic creation of new crown vectors as response to a loss of crown vectors on the crown bottom due to competition from neighbor trees. If one complete layer of crown points with the same height is deleted (A), the crown onset point moves upwards to the height of the next crown layer (B), which changes the orientation of all vectors. This leads to an increase of the angle α to the stem axis. If α is greater than 5 $^\circ$ (C), new crown vectors are created to complete the tree crown again (D).

The crown onset point with height O moves to the next minimum height of the crown points, if a complete lower crown part is deleted (see Fig. 9 A). The maximum upward movement depends on the vertical distance between crown points. The crown points itself remain unaltered, but the crown vector orientation changes, so that new vectors can be created at the crown top if the angle α is greater than 5 $^\circ$ (see Fig. 9 C). This mechanism provides an optimum of crown space occupation. A maximum of 10 new crown points is assumed to be created at every time step by calibration.

The interplay between crown point loss due to competition or senescence and crown vector growth changes the trees′ crown space occupation.

The horizontal projection of the crown points forms a polygon of n crown points. This crown projection area can increase or decrease, as a result of the interaction described above.

Tree diameter DBH is derived from the crown projection area cpa and calculated by

$$DBH = MaxD * (1 - e^{-i*cpa})^{potD} \qquad (12)$$

where i, $MaxD$, and $potD$ are parameters. The parameter $potD$ alters the crown efficiency, which is the basal area increment per crown surface area increment (Fichtner *et al.*, 2013). Parameters i and $MaxD$ are the result of parameterization, while $potD$ was calibrated. While the crown projection area can decrease, the diameter cannot. The diameter at breast height increases if the crown projection area grows.

5.3 Sensitivity analysis

The BEEP model produces a range of outputs that depend on the numerical and algebraic formulations described above as well as on model parameters (see Table 2) to varying degrees. As the model describes only a small subset of possible mechanisms and processes in a forest ecosystem, the model formulations and the model concept as such is subject to uncertainty. It is unclear, if the seemingly positive results are based on misconceptions about the mechanisms or interactions between the elements of a forest. Sensitivity analysis is performed In order to analyze how the model actually performs and reacts to variations of the model input (Pianosi *et al.*, 2016). In particular, sensitivity analysis tests if variations in the model output can be attributed to changes of its input parameters. This sensitivity is closely related to model calibration (see section 5.5) (Grimm & Berger, 2016).

Sensitivity analysis can be achieved with both global and local approaches. While local sensitivity analysis focuses on the variation of an input factor

around a specific value, global sensitivity analysis extends the considered variation to the entire space of variability (Pianosi *et al.*, 2016). Input parameter values can be varied one at a time (OAT) or altered simultaneously (All-At-a-Time or AAT). The sensitivity analysis applied in this study follows the procedures proposed by Campolongo *et al.* (2011) and is henceforth described. The parameters tested on its relative importance are provided in Table 2. A total number of 14 parameters was included in the sensitivity analysis, some of which were already introduced in Table 1 and section 5.2.

Table 2: Parameters included in the sensitivity analysis with specific parameter ranges.

Parameter	Parameter range	Explanation
Area	0.2 − 1 [ha]	Simulation area
MaxHMean	20 − 50 [m]	Mean maximum tree height
MaxHSd	0 − 5 [m]	Standard deviation of MaxH
MaxHpMean	0.0085 − 0.04	Mean pace of height increment
MaxHpSd	0.0001 − 0.001	Standard deviation of MaxHp
potDMean	0.33 − 1	Mean potential diameter increment
potDSd	0.0001 − 0.01	Standard deviation potD
MortIndexMean	0.5 − 0.99	Mean mortality index
MortIndexSd	0.001 − 0.05	Standard deviation mortality index
minCrown	10 − 20	Minimum crown point number
CanopyPACL	0.1 − 10 [m]	Height difference for PACL computation
minPACL	0.01 − 0.05	Minimum PACL for trees
VisionCone	20 − 90 [°]	Vision cone angle
Regenerate	1 − 10	Number of saplings per mature tree

The model output is characterized by a number of indices that inform about the structure of the simulated forest. There are six indices used to quantify the model output differences:

71

1. the basal tree diameter [cm]

2. the stem number per hectare

3. the Clark-Evans index, which informs about the regularity or irregularity of stem foot positions

4. the Crown Shift Index (CSI), which informs about the regularity of crown centroids compared to stem foot positions

5. the Structural Complexity Index (SCI), which informs about the amount of horizontal and vertical forest structure

6. the Shannon-Weaver index (SI), which informs about the vertical forest structure.

The basal tree diameter D_g is calculated as the quadratic mean diameter of all trees in the simulated forest stand:

$$D_g = 2 * \sqrt{\frac{g}{\pi}} \tag{13}$$

where g is the average tree basal area at 1.3 m above ground.

The stem number per hectare is simply the ratio between stem number and simulation area.

The horizontal forest structure was analyzed with the Clark-Evans aggregations index R. The Clark-Evans aggregation Index R (Clark & Evans, 1954) was calculated for stem foot points with the package spatstat (Baddeley *et al.*, 2018) to describe the horizontal forest structure. The edge correction according to Donnelly *et al.* (1978) was used for the calculation of the theoretically expected value for the mean nearest neighbor distance under a Poisson process. Clark-Evans R is defined as the ratio between the distance of a point to its nearest neighbor r_A and the mean expected value of a randomly distributed population r_E.

$$R = \frac{r_A}{r_E} \tag{14}$$

Clark-Evans indices greater than 1 indicate a regular point distribution. Values below 1 indicate point aggregation.

The spatial point patterns of stem foot points and crown centroids were analyzed with Besag's transformation (Besag, 1977) of Ripley's K-function (Ripley, 1976). The crown centroid is the center of gravity of the horizontal crown projection that forms a polygon of n crown points (see Fig. 16).
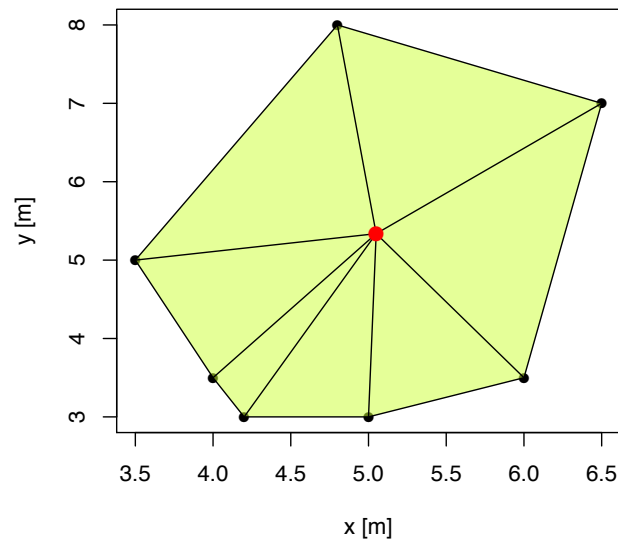
Figure 16: Crown projection area with the crown centroid (red dot) and crown points (black dots). The center of gravity of this polygon is calculated as the mean of the gravity centers of the triangles in which the polygon can be split, weighted by the respective triangle area.

The center of gravity of this polygon is calculated as the mean of the gravity centers of the triangles in which the polygon can be split, weighted by the respective triangle area. Crown centroid calculation was performed with the R-packages rgeos (Bivand & Rundel, 2017) and sp (Pebesma & Bivand, 2005). Besag's transformation of Ripley's K-function was calculated with

the R-package ads (Pelissier & Goreaud, 2015) and is defined as:

$$L(r) = \sqrt{\frac{K(r)}{\pi}} \tag{15}$$

where $K(r)$ is Ripley's K-function and $L(r)$ is Besag's transformation. $L(r)$ is calculated for a set of sample radii from 0 m to 10 m in 0.1 m intervals. $L(r)$ values were calculated for comparison with empirical data and for the calculation of the CSI-index. The CSI is a measure of the enhanced regularity of the crown centroids compared to the stem foot positions, which is a result of the horizontal crown displacement (see Fig. 17).
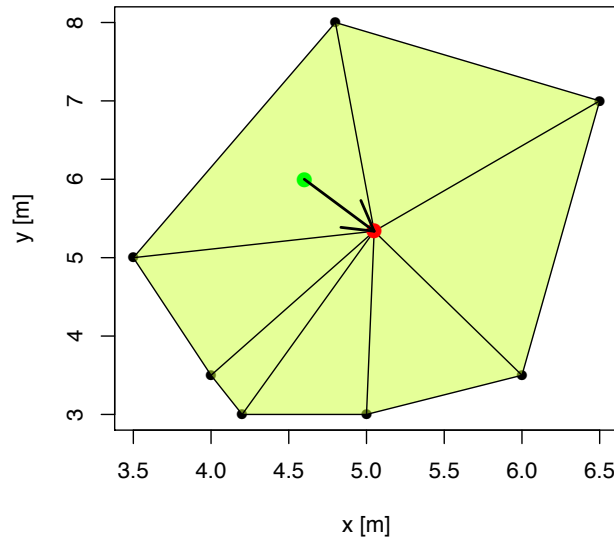
Figure 17: Crown displacement (black arrow) as the horizontal distance between the stem foot point (green dot) and the crown centroid (red dot).

For CSI computation, all radii r were subtracted from the $L(r)$ values, which yielded negative $L(r) - r$ values. The CSI was calculated as the difference between the centroid and stem area under the curve (AUC) which was calculated from the negative $L(r) - r$ values for sample radii ranging from 0 m to 10 m in 0.1 m intervals. The AUC is the area under the curve

74

for all $L(r) - r$ values less than zero (see Fig. 18). If the centroid's AUC is greater than the AUC of the stem foot points, the CSI is positive and the centroids are more regularly distributed.

CSI Calculation
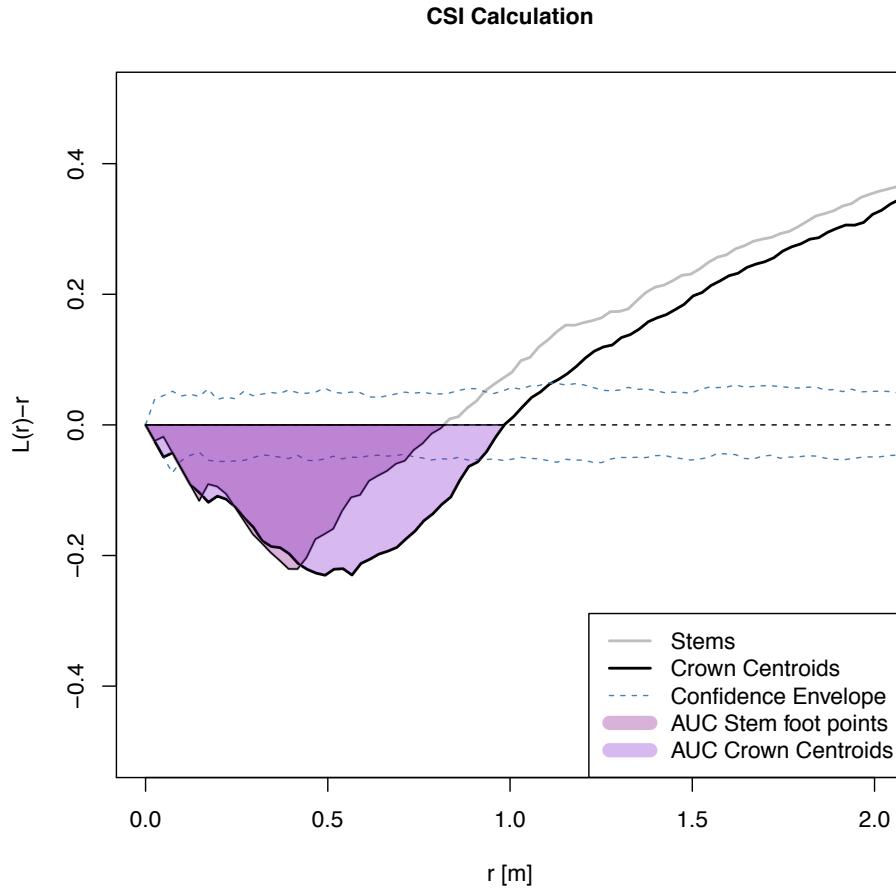
Figure 18: The difference between the areas under the curve (AUC) calculated from the negative $L(r) - r$ of the crown centroids and the AUC calculated from the negative $L(r) - r$ of the stem foot points was used as the Crown-Shift-Index CSI that quantifies the enhanced regularity of crown centroids due to crown displacement. Positive CSI values indicate an enhanced regularity.

The vertical forest structure was analyzed with the Shannon index (McArthur & McArthur, 1961) which was calculated over a set of 11 height classes H ranging from 0 m to 55 m, each of which is characterized by a height of 5

m.

$$SI = -\sum_{i=1}^{H} p_i \ln p_i \tag{16}$$

where p_i describes the relative abundance of a particular height class I, which is the number of trees in a particular height class divided by the total number of trees. The greater the SI values, the greater is the vertical structure of the forest.

The Structural-Complexity-Index SCI (Zenner & Hibbs, 2000) was calculated to describe the horizontal and vertical forest structure in one measure. First, a x-y spatial point data set of stem foot points was triangulated with the R-package deldir (Turner, 2018), which gave a network of non-overlapping triangles. Second, every vertex was assigned a z-coordinate given by the particular tree height. This second step yielded a three-dimensional surface of triangles covering the forest heterogeneity both in the horizontal and in the vertical direction (Fig. 19). Third, the SCI was gained by dividing the sum of all surface triangle areas through the sum of the projected triangle areas. The SCI value is, thus, a measure of forest rugosity. The greater the SCI values, the greater is the forest structure described by the index.
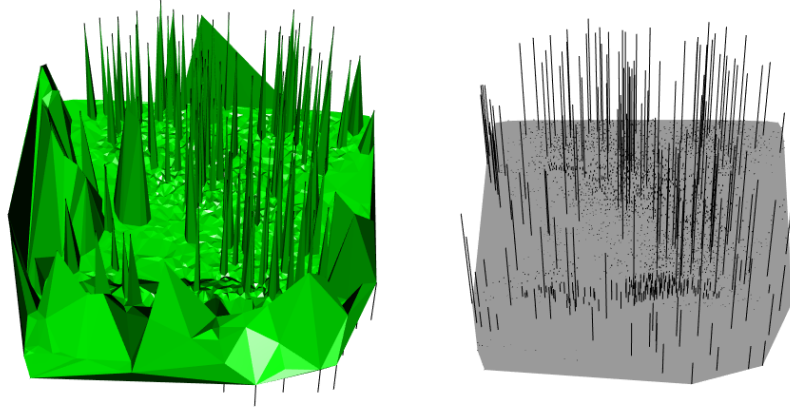
Figure 19: The Structural Complexity Index (SCI) as a measure of the forest rugosity is calculated by dividing the sum of all surface triangle areas (green) through the sum of the projected triangle areas (grey). Black lines show the stem axes of the trees. The displayed forest structure is drawn from one simulation run at time step 1000.

Campolongo *et al.* (2011) proposed a radial sampling design for drawing parameter values for the computation of sensitivity indices. Hereby, starting from a random point in the hyperspace of the input factors (see Table 2), one step is done for each factor where the particular parameter values are varied. This procedure is known as a One-At-a-Time (OAT) approach. This radial sampling (Saltelli *et al.*, 2010) was found to be superior compared to the method of Morris (Morris, 1991). A total number of 10 parameter values was equally drawn out of every parameter range specified in Table 2. Parameter values were drawn according to quasi-random Sobol-number sequences (Sobol *et al.*, 1976) for every parameter, which ensures an efficient exploration of the parameter hyperspace. This procedure was the basis for a model screening which aims at identifying the non-influential factors in a model using only a small number of model evaluations. Here, the elementary effect method is used, where factors are varied according to an OAT approach. So called elementary effects are computed which define the

ratio between the change in model output y and the parameter step Δ_i in the input domain. Unlike classical sampling strategies, a radial design computes elementary effects i over different parameter step sizes (x_i^u - x_i^v), where u and v denote two points along the sampling trajectory for the factor k in the input parameter hyperspace. The elementary effect EE_i is computed by:

$$EE_i = \left| \frac{y(x_i^{(u)} x_{\sim i}^{(u)}) - y(x_i^{(v)} x_{\sim i}^{(u)})}{x_i^{(u)} - x_i^{(v)}} \right| \tag{17}$$

where x_i is the focused parameter at the point u in the hyperspace and $x_{\sim i}$ denote all other parameters fixed at the same point. The screening test μ is then computed as the average of all elementary effects for the factor k, which yields the relative factor importance μ_k. This screening experiment allows a first insight into the model behavior. Further, detecting factor interactions is of key importance, which can be assessed using variance-based sensitivity measures that measure first-order effects and interactions of any order. As recommended by Campolongo et $al.$ (2011), the global sensitivity index ST is computed according to Jansen et $al.$ (1999):

$$ST = \frac{1}{2r} \sum_{j=1}^{r} (y(a_1^{(j)}, a_2^{(j)}, ..., a_k^{(j)}) - y(a_1^{(j)}, a_2^{(j)}, ..., b_i^{(j)}, ..., a_k^{(j)}))^2 \tag{18}$$

where a and b are two points along the trajectory of factor k and r is the number of steps taken in the parameter hyperspace.

For comparison purposes, the factor step sizes were standardized by their respective parameter range, the model output differences were standardized by their observed range in the experiment. The BEEP model was initialized as in section 5.2.5 and run for 200 time steps. This time span was chosen to allow beech regeneration to establish and old trees to die, which impacts the resulting forest structure and, hence, the model output indices described above. For the screening experiment, a total number of 5 steps in the hyperspace were accomplished accounting to 70 simulations using the radial sampling design. For the total sensitivity indices ST, 9 steps and 126 simulations were used for calculation.
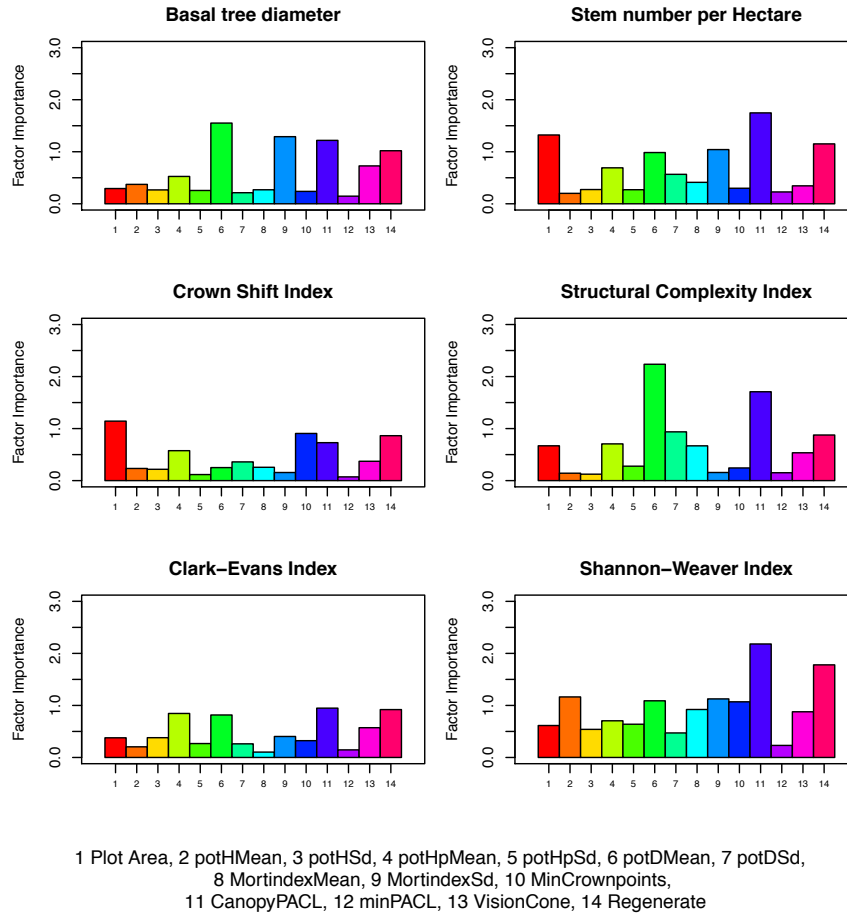
Figure 20: Factor importances for model output indices. The factor importance shows the relative importance of a specific parameter that impacts the model output.

The screening experiment (Fig. 20) shows that the sensitivity of the Crown-Shift-Index CSI and Clark-Evans Index is much less than the sensitivity for the other model output indices. Of major importance are the factors CanopyPACL and MinCrownpoints that impact tree crown space competition as well as the mortality index which specifies when trees die. Further, the simulation area and the number of saplings that every mature tree produces (Regenerate) impacts almost all model output indices. Although not being connected with the structural indices, the factors pot-

79

DMean and potDSd seem to have a great impact. A possible explanation is the diameter threshold that is used to classify trees for being established and, hence, included in the index calculation. Against expectations, the factors influencing height and crown growth, MaxH and MaxHp, seem to be of minor importance. The angle of the vision cone that impacts the identification of neighboring crown points as well as the minimum PACL that a tree must receive to persist are of minor importance.

1 Plot Area, 2 potHMean, 3 potHSd, 4 potHpMean, 5 potHpSd, 6 potDMean, 7 potDSd,
8 MortindexMean, 9 MortindexSd, 10 MinCrownpoints,
11 CanopyPACL, 12 minPACL, 13 VisionCone, 14 Regenerate
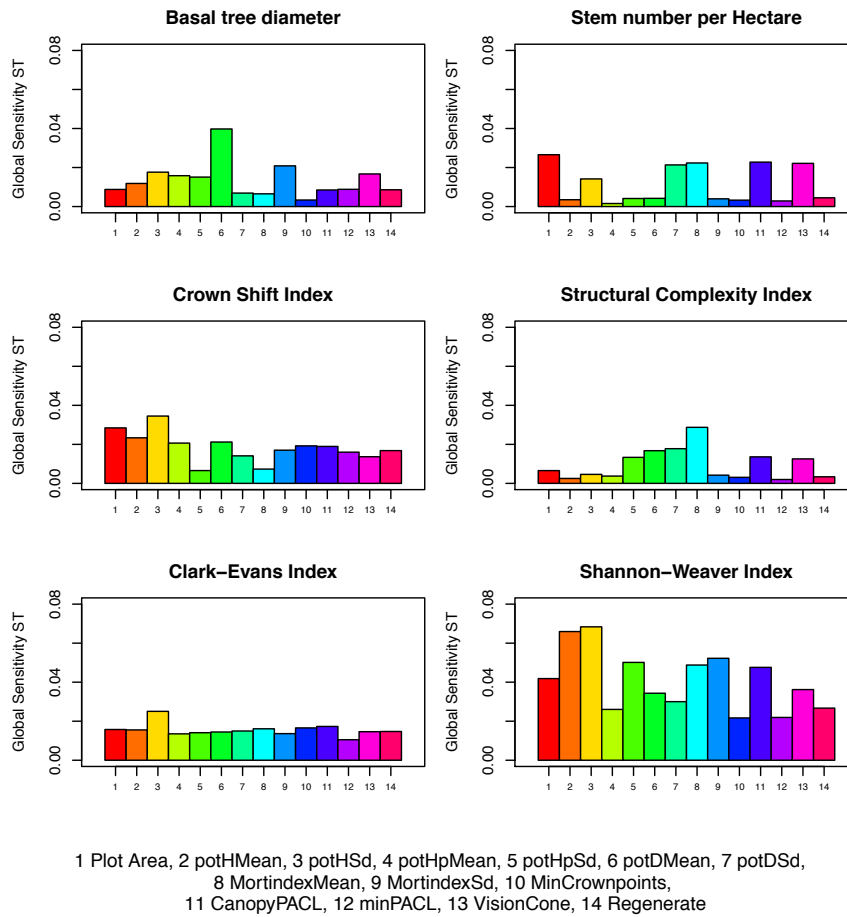
Figure 21: The global sensitivity index for model output indices. The global sensitivity index ST measures the total order sensitivity of a factor including factor interactions.

A different perspective reveals the global sensitivity index *ST*. Here, the

sensitivity of the basal tree diameter and Clark-Evans index is much less than the sensitivity of all other model output indices. The Crown-Shift-Index CSI and the Shannon-Weaver Index SI are now much more sensitive to changes in the parameter MaxHMean and MaxHSd that alter the height and crown growth of the trees. The mortality index, the CanopyPACL, and the parameters potDMean and potDSd still have a great impact on the stem number per hectare, the Structural Complexity Index SCI and the Shannon-Weaver Index SI. Surprisingly, the parameter VisionCone now has a stronger impact on the stem number per hectare, the SCI and the SI, while the effect of the sapling number per mature tree is lower than in the screening experiment.

The differences between the screening experiment and the global sensitivity measures shows a considerable amount of interaction between the parameters that impacts the model output. As a result of the sensitivity analysis, the parameter value for the CanopyPACL, which alters the minimum height difference in the radiation submodel, was set to zero, so that every tree greater than the focal tree is identified as potential competitor for PAR. The parameter VisionCone was set to an opening angle of 60 ° as described in section 5.2.10 in order to achieve maximum crown point detection and to avoid artificial canopy gaps due to large opening angles. The parameters Regenerate, minCrown, and minPACL were set to their values according to field observations and crown model structures presented in section 5.2.7 and 5.2.10, respectively. The parameters for the mortality index MortIndexMean and MortIndexSd were set to the values given in section 5.2.9 that enable irregular mortality between 75 and 98 % of a tree's potential height. As MortIndexMean and MortIndexSD are based on assumptions, the exact simulation results must be treated with care.

The sensitive parameters were calibrated with inventory data gained from the Schattiner Zuschlag (section 5.5).

5.4 Model parameterization

Inventory data from the 'Schattiner Zuschlag' from the years 1992, 2003, and 2013 was used to parameterize the height-age relationship. First, only inventory plots of pure beech forest were extracted. Second, maximum heights for every tree age were used to fit a potential height growth relationship by applying the Chapman-Richards equation:

$$H = MaxH * (1 - e^{-MaxHp*age})^c \tag{19}$$

where H is the tree height, $MaxH$ is the maximum potential tree height, and $MaxHp$ alters the pace of height increment. As observed tree heights over tree ages are considerably influenced by competition for PAR, competition effects must be excluded by only considering maximum observed heights for every tree age. This was achieved by extracting those observed tree heights that were greater or equal than the 95 % quantile of the heights for every age. To cover the range of observed maximum heights in Fig. 22, the maximum observed tree height of 48.6 m was set as parameter $MaxH$. Parameter c was set to 2 and parameter $MaxHp$ was varied from 0.0085 to 0.04. The resulting height-age relationships are shown in Fig. 22.
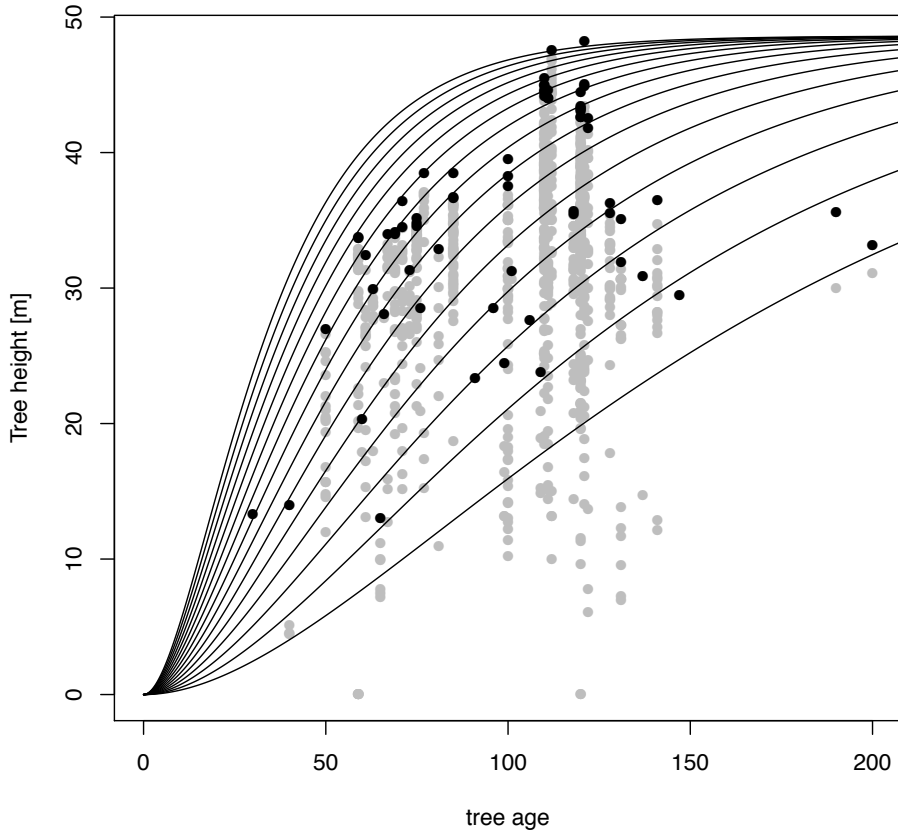
Figure 22: Tree height-age relationships fitted to observed maximum tree heights (black dots) at every tree age. Grey dots denote the raw height measurements for the respective tree age. The relationships span over the range of parameter MaxHp varied from 0.0085 to 0.04 in eqn. 19.

The parameters MaxHSd (standard deviation of MaxH at the initialization), MaxHpMean (average MaxHp at the initialization), and MaxHpSd (standard deviation of MaxHp at the initialization) were further calibrated (section 5.5).

The observed data from Schattiner Zuschlag, Langula, and Farbikschleichach was used to parameterize the relationship between tree diameter DBH and crown projection area cpa. Fig. 23 shows the observed crown pro-

jection areas calculated from the measured crown radii [m] at those sites. The relationship was parameterized with a maximum diameter $MaxD$ of 150 cm and i of 0.0026 using again the Chapman-Richards function.

$$DBH = MaxD * (1 - e^{-i*cpa})^{potD} \tag{20}$$

Fig. 23 shows the fitted range of relationships for varying values of the parameter potD from 0.33 to 1.1. The parameter potD was set to its average of 0.7. In the initialization (section 5.2.5), a tree is assigned the potD value drawn from a normal distribution with mean 0.7 and a standard deviation of 0.1, which ensures that relationships between diameter at breast height and crown projection area, in other words crown efficiencies, can vary over the observed range. The parameter potD is no subject to further calibration, as the crown efficiency (Fichtner *et al.*, 2013) is driven by tree internal physiological processes that are not accounted for in the BEEP model and, thus, treated as stochastic.
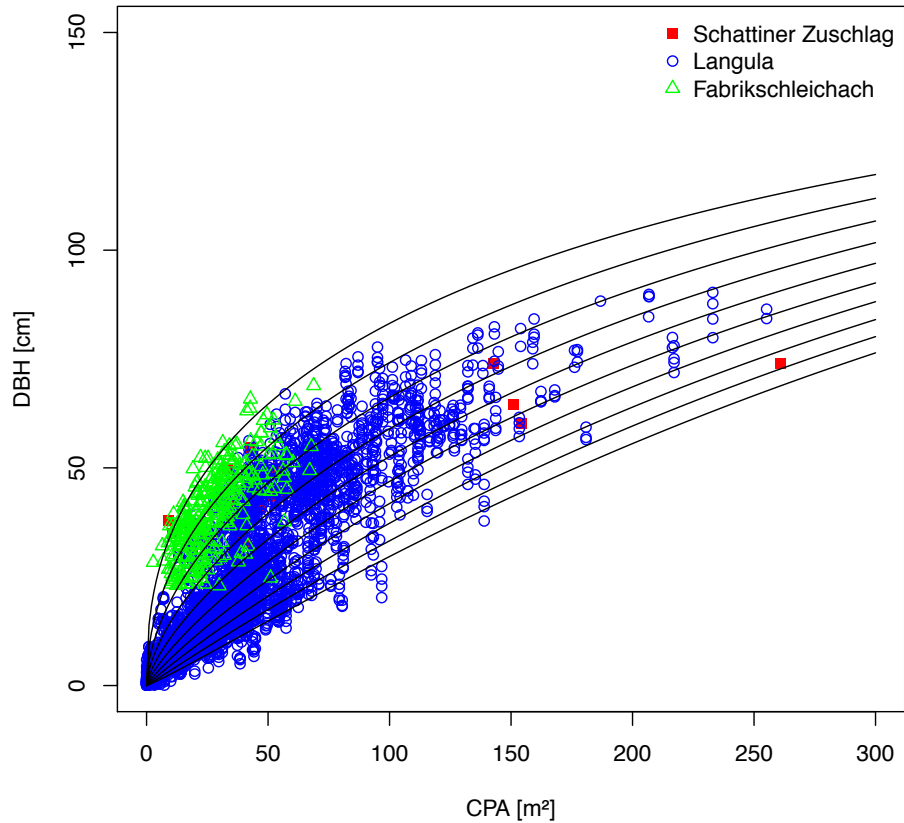
Figure 23: Relationships between observed tree diameters (DBH) and crown projection areas (CPA) for three different sites located at Schattiner Zuschlag, Langula, and Fabrikschleichach. The relationships are varied according to the parameter potD ranging from 0.33 to 1.1 in eqn. 20.

5.5 Model calibration

Calibration was accomplished for the standard deviation with which the parameter MaxH is initialized, while the mean value of 48.6 m for MaxH (maximum tree height) is derived from inventory data from the Schattiner Zuschlag (section 4.1.1). For the parameter MaxHp that alters the pace of height increment both mean and standard deviations were subject to

calibration. In order to find the best parameter combination, the model results are compared against a set of empirical parameters.

Based on the inventory data from the Schattiner Zuschlag, pure beech stands with age ranges between 100 and 130 years were selected and following parameters extracted: the stand basal area [m^2/ha], the stem number per ha, and the average tree height. The selected age range is based on the average age of all inventory plots in 2013 (Fig. 2), which is 120. The range of average plot heights and the basal areas over the stem number per hectare is displayed in Fig. 24. As the median average plot height is 32.5 m, this value is used for calibration as average tree height at age 120. Further, calibration assumes undisturbed forest development for which maximum stand basal areas can be assumed. Therefore, the stem number per hectare is set to 750 and the stand basal area to 66.6 m^2/ha (Fig. 24).
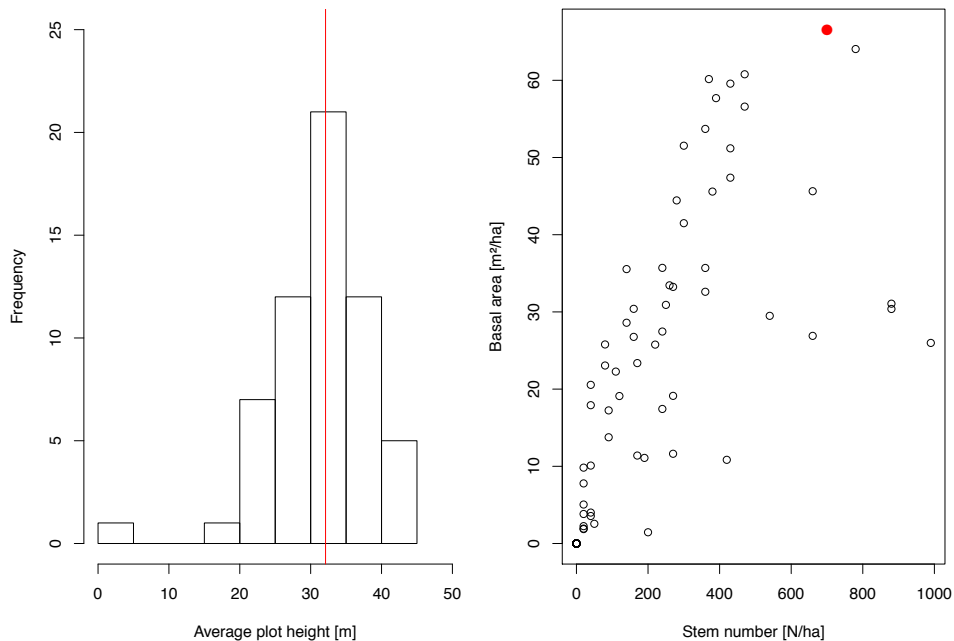
Figure 24: Frequency distribution of average plot heights (left) and stand basal areas dependent on stem numbers per hectare (right). The median average plot height is marked with a red line. The highest stand basal area is marked with a red dot.

Another parameter used for calibration is the slope of the self-thinning trajectory that describes the relationship between the number of living trees and tree size. For beech, this slope is reported as ranging from -1.723 to -2.244 for unmanaged beech forest stands in Germany (Pretzsch, 2006; Pretzsch & Mette, 2008; Condés *et al.*, 2017). For calibration, the average value of -2 was used.

The calibration was implemented using a full-factorial design, which means the full exploration of the possible parameter space spanned over the input parameters MaxHSd (standard deviation of MaxH), MaxHpMean (Mean of MaxHp), and MaxHpSd (standard deviation of MaxHp). One simulation was run for every unique parameter combination. Simulation were initialized as described in section 5.2.5 and run for 120 time steps. For every parameter MaxHSd, MaxHpMean, and MaxHpSd, the parameter ranges were split into six levels. MaxHSd ranged from 0.1 to 5, MaxHpMean ranged from 0.0085 to 0.04, and MaxHpSd ranged from 0.00001 to 0.0005. A total of 216 simulations were run and results for the self-thinning slope, the stand basal area, the stem number per hectare, and the average tree height were assessed based on their deviations from empirical values. The deviation D was computed from the simulation result for a simulated parameter r_s against the empirical parameter r_e with n being the number of test parameters:

$$D = \frac{\sum_{i=1}^{n} \left| \frac{r_s}{r_e} - 1 \right|}{n} \tag{21}$$

The simulation results with their unique parameter combinations were subsequently ranked based on their deviation D. The results revealed that the parameter ranges could be restricted for MaxHpMean between 0.015 and 0.018 and between 0.00019 and 0.00022 for MaxHpSd, as all other ranges increased the deviation. A second more detailed calibration run was accomplished with readjusted parameter levels. The parameter MaxHpMean was split into 10 levels for the adjusted range, while 5 levels were set for the

other parameters. The range for MaxHSd was kept between 0.1 and 5. A total of 250 simulation runs were conducted.

The results of the second calibration run showed good approximations of the empirical values (Table 3.)

Table 3: Simulated results for the best parameter combination and respective empirical values after calibration. Simulations were run for 120 time steps. Results are provided for time step 120. ST-slope denotes the slope of the self-thinning trajectory that describes the relationships between tree number and size.

Parameter	Simulated value	Empirical value
Basal area [m^2/ha]	60.7	66.6
Stem number [N/ha]	784	750
Average height [m]	37.2	32.5
ST-slope	-1.8	-2

The parameter MaxHSd was subsequently fixed at 0.1, the parameter MaxHpMean was set to 0.017 and the parameter MaxHpSd was set to 0.00022. A summary of parameterized, calibrated and estimated parameter values for the parameters examined in the sensitivity analysis is given in Table 4.

Table 4: Parameter values used for the BEEP model after calibration and parameterization.

Parameter	Parameter	Source
Area	0.5 ha	derived from Tabaku (2000)
MaxHMean	48.6 m	observed (section 4.1.1)
MaxHSd	0.1 m	calibrated
MaxHpMean	0.017	calibrated
MaxHpSd	0.00022	calibrated
potDMean	0.7	parameterized
potDSd	0.1	parameterized
MortIndexMean	0.94	estimated (section 5.2.9)
MortIndexSd	0.035	estimated (section 5.2.9)
minCrown	10	assumed for crown submodel
CanopyPACL	> 0	assumed for radiation submodel
minPACL	0.03	derived from Emborg (1998)
VisionCone	60 [°]	assumed for crown model
Regenerate	3	derived from Muck *et al.* (2009)

5.6 Model validation

Model validation aims at comparing model outputs with independent empirical data that was not used for parameterization or calibration (Schmolke *et al.*, 2010). Two submodels were validated against empirical data - the radiation submodel and the crown submodel. Deviations from empirical findings suggest that model routines need to be improved and re-implemented to enhance model accuracy. However, re-implementation of the crown growth model nested in BEEP could not be achieved yet due to missing long-term data with high resolution that enables a correction of the model routines and associated parameters.

5.6.1 Validation of the radiation submodel

Simulated percentages of above canopy light (PACL) under closed canopies and in gaps of varying size have been validated against results obtained from literature (section 4.2.2). A total of 10 simulation runs were performed for 100 time steps with initial stand conditions as described in section 5.2.5. At time step 100, the median PACL was calculated for 100 points on a grid with 1 m spacing located in the plot center on the ground for closed-canopy and gap conditions. Gaps were artificially created near the plot center by removing a number of canopy trees up to a maximum of 25 trees. The calculated median PACL was then related to the created gap size. Comparison between simulated and observed PACL values is provided in Fig. 25.
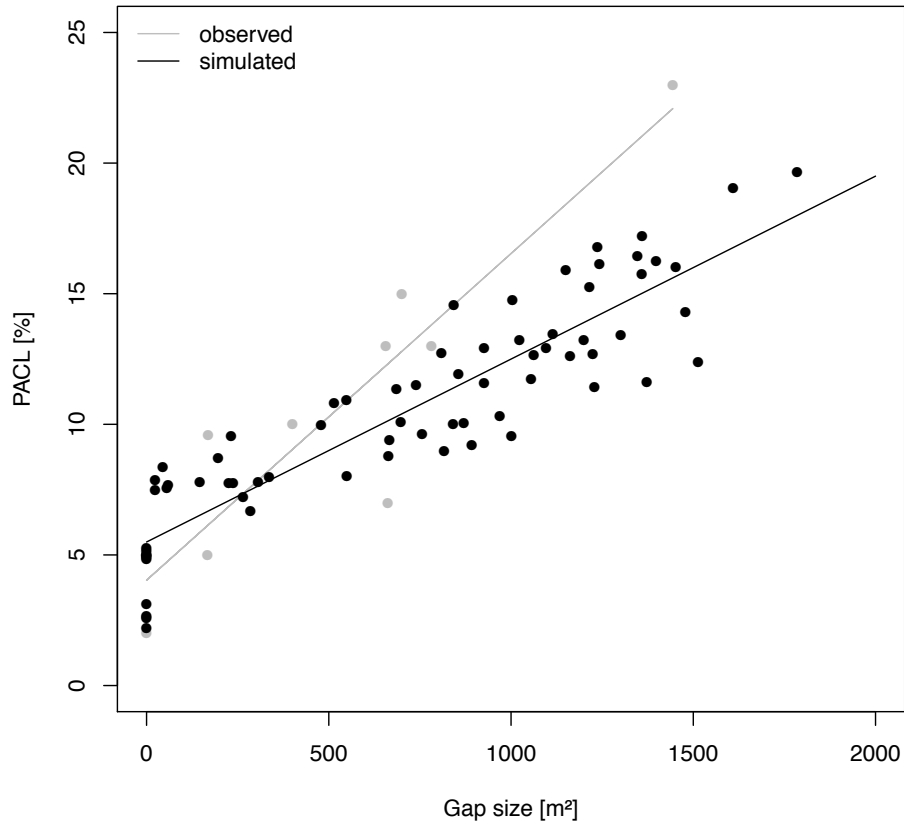
Figure 25: Empirical and simulated percentages of above canopy light (PACL) over gap size. The relationship between the empirical PACL values and gap sizes can be characterized by a linear model with R^2 of 0.82 and slope of 0.01. Simulated PACL values over gap sizes can be likewise characterized by a linear model with R^2 of 0.82, but different slope of 0.007.

The simulated PACL values grow less with gap size than observed. This difference may stem from highly variable PAR intensities found on different gap edges (Gálhidy *et al.*, 2006), but also from the small empirical sample size, especially for large gap sizes. No adjustments to the radiation submodel have consequently been made.

5.6.2 Validation of the crown model

The best data source to accomplish such a validation would be long-term crown growth data from near-natural beech forests. However, beech trees were analyzed only once using Terrestrial Laserscanning (TLS), which provided three-dimensional point-data from near-natural forests. This data cannot be used for validating predicted crown growth, but for validating the crown shape, proportions and dimensions, which enables inferences about the crown model used in BEEP. The data used for validation is described in section 4.2. The analysis focused on the following parameters: the crown volume, the crown length, the regularity of the crown shape, and the crown displacement. The analysis was carried out on 2293 simulated canopy trees (height greater than 20 m) from 10 simulations initialized as described in section 5.2.5. Simulations were run for 100 time steps in order to develop a closed forest canopy that is comparable to the measured forest plots at Schattiner Zuschlag. Statistical tests on significant differences were not conducted because of the possibility of arbitrary sample sizes that can be generated with simulations, which produces artificial high p-values (Fritz & Morris, 2012).
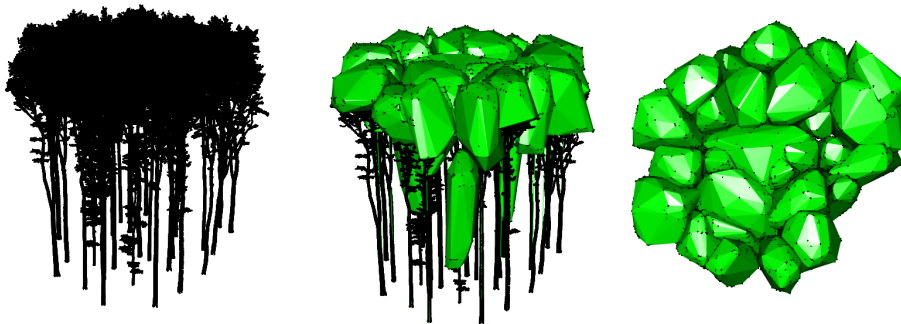
Figure 26: TLS-Point Data showing a group of canopy trees grown in the Schattiner Zuschlag, Lübeck, North-Germany. Green facets show the modeled BEEP-crowns on the 3D-point data for comparison.

To compare the empirical crown data with the simulated crowns from the BEEP model, BEEP-crowns were modeled on the 3D-point data derived from the plot scans (Fig. 26). The crown volume and the crown length relate to the upper crown above the height of the greatest crown width (green facets in Fig. 26). The crown displacement is defined as the horizontal distance between the stem foot point and the crown centroid, which is defined as the center of gravity of the respective crown projection area. The regularity of the crown shape was measured as the deviations of the crown vector lengths from their mean value. In particular, the deviation of the crown projection area from a perfect circle was specified as the circle deviation, which is the average difference between a particular crown vector length and the mean of all vector lengths (see Fig. 27). The vector lengths are specified for the crown vectors in x-y-direction. On the contrary, the deviations of the crown shape from a half-sphere was defined as the average difference of the 3D vector lengths from their mean value (see Fig. 27).
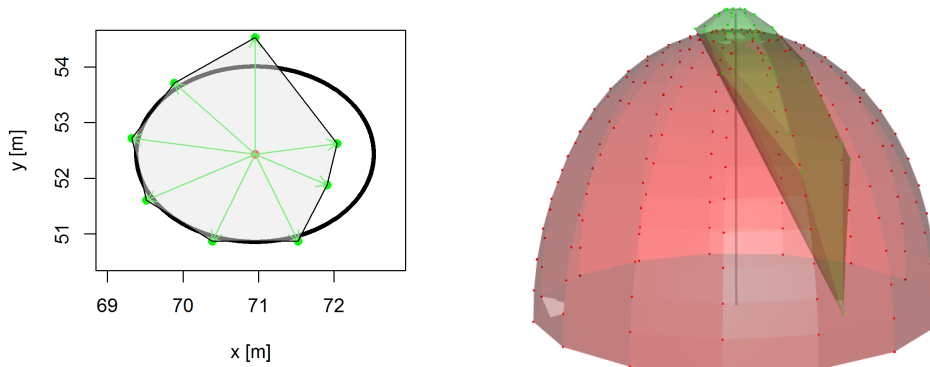
Figure 27: Deviations of the crown shape from a circle (left) and a half-sphere (right). Circle deviations are calculated from the differences between the crown vector lengths (green) and the mean vector length (black circle). Sphere deviations are calculated from the differences between the 3D crown vector lengths (vector tips lie on the green facets) and the mean vector lengths (vector tips lie on the red hemisphere).

93

The comparison in Fig. 28 shows that simulated crown lengths are much lower, which leads to smaller upper crown volumes. While empirical crown lengths and volumes follow almost a Gaussian distribution, the simulated distribution are highly skewed, which indicates irregularities in the crown simulation. Considering the mean circle deviation, both simulated and empirical values are very close, but high deviations within the simulated crowns occurred In contrast, empirical crowns show on average more deviations from a spherical shape, which may be based on the regular crown arrangement of the BEEP model. In terms of the crown displacement, simulated displacements exceed observed displacements by far.
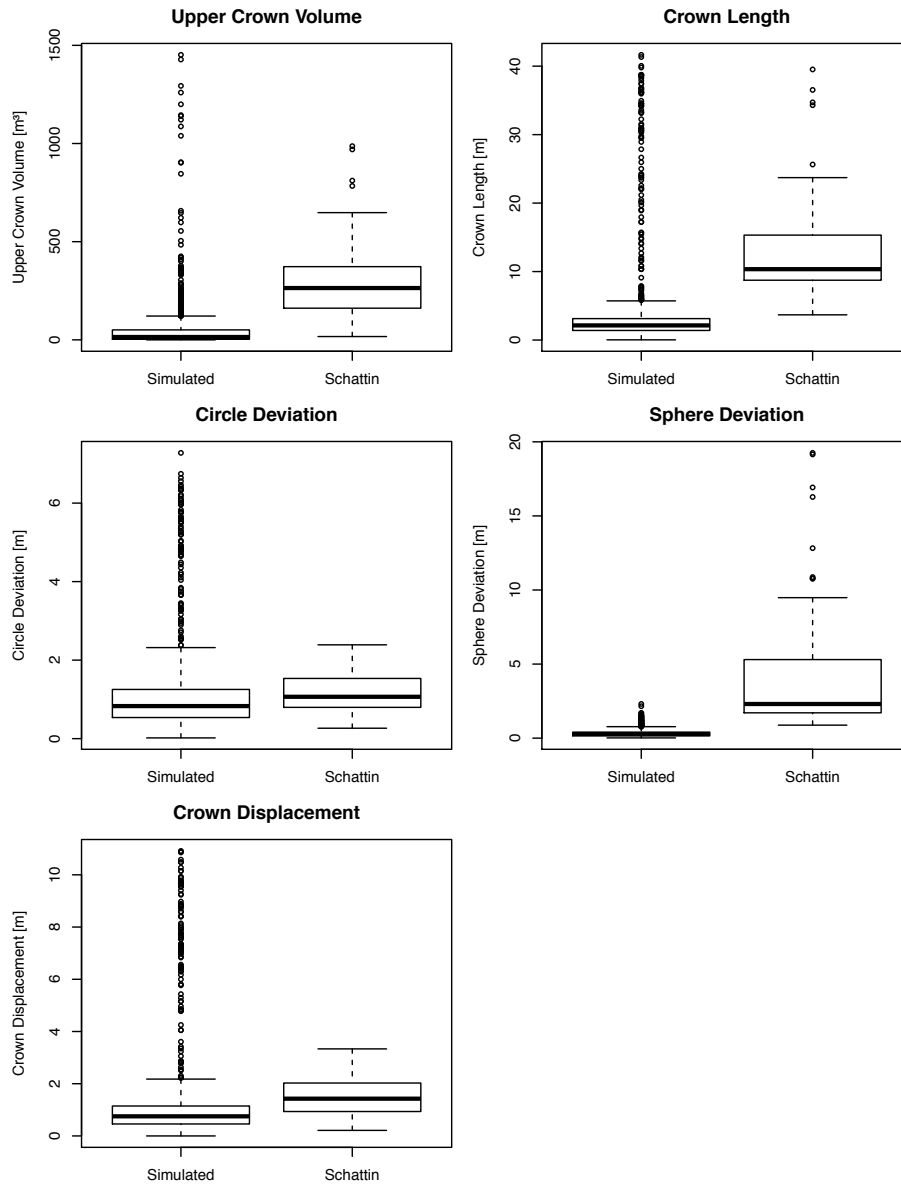
Figure 28: Comparison between simulated (Simulated) and empirical (Schattin) tree crown parameters: the upper crown volume, the crown length, the circle deviation, the sphere deviation, and the absolute crown displacement.

The presented results lead to the conclusion that the BEEP crown model is able to capture the horizontal crown plasticity, but show deficiencies in the vertical crown development, especially in modeling the crown depth

as well as in the magnitude of crown displacements. It can be assumed that the BEEP crown model is still too regular and the possibilities to occupy free crown space are constrained. Otherwise, the simulated crowns would be more irregular. These validation results constraint possible conclusions drawn from simulation results in this study and underpins the need to improve the crown model with multitemporal laserscanning data from near-natural beech forests.

6. Simulation experiments

In order to reveal the effects of plastic tree crowns on forest structure, it was necessary to create a modified model version with rotation-symmetric tree crowns. For analyzing the effect of selective thinning on forest structure, the BEEP model was enhanced with a model routine that implements thinning intervention. Simulations were conducted for every model version. Results between simulation experiments are compared in terms of the following measures:

1. the vertical forest structure assessed with the SI (section 5.3)

2. the horizontal and vertical forest structure assessed with the SCI (section 5.3)

3. the regularity or aggregateness of stem foot positions and crown centroids assessed with the Clark-Evans-index (section 5.3)

4. the amount of enhanced regularity of crown centroids compared to stem foot positions assessed with the CSI (section 5.3)

5. the age range of canopy trees taller than 20 m, which is the difference between maximum and minimum tree age

6. the diameter range of canopy trees taller than 20 m, which is the difference between maximum and minimum tree diameter

7. the number of development phases according to Tabaku (2000) (section 6.4)

Details on the simulation experiments are provided in the following.

6.1 Simulation with plastic tree crowns

The first model experiment aims at answering the question if the BEEP model reproduces observed patterns of near-natural beech forests, which are in particular:

1. a multi-layered vertical forest structure

2. a small-scale heterogeneous forest structure with a mosaic of developmental stages

3. a reversed-J-shaped or bimodal diameter distribution

4. a large age range of canopy trees of more than 100 years

5. varying spatial point patterns of stem foot positions which tend to be regular in the long run.

For the first experiment, 10 simulation runs were implemented with the BEEP model to account for model uncertainty. A higher number of simulation runs was not feasible due to computational constraints. The initial conditions for every simulation were held constant. Each simulation was run for 2000 time steps on an area of 0.5 ha. The simulation time was set to 2000 time steps to allow several tree generations to develop and the forest structure to emerge. Simulation stopped after 2000 time steps. Edge effects were reduced by truncating a boundary of 10 m from the edges and excluding the simulated individuals from analysis.

Four indices were calculated to describe the forest structural development over the simulation period: the Clark-Evans Index R, the Crown-Shift-Index (CSI), the Structural Complexity Index (SCI) as well as the

Shannon-Waever Index (SI). All indices were already introduced in the sensitivity analysis section 5.3. The simulated indices were compared to those calculated from empirical forest stands from unmanaged beech forests described in section 4.3. This comparison aimed not at reproducing the exact forest stands in terms of age and size distributions, but rather attempted to reveal whether the simulation model is able to reach the levels of empirical indices. Analysis was carried out for time steps $1000 - 2000$, while the first 1000 time steps were discarded to allow transient oscillations.

6.2 Simulation with rotation-symmetric tree crowns

The second experiment was specifically designed to answer the second research question concerning the effects of tree crown plasticity on the forest structure and dynamics. Similar to the first experiment with plastic tree crowns, 10 simulation runs were accomplished using the same initial conditions described in section 6.1. As the BEEP model already incorporates crown plasticity, a variation with rotation-symmetric tree crowns without any plasticity was implemented. Thus, the second simulation experiment aimed at a comparison between the original BEEP model and a modified version using rotation-symmetric crown shapes without plasticity. To achieve this comparison, the modified BEEP model contains slight changes in the height and crown growth submodel as well as in the mortality submodel. All changes were deliberately held small to reduce bias effects based on the model modification itself. Simulations with rotation-symmetric tree crowns were run under the same specifications as for the first simulation experiment with plastic tree crowns.

The modified model allows tree crown intersection. Trees do not loose crown points any more, which renders their crown shape always symmetric. However, the rotation-symmetric shape can change from spherical to paraboloidal due to reactions to varying levels of PACL. The amount of

crown intersection is used as a proxy for the competition strength that neighbor tree crowns exert. This competition strength weakens the crown growth for all crown vectors. Thus, competition effects from neighboring crowns lead to a symmetric competition response instead of a asymmetric (plastic) response in the original model. This concept has already been used in 2D zone-of-influence plant interaction models (Lin *et al.*, 2012).
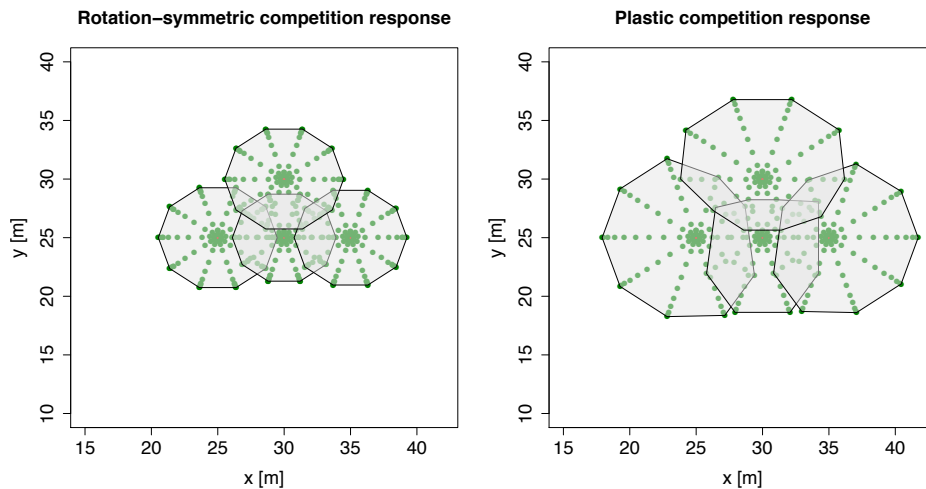
Figure 29: Comparison between rotation-symmetric and plastic competition response. Tree crowns are grown for 100 time steps. The rotation-symmetric response leads to smaller tree crowns because of competition affecting the growth of all crown vectors. Green dots show the crown points, grey polygons the respective crown projection area.

Fig. 29 shows the difference in crown shapes that occur after a simulation period of 100 time steps. Crown points, nevertheless, "sense" each other as in the original model, but in the modified version, the total number of crown points that encounter neighbor crown points in their vision cone is simply counted as C. This number is the proxy for the competition strength that neighbor crown exerts. If a particular tree is surrounded by more than three neighbors, its crown cannot extend a certain radius, because the crown growth is severely reduced. The reduction is achieved by an additional factor that influences the shoot reduction factor (see section 5.2.10). If more than

10 crown points detect neighbor crown points in their vision cone, the crown growth of the particular tree ceases, because it is assumed that the tree is surrounded from all directions. The number of 10 crown points is based on the regular crown point arrangement in layers. The reduction factor RF is calculated as

$$RF = -0.0008 * C + 0.0091 \tag{22}$$

where C is the number of crown points that detect neighbor crown points in their vision cone. Consequently, the shoot reduction factor SR from section 5.2.10 is reformulated as

$$SR = RF * PACL - 0.0091 \tag{23}$$

where $PACL$ is the Percentage of Above Canopy Light. Tree mortality is, hence, adapted. That is, trees do not die if their respective crown point number falls below 10, but if the difference between the point number and C falls below the threshold of 10. In other words, if less than 10 crown points detect no neighbor crown points in their vision cone, the tree is deleted. Simulation were initialized similarly to the simulation experiment with plastic tree crowns.

All other specifications from the submodels presented in section 5.2 experienced no changes.

6.3 Simulation with plastic tree crowns and selective thinning

The third simulation experiment aimed at answering the research question what effects does thinning have on forest structure and dynamics. A total number of 10 simulations runs with initial conditions described in section 6.1 were accomplished. The following hypotheses have been stated:

1. Tree crown plasticity causes crown centroids to be more regularly distributed than stem foot positions, while thinning causes the spatial patterns to be less regular.

2. Tree crown plasticity and thinning decrease the aboveground competition for crown space and PAR.

3. Tree crown plasticity enhances, thinning decreases the horizontal and vertical forest structural diversity.

4. Tree crown plasticity contributes to a small-scale heterogeneous forest structure, while thinning causes the forest structure to be less heterogeneous.

To test thinning effects, a new model routine with selective thinning intervention was implemented. This routine is based on the management concept of the forest district Lübeck (Sturm, 1993; Westphal *et al.*, 2004), where trees are harvested with a minimum diameter at breast height of 65 cm (target trees). As thinning intervention is not continuously implemented (Sturm, 1993; Westphal *et al.*, 2004), the model routine removes target trees every 5 time steps. It is assumed that thinning intervention does not damage neighbor trees surrounding the target tree and no skid trails are established which accounts for the low-interference management that the foresters of the forest district Lübeck apply. Simulations with plastic tree crowns and selective thinning were run under the same specifications as for the first experiment without selective thinning.

6.4 Assessing forest development phases

Forest dynamics cannot be directly measured, but it can be statically assessed in time and space (Münch, 1993) by defining development characteristics that can be summarized into phases (Leibundgut, 1959). Due to this discretization, the time of existence of a particular phase, its spatial extension, and phase orders can be characterized. Different approaches for classifying forest stands into different development phases have been conceived in order to avoid simple age classes, for example Leibundgut (1959)

and Meyer (1995). This study classifies development phases according to Tabaku (2000), who developed a new consistent classification scheme. The original classification had to be slightly changed due to missing dead wood calculations in the BEEP model. The classification is achieved on a raster field r of 156.25 m^2.

The scheme uses following measures for classification of a raster field:

1. the maximum diameter D_{max}

2. the ratio between the sum of tree crown projection areas and the raster area (crown projection cover CPC)

3. the ratio between the area covered by natural regeneration and the raster area (natural regeneration cover NRC)

4. the ratio between maximum tree height on a raster field and maximum possible tree height (H_{max})

5. the standardized quantile difference of the diameter distribution QUA_r

The area covered by natural regeneration on a raster field r was calculated as area of a convex hull of tree positions using the R package geometry. The standardized quantile difference for the diameter distribution QUA_r at a given raster field r was calculated as (Tabaku, 2000)

$$QUA_r = \frac{(Perc_{75} - Perc_{25})}{D_M} * 100 \qquad (24)$$

where $Perc_{75}$ and $Perc_{25}$ denote the 75 and 25 percentile of the diameter distribution, respectively, and D_M denotes the median diameter. Based on these criteria, Tabaku (2000) classified a gap phase, an initial phase, a regenerating phase, an early-optimum phase, a mid-optimum phase, a late-optimum phase, a terminal phase, a degradation phase, and a selective phase. The criteria used for classification is provided in Table 5.

Table 5: Classification criteria for development phases adopted from (Tabaku, 2000). D_{max} denotes the maximum diameter, CPC denotes the crown projection cover, NRC denotes the natural regeneration cover, H_{max} denotes the maximum tree height, and QUA_r denotes the standardized quantile difference of the diameter distribution.

Phase	D_{max}	CPC	NRC	H_{max}	QUA_r
Gap	–	< 0.3	< 0.5	–	–
Initial	< 20	> 0.3	–	–	–
Regenerating	< 20	–	> 0.5	–	–
Early-Optimum	20 − 40	> 0.3	–	< 0.85	
Mid-Optimum	> 40	> 0.3	–	< 0.85	< 100
Late-Optimum	> 60	> 0.3	–	< 0.85	< 100
Terminal	> 20	> 0.3		> 0.85	< 100
Degradation	> 60	> 0.3	< 0.5	–	–
Selective	–	–	–	> 0.85	> 100

The raster grid with which development phases are classified is fixed (Tabaku, 2000), which supports the risk of undetected phases. Therefore, raster search was implemented dynamically by systematically shifting a raster field over the simulated area in 0.1 m steps. This was done for simulated stands of time steps $1000 − 2000$. The number of detected unique phases was then compared between the simulations.

6.5 Testing differences between simulation results

The simulations carried out in this study produce time series data of large sample sizes of 20,000 observations for 10 simulation runs for one experiment. Testing on statistical significance between results is, therefore, absurd, because statistical power is determined by replication, which can be increased at any time by the experimenter. Further, the testable null hypothesis is not 'unknown' but obvious to the experimenter. This leads to the conclusion

that significance tests should not be applied alone under these circumstances (White *et al.*, 2013). Rather, effect size estimates (Fritz & Morris, 2012) provided in this study along with significance tests enable a assessment of the effects that different model variations of BEEP produce. Effects sizes are used to describe the magnitude of an effect compared to a control. For example, one part of a experimental group receives no medication (control), while another does receive a special treatment (effect group).

A multitude of possible effect size measures has been developed, while most of them are designed for normality assumptions, that is, the sample data needs to be normal and follow a Gaussian distribution. Normality has been tested for all simulation results with a Shapiro-Wilk-test (Sachs, 2004), which revealed non-normality. This led to the application of non-parametric tests and effect sizes. In order to test for differences between simulated series', the Mann-Whitney-Wilcoxon test (Sachs, 2004) was applied, which produced significant results because of the large sample sizes. In addition, the non-parametric effect size measure r was calculated based on z-values derived from the U test statistic of the Mann-Whitney-Wilcoxon test by (Cohen, 1988)

$$r = \frac{z}{\sqrt{N}} \tag{25}$$

where N is the sample size. According to Cohen (1988), a large effect size is greater or equal than 0.5, a medium effect 0.3, and a small effect 0.1.

Instead of the p-values derived from the Mann-Whitney-Wilcoxon test, effect sizes are provided for comparison between two series. Tests were performed between two simulation series, which were treated as independent samples. The simulation with plastic tree crowns was, thereby, treated as control, the simulation with rotation-symmetric tree crowns or plastic tree crowns with selective thinning application as variation. Thus, the effect sizes inform about the effect strength of a model variation relative to the BEEP model variant with plastic tree crowns without selective thinning.

7. Results

7.1 Simulation with plastic tree crowns

An example of the simulated forest at time step 1000 is shown in Fig. 30. The forest structure is multi-layered, while the canopy is interspersed with gaps in which regeneration has established. The average crown displacement for canopy trees taller than 20 m range between 0 and 11.5 m with the median 1 m. This median is lower than observed average crown displacements from near-natural beech forests of 1.95 m (Schröter *et al.*, 2012) and 1.5 m (Bulušek *et al.*, 2016). Maximum values of 11.5 m exceed plausible crown displacements by far, as the maximum observed crown radius is already 8 m (section 4.1.2), which indicates a need to constrain simulated crown growth.
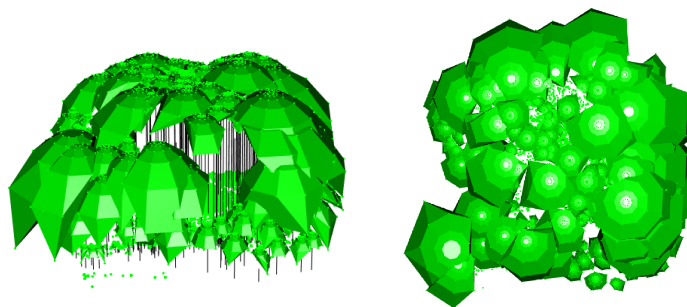
Figure 30: One simulated forest at time step 1000. The forest is shown from side (left) and top view (right). Green facets show the simulated crown surface area, black lines show the stem axes of the trees.

7.1.1 Forest structure in comparison to Serrahn beech forests

The SCI as a measure of forest rugosity informs about the amount of horizontal and vertical forest structure, while the SI informs about the vertical structure. The greater the SCI and SI values, the greater is the associated forest structure. The CSI informs about the enhanced regularity of crown centroids compared to stem foot positions, which is a result of the crown plasticity. The CSI in Fig. 31 was only calculated for canopy trees taller

105

than 20 m for comparison purposes. The development of the CSI values reveals very little fluctuations around zero. During the simulation, periods with positive and negative CSI alternate. The CSI ranges from -2.3 to 2.2. This is in stark contrast to the large positive values of Schröter *et al.* (2012) in (Fig. 31), which reveals considerably enhanced regularity of crown centroids compared to stem foot positions.

The SI shows considerable cyclic fluctuation, while the observed values of Schröter *et al.* (2012) are lower than the median simulated SI, which is likely caused by missing natural regeneration in the data set of Schröter *et al.* (2012) that artificially reduces the vertical forest structure assessed with the SI. The SCI likewise fluctuates to a considerable degree, but anti-cyclically to the SI. This can be explained with the calculations of both indices. The SI simply informs about the vertical forest structure over tree height classes. If the SI culminates, trees of all classes can be found on the simulated area, which reduces the forest rugosity, because maximum height differences between neighboring trees decrease. As forest rugosity depends on those maximum height differences between neighboring trees, the SCI culminates if trees can only be found in the lower and higher height classes, which in this case reduces the SI. Similar to the SI, the median SCI is higher than observed from Schröter *et al.* (2012), which can be again explained by the missing regeneration in the inventory data set.
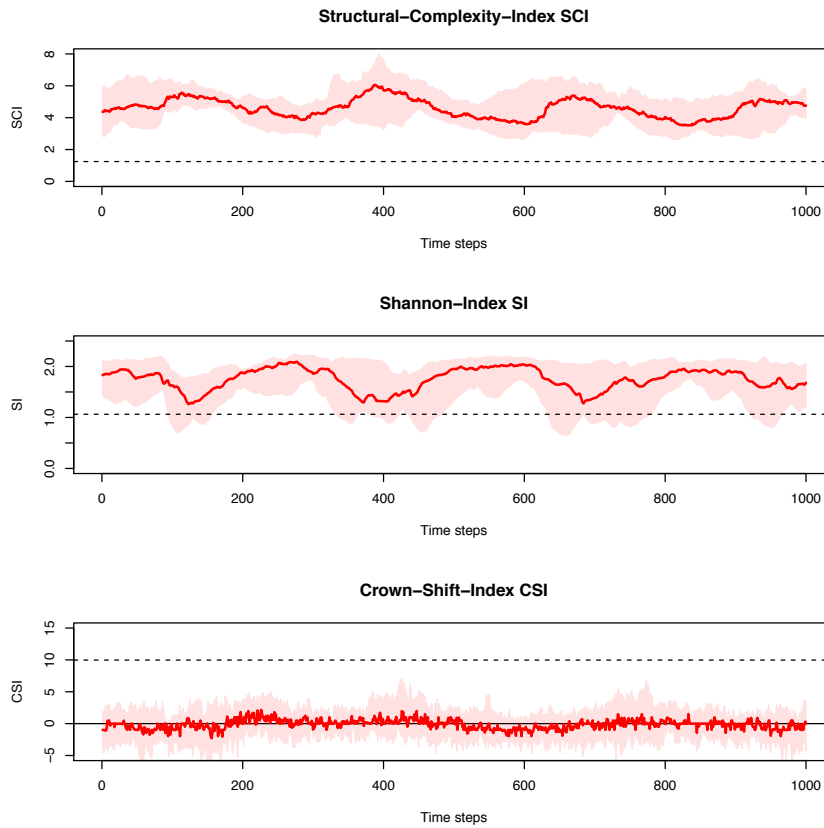
Figure 31: Forest structure in comparison to Serrahn beech forests. *SCI* and *SI* are calculated at the stand level for every time step. Bold red lines show the median over all simulated values, while the respective 95 % confidence envelopes are displayed in pale red. Black dashed lines show the indices calculated for a beech forest stand with trees of ages between 180 and 240 years near Serrahn, North-East Germany (Schröter *et al.*, 2012). Greater *SI* values indicate an enhanced vertical forest structure. Greater *SCI* values indicate an increased level of vertical and horizontal forest structure. Positive values of the Crown-Shift-Index *CSI* indicate crown centroids to be more regularly distributed than stem foot points.

7.1.2 Forest structure in comparison to Sudetes and Serrahn beech forests

Fig. 32 shows simulated Clark-Evans indices for stem foot positions in comparison to observations in old-growth beech forest in the Czech Republic

(Bílek *et al.*, 2011; Bulušek *et al.*, 2016) and North-East-Germany (Schröter *et al.*, 2012). K35 denotes a forest stand in the Krkonoše National Park, O7 is located in the Orlické hory Protected Landscape Area, and B8 is located in the Broumovsko Protected Landscape Area. The permanent research plots PRP 06 and PRP 07 are located in the Voděrady National Nature Reserve. The plot PAR S is located in the beech forests of Serrahn.

The simulated Clark-Evans indices show cyclic fluctuations. The median indices are always lower than 1 indicating a more aggregated spatial pattern of stem foot positions. All observed indices from different beech forests lie above the simulated median values. The indices of PRP 06, PRP 07, and PRP S are closer to the median simulated indices than those of K35, O7, and B8. Except for PRP 07, all observed indices are greater than 1 indicating regular stem foot position patterns. These levels of regularity could not be reached by simulations with plastic tree crowns.

Stem foot points tree layer
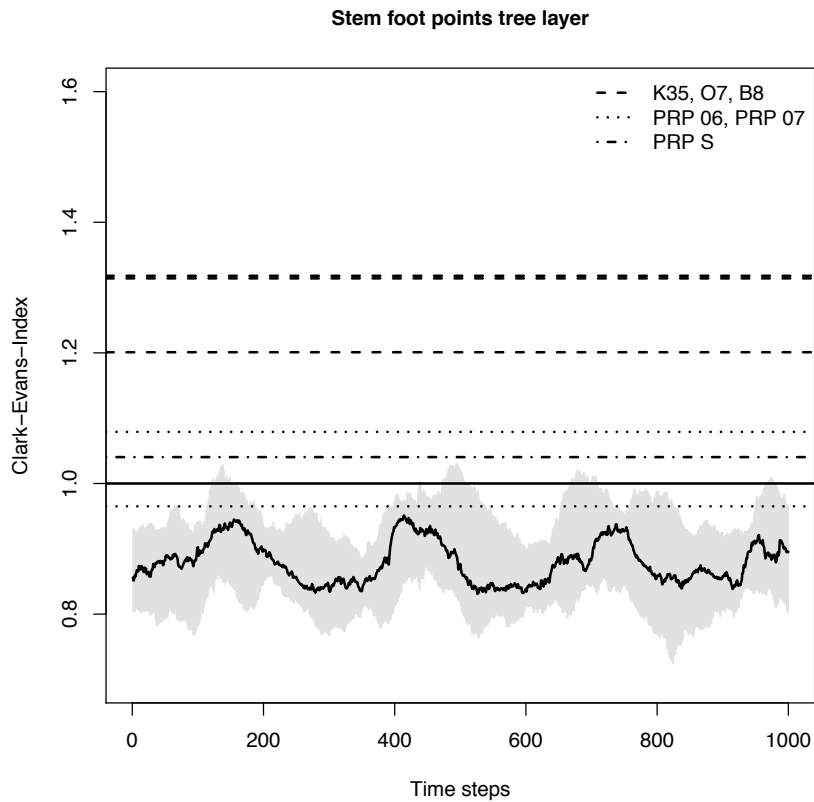
Figure 32: Stem foots spatial distribution in comparison to Sudetes and Serrahn beech forests. The black solid line show the median Clark-Evans indices for stem foot positions over all simulations together with the 95 % confidence envelopes in gray color. Black dashed lines show the indices for different beech forest stands located in the Krkonǒve National Park (K35), the Broumovsko (B8) and Orlické hory Protected Landscape Areas (O7) (Bulušek *et al.*, 2016), in Voděrady (PRP 06, PRP 07) (Bílek *et al.*, 2011), and in Serrahn (PRP S) (Schröter *et al.*, 2012). Clark-Evans indices greater than 1 show a regular point pattern, indices smaller than 1 show an aggregated point pattern. The simulated Clark-Evans indices do not reach the level of regularity of the empirical stem foot positions.

Fig. 33 shows simulated Clark-Evans indices for crown centroids again in comparison to observations from field sites described above. Simulated crown centroids show cyclic fluctuations that to a large part is lower than 1 indicating aggregated spatial point patterns, while some median values also

109

reach Clark-Evans indices above 1 indicating regularity. However, similarly to stem foot positions, observations from near-natural beech forests show enhanced regularity compared to simulated crown centroids. Thus, neither stem foot positions nor crown centroids reach the regularity of observed spatial patterns in near-natural beech forests.

Crown centroids tree layer
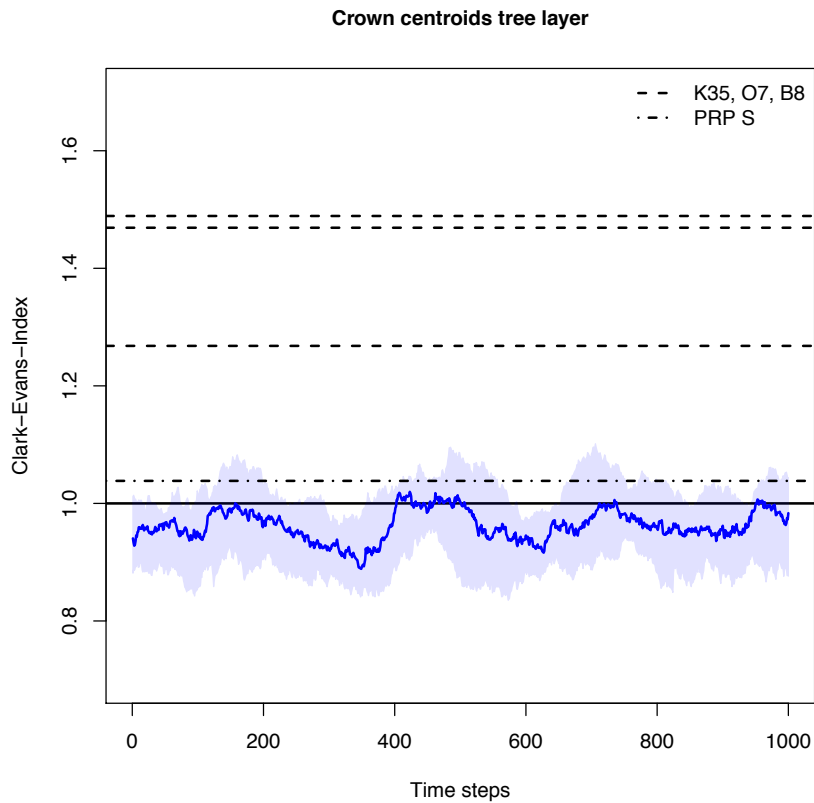
Figure 33: Crown centroids spatial distribution in comparison to Sudetes and Serrahn beech forests. The black solid line show the median Clark-Evans indices for crown centroids over all simulations together with the 95 % confidence envelopes in gray color. Black dashed lines show the indices for different beech forest stands located in the Krkonove National Park (K35), the Broumovsko (B8) and Orlické hory Protected Landscape Areas (O7) (Bulušek *et al.*, 2016), and in Serrahn (PRP S) (Schröter *et al.*, 2012). Clark-Evans indices greater than 1 indicate a regular point pattern, indices smaller than 1 indicate an aggregated point pattern. The simulated Clark-Evans indices do not reach the level of regularity of the empirical crown centroids.

7.1.3 Tree age ranges of canopy trees and diameter distributions

Fig. 34 shows the age range development for canopy trees taller than 20 m. The age range informs about the difference between the maximum and minimum tree age of canopy trees. Simulations with plastic tree crowns show that age ranges extend 100 years, while median ranges fluctuate between 200 and 350 years.

Figure 34: Age ranges for canopy trees taller than 20 m. The solid line shows the median over all simulations while the 95 % confidence envelopes are given in pale red.

Fig. 35 shows the diameter distributions of all time steps and simulations with plastic tree crowns. The reversed-J- shape is dominant, while a considerable number of large-diameter trees is also distinguishable.
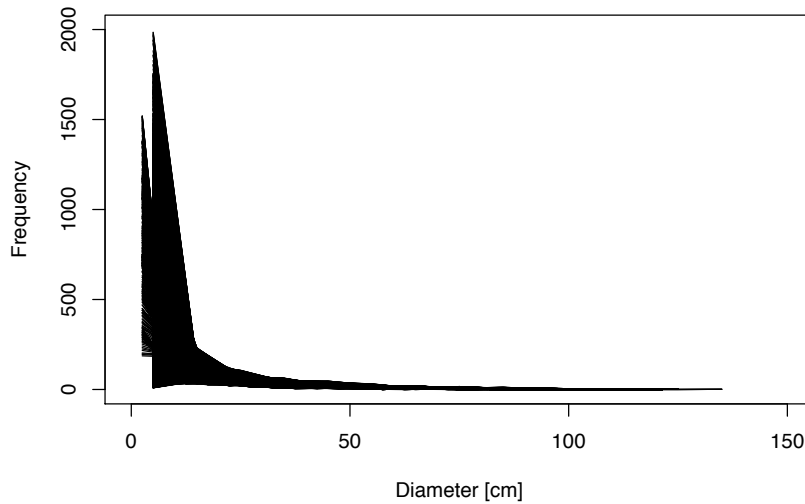
Figure 35: Diameter distributions of 10000 simulated forest stands from 10 simulation runs. The distributions show a dominant reversed-J-shape with a considerable number of large-diameter trees.

7.2 Simulation with plastic tree crowns, rotation-symmetric tree crowns and selective thinning in comparison

The following section deals with the simulation results of all three experiments in comparison. Simulations were run with plastic tree crowns, rotation-symmetric tree crowns as well as with plastic tree crowns and selective thinning. Differences between simulation results are described by means of the non-parametric effect size measure r (section 6.5).

7.2.1 Forest horizontal structure assessed with Clark-Evans-indices

Clark-Evans indices for stem foot positions have been calculated for all simulation runs shown in Fig. 36. Median simulated Clark-Evans indices are lower than 1 indicating aggregated stem foot positions.

Clark Evans indices stem foot positions
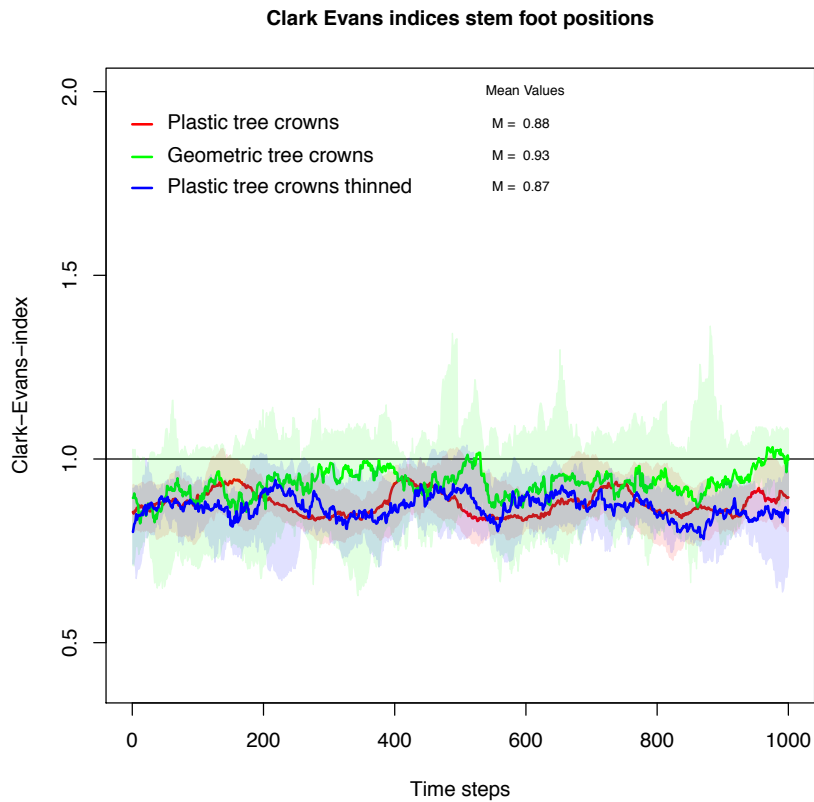
Figure 36: Clark-Evans indices computed for stem foot positions for all simulation experiments. 95 % confidence envelopes are given in the same color as the series for the median index values over all simulations (solid lines). Mean values (M) are given for every series. The effect size r between simulations with plastic tree crowns and selective thinning is 0.04, the effect size r between simulations with plastic tree crowns and rotation-symmetric tree crowns is 0.08. Both effect sizes indicate very small effects of model variation on Clark-Evans indices.

Average indices show very small differences between the series, which is supported by very small effect sizes of 0.04 for rotation-symmetric tree crowns and 0.08 for selective thinning. Fig. 37 shows the Clark-Evans indices computed for simulation with plastic tree crowns and simulations with selective thinning.

113
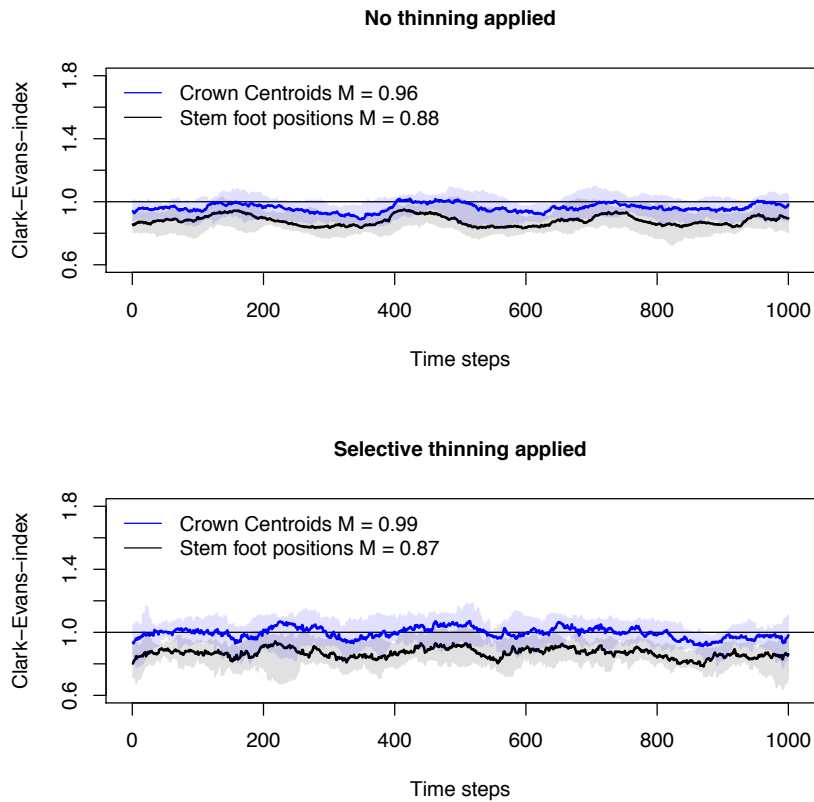
Figure 37: Clark-Evans indices computed for simulation with plastic tree crowns and selective thinning. Blue and black solid lines show the median values over all simulations for crown centroids and stem foot positions, respectively. 95 % confidence envelopes are given in the same colors. Crown centroids are more regularly distributed than stem foot positions. Mean values (M) are given for every series. Selective thinning has a very small effect size r of 0.04 on Clark-Evans indices of stem foot positions, but medium effect size r of 0.53 on Clark-Evans indices of crown centroids.

In both experiments, crown plasticity leads to a more regular distribution of crown centroids. Selective thinning had a very small effect size of 0.04 on the indices of stem foot positions, but medium effect size of 0.53 for crown centroids. Therefore, selective thinning influences the crown centroid distribution more than the stem foot positions. Under selective thinning application, average indices for crown centroids are 0.99 compared to 0.96.

114

Thus, thinning promotes the regularity of crown centroids to a small degree.

7.2.2 Forest vertical structure assessed with Shannon-Weaver indices

Fig. 38 shows the Shannon-Weaver indices for all simulation experiments. All series show large fluctuations over the simulation period. Highest average indices with 1.71 are reached by simulations with plastic tree crowns. Both rotation-symmetric tree crowns and selective thinning have very small effect sizes of 0.08 and 0.04 on the vertical forest structure assessed with the SI.
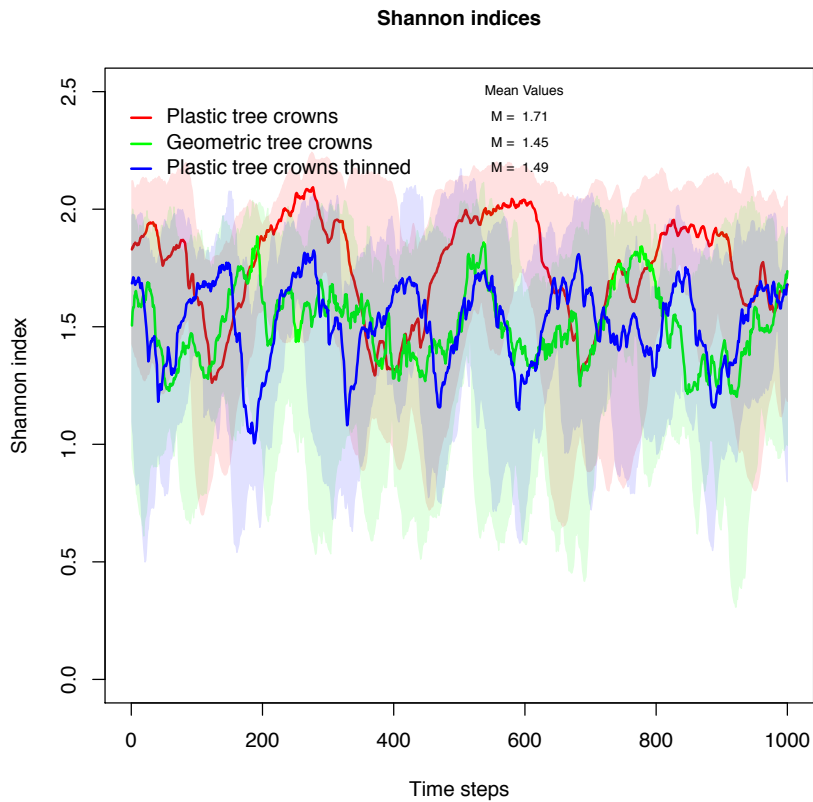
Figure 38: Shannon-Weaver indices (SI) for all simulations in comparison. The SI informs about the vertical forest structure. The greater its value, the greater is the associated vertical forest structure. 95 % confidence envelopes are given in the same color as the series for the median index values over all simulations (solid lines). Selective thinning and rotation-symmetric tree crowns have only small effect sizes r of 0.04 and 0.08 on the vertical forest structure.

7.2.3 Forest vertical and horizontal structure assessed with stand complexity indices

Fig. 39 shows the structural complexity indices for all simulation experiments. In contrast to Fig. 38, large differences between the experiments become observable. Both rotation-symmetric tree crowns and selective thinning have strong effects sizes of 0.85 and 0.86 on the SCI. Thinning and

116

rotation-symmetric tree crowns produced considerably lower horizontal and vertical forest structure assessed with the SCI as simulation with plastic tree crowns alone.

Structural complexity index
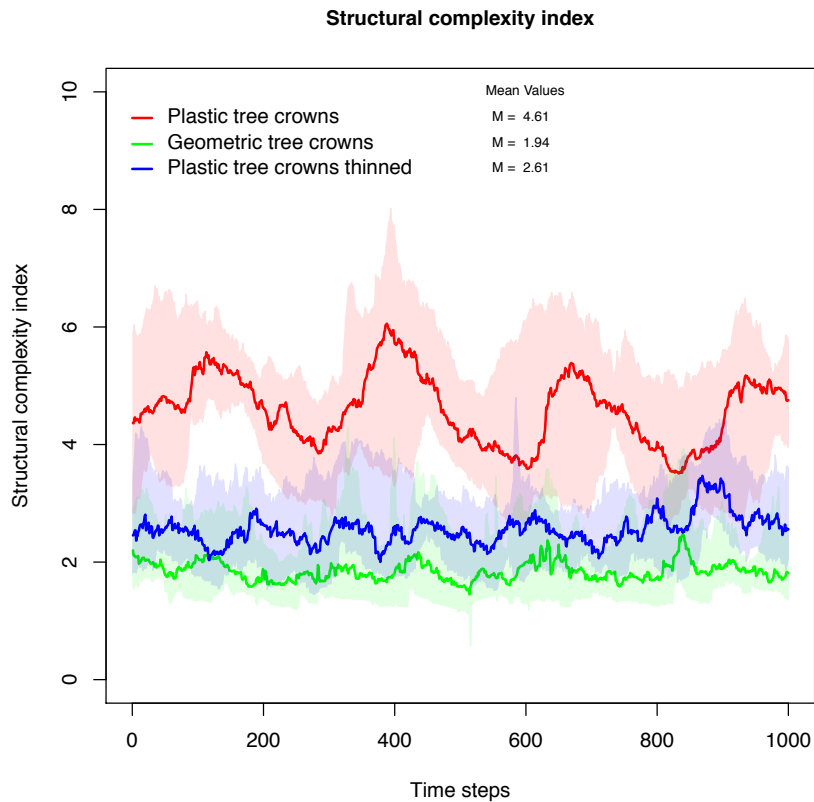
Figure 39: Structural complexity indices (SCI) of all simulation experiments in comparison. Solid lines display the median over all simulations, while 95 % confidence envelopes are given in the same color. Both selective thinning and rotation-symmetric tree crowns have strong effect sizes r of 0.85 and 0.86 on the horizontal and vertical forest structure assessed with the SCI.

7.2.4 Relative regularity of crown centroids compared to stem foot positions assessed with the crown-shift-index

Fig. 40 shows the Crown-Shift indices for simulations with plastic tree crowns and with selective thinning.

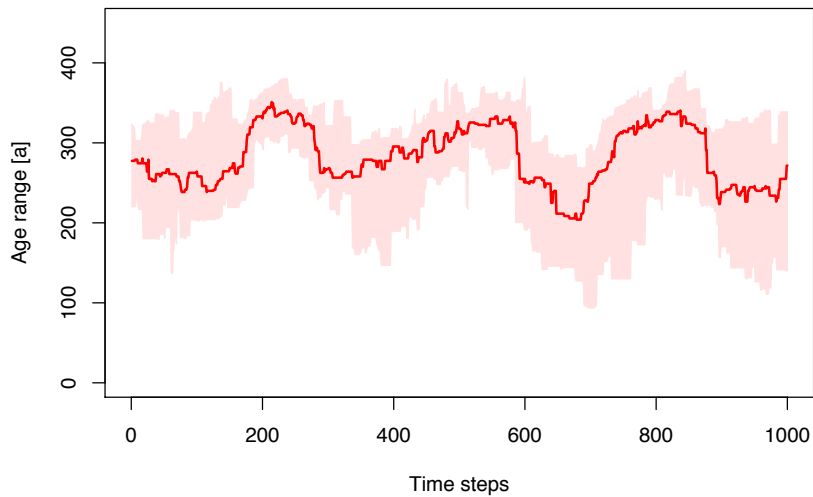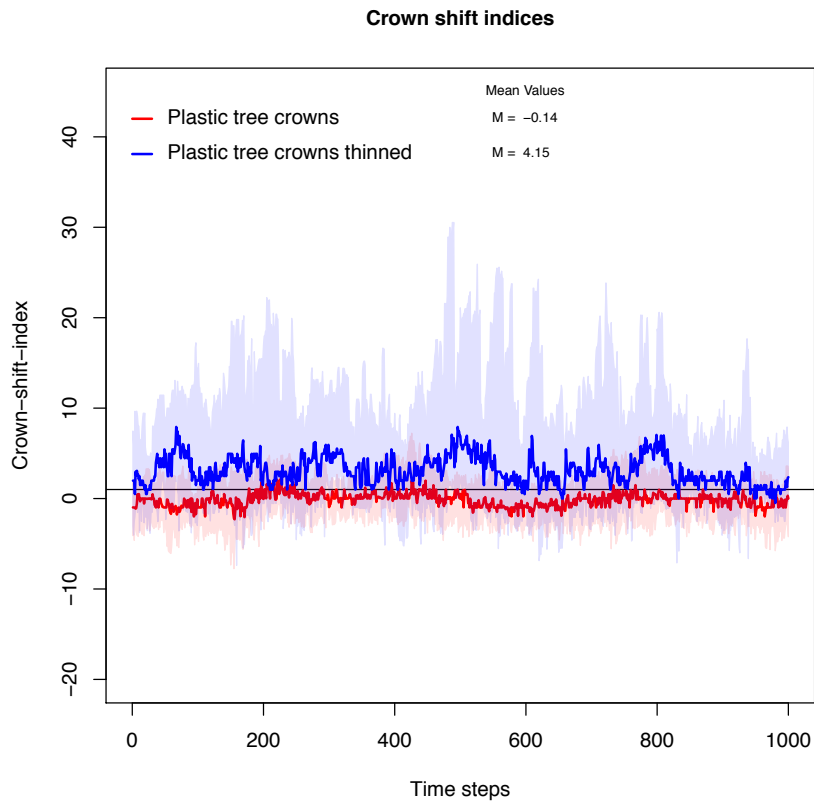**Figure 40:** Crown-Shift indices (CSI) for simulations with plastic tree crowns and with selective thinning for canopy trees taller than 20 m. Solid lines display the median over all simulations, while 95 % confidence envelopes are given in the same color. Selective thinning has a strong effect size r of 0.6 on the CSI.

The second experiment with rotation-symmetric tree crowns is absent due to missing crown plasticity. The greatest CSI values are reached by application of selective thinning, which has a strong effect size of 0.6 on the CSI. Thus, selective thinning leads to enhanced spatial regularity of crown centroids compared to stem foot positions.

7.2.5 Age ranges of canopy trees in comparison

Fig. 41 shows the age ranges for canopy trees taller than 20 m for all simulation experiments. Both rotation-symmetric tree crowns and selective

thinning had strong effects sizes of 0.76 and 0.75 on canopy age ranges, while maximum average ranges of 277 years were reached by simulations with plastic tree crowns.

Age range for canopy trees
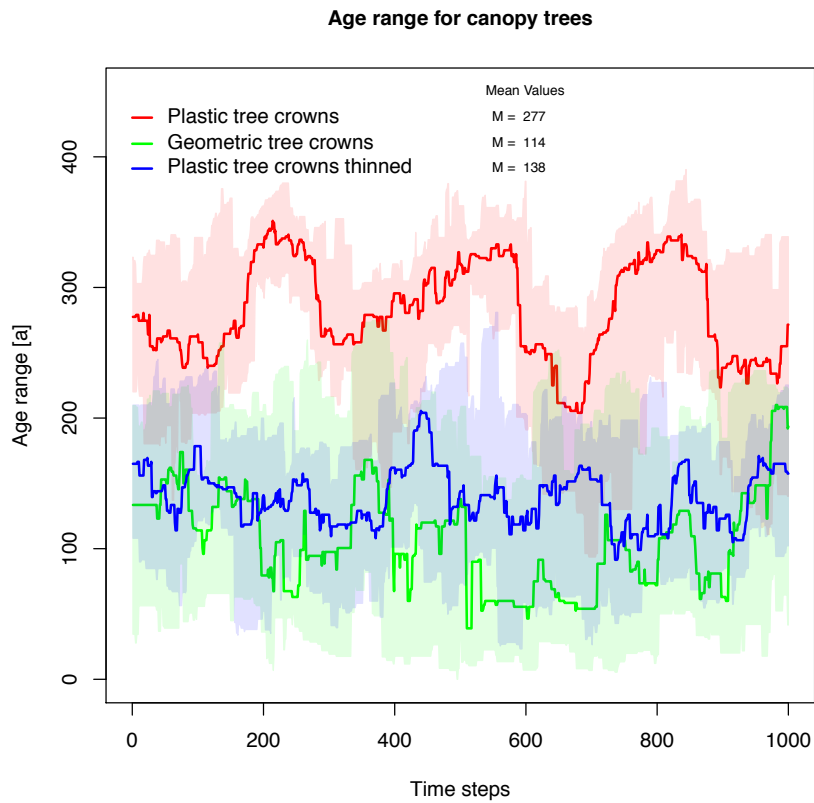
Figure 41: Age ranges of canopy trees taller than 20 m for all simulation experiments in comparison. Solid lines display the median values over all simulations, while 95 % confidence envelopes are given in the same color. Both selective thinning and rotation-symmetric tree crowns have strong effect sizes r of 0.75 and 0.76 on the age ranges of canopy trees.

7.2.6 Diameter ranges of canopy trees in comparison

Fig. 42 shows the diameter ranges for canopy trees taller than 20 m for all simulation experiments. The diameter range informs about the difference between minimum and maximum tree diameters in the simulated for-

est canopy. Contrary to canopy age ranges, selective thinning had only a small effect size of 0.19, while rotation-symmetric tree crowns had a strong effect size of 0.86 on diameter ranges of canopy trees. The highest average diameter range is reached by simulation with plastic tree crowns with 97 cm.

Diameter range of canopy trees
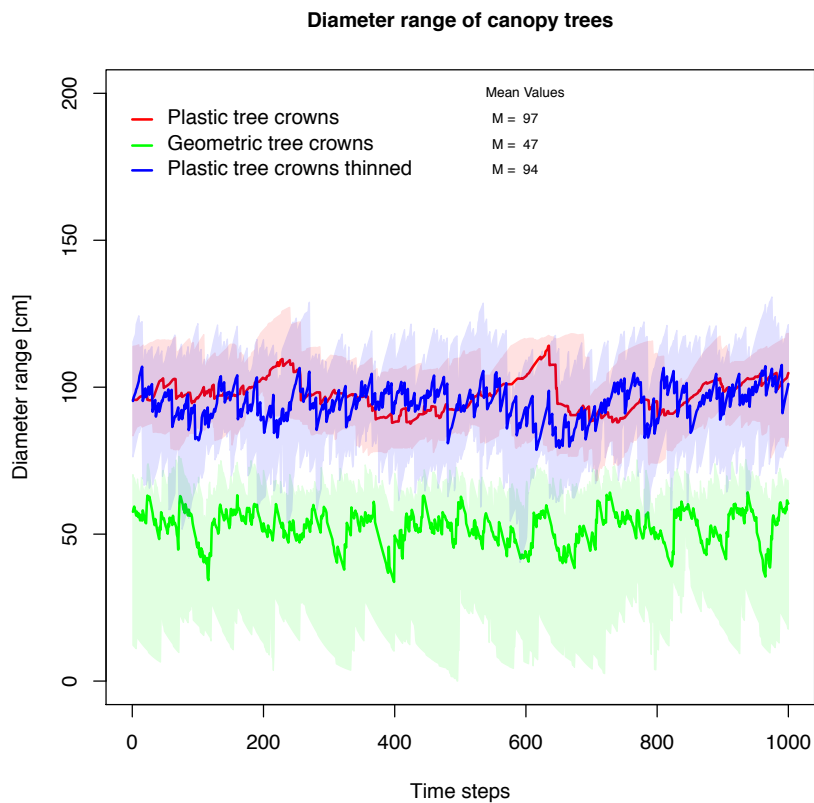
Figure 42: Diameter ranges for canopy trees taller than 20 m for all simulation experiments in comparison. Solid lines display the median values over all simulations, while 95 % confidence envelopes are given in the same color. Selective thinning has a small effect size of 0.19, while rotation-symmetric tree crowns have a strong effect size of 0.86 on diameter ranges of canopy trees.

7.2.7 Number of forest development phases in comparison

Fig. 43 shows the number of forest development phases detected according to section 6.4 for all simulations in comparison.

Forest development phases
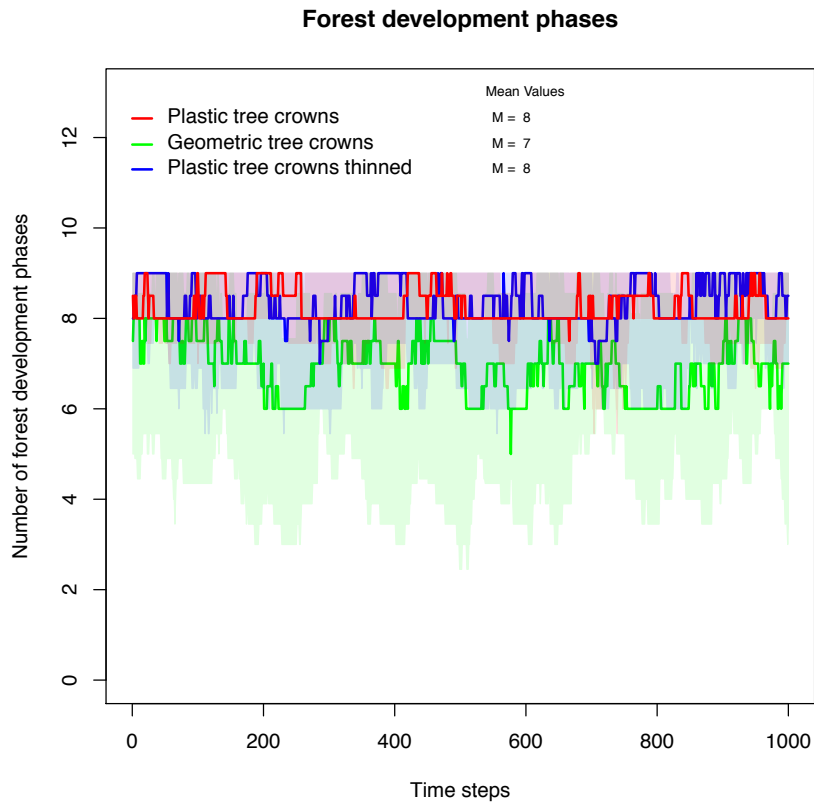
Figure 43: Number of forest development phases in comparison. Solid lines display the median values over all simulations, while 95 % confidence envelopes are given in the same color. Selective thinning has a small effect size of 0.19, while rotation-symmetric tree crowns have a medium effect size of 0.53 on the number of forest development phases on the simulated area.

Selective thinning had a small effect size of 0.19, while rotation-symmetric tree crowns had a medium effect size of 0.53 on the number of detected phases. Average numbers of 9 phases are both detected for simulations with plastic tree crowns alone and with selective thinning applied.

8. Discussion

This study is the first to investigate the influence of tree crown plasticity on the structure and dynamics of near-natural beech forests by means of individual-based modeling. The applied model framework allows to analyze how patterns and structures observed at the ecosystem-level emerge from complex individual interactions. Thereby, beech forests are treated as Complex Adaptive Systems (CAS) assuming that complex system behavior is driven by non-linear spatiotemporal interactions that span over different organizational levels. However, despite the overwhelming complexity of organismic interactions found in beech forests, the experimental focus is solely placed on aboveground tree interactions while interactions below ground are deliberately excluded in order to test if this suffices to reproduce patterns from empirical studies in near-natural beech forests. Aboveground competition for Photosynthetic Active Radiation (PAR) is described process-based in that radiation interception by tree crowns is calculated through a ray-tracing algorithm which recognizes the plasticity of tree crowns. The latter is described phenomenologically through a vector-based approach, which spans tree crown surfaces by vectors emanating from a crown onset point. Individual tree crowns can adapt their crown shape according to available crown space which is constricted by tree neighbors. The developed model BEEch Plasticity (BEEP) allows to simulate beech forest growth in 3D and to apply different management treatments, such as thinning. The results from the simulation experiments conducted in this study are discussed in the following.

8.1 Reproduced patterns from near-natural beech forests

The first simulation experiment with plastic tree crowns aimed at reproducing patterns observed from near-natural beech forests (first research question). The following sections discuss the results presented in section 8.1 in

terms of the hypothesis derived from the first research question.

8.1.1 Multi-layered forest structure

The development of the Shannon-Weaver indices SI, which informs about the vertical structure of the simulated forest, clearly show that a multi-layered forest structure developed over the simulation period. This result is in accordance with empirical observations (Hobi *et al.*, 2015a). Simulated SI values reach observed levels from a senescent old-growth beech forest in North-Germany (Schröter *et al.*, 2012) and exceed them, because of absent natural regeneration in the study of Schröter *et al.* (2012). The hypothesis that the BEEP model is able to reproduce a multi-layered forest structure can be confirmed. The developed forest structure shows cyclic fluctuations, but remains stable around an average SI value of 1.71 (Fig. 38) in the long run, which is supported by discarding the first 1000 time steps of the simulation in order to allow transient oscillation.

8.1.2 Small-scale heterogeneous forest structure

The small-scale heterogeneous forest structure can be observed in four ways: by the development of the structural-complexity-index SCI, the development of the Shannon-index SI, by the age ranges of canopy trees, and by the number of development phases. Large age ranges of canopy trees suggest that those trees emerged from tree cohorts with different ages and sizes in close proximity to each other. Increasing SCI and SI values over the simulation period indicate a horizontally and vertically divers forest structure, which can be termed heterogeneous. The SCI values exceed observed indices from the Serrahn beech forest (Schröter *et al.*, 2012) by far, which might stem from the absence of tree regeneration in the inventory of the mentioned study. The interplay of tree mortality and crown plasticity leads to long periods over which the canopy is interspersed with small gaps. These

gaps may close again, which might lead to the death of already established regeneration. As a consequence, the beech regeneration greatly differs in terms of age, height, and diameter, and this result is congruent with the findings from central Bohemian beech forests (Bílek *et al.*, 2014) and Ukrainian beech forests (Hobi *et al.*, 2015a).

The question about the scale on which the heterogeneous forest structure is observed may be difficult to answer, because the sizes of development phases of old-growth forests vary on the scale applied by the observer (Commarmot *et al.*, 2005). However, the characteristic mosaic pattern should be observable on an area of less than 1 ha (Tabaku, 2000; Piovesan *et al.*, 2005; Alessandrini *et al.*, 2011). The sizes of developmental phases in the simulation experiment are smaller than 0.5 ha and refer to cohorts of trees (Fig. 43). The simulation with plastic tree crowns produced on average 9 detectable development phases of 156.25 m^2 on a simulation area of 0.5 ha. This pattern is comparable to the results obtained from the model BEFORE (Rademacher *et al.*, 2004), which clearly demonstrates that beech forests consist of a mosaic of areas with different developmental stages (on average 0.3 ha), although the grid pattern with cell sizes of 204 m^2 impact the size of detectable phases, as phase sizes below cell size cannot be described. As the raster size of 12.5 x 12.5 m applied in this study can be occupied by one large beech tree alone, if the particular tree has a crown width of 20 m for example, then the scale of observation cannot be decreased further, because it is already at the scale of an individual tree. Thus, based on the findings from the sheer number of development phases, the forest structure can be described as small-scale heterogeneous.

The dynamic raster search with which development phases have been detected in this study is in contrary to Tabaku (2000), who applied a fixed raster grid. Thus, the number of phases in the simulation cannot be easily compared to this field observations, as the dynamic raster search may arti-

ficially increase the number of phases. On the other side, a fixed raster may underestimate the total number of detectable phases.

A very important mechanism that drives the mosaic pattern is the mortality submodel. As described in the model description (see section 2.2.9), the tree senescence, which means the process of decreasing tree vitality and subsequent tree death as irregular mortality, is based on the tree dimension, particularly the tree height. Tree senescence is initiated with a mortality index drawn from a normal distribution. Thus, trees may die as single individuals or in groups depending on their mortality index, height, and position. However, empirical studies strongly suggest that structures and processes in old-growth beech forest are driven by gap dynamics that in turn rely on disturbance events, mostly storms (Piovesan *et al.*, 2005; Nagel & Diaci, 2006; Trotsiuk *et al.*, 2012). Single or groups of trees are destroyed which lead to the observed gap patterns by Hobi *et al.* (2015b), with large-scale disturbances being very rare. Thus, it can be assumed that tree deaths caused by wind disturbance events occur in clusters. This death of tree groups is only mimicked in the BEEP model by trees which mortality indices, dimension, and positions are close to each other.

It can be argued that tree morality in the simulation must occur in clusters of groups of trees due to the above-mentioned development phases, which is similar to the observed gap patterns in old-growth beech forests (Hobi *et al.*, 2015b). However, the mortality model used in the simulation experiment may not come up to the observed patterns of beech tree mortality, because it does not take into account important drivers of tree mortality, such as drought stress (Hülsmann *et al.*, 2016). This can only be improved by the incorporation of adequate empirical or mechanistic mortality models based on long-term data derived from monitoring plots in near-natural beech forests. Therefore, the BEEP model is able to reproduce a small-scale heterogeneous forest structure, but the results are strongly influenced by the

applied mortality submodel. Thus, it remains uncertain, if the small-scale pattern could have been produced by other model formulation in the mortality submodel. The sensitivity analysis already showed that forest structure result are very sensitive to assumptions made in the mortality submodel. However, the hypothesis that the BEEP model is able to reproduce a small-scale heterogeneous forest structure can be confirmed.

8.1.3 Shape of diameter distributions

The simulation results show a typical reversed-J-shaped diameter distribution with high numbers of tree regeneration and old large-diameter trees. The results are in accordance with empirical observations (Heiri *et al.*, 2009; Kucbel *et al.*, 2012). However, most studies from empirical beech forests describe a mixture of reversed-J-shape, bimodal or rotated-sigmoid shape (Piovesan *et al.*, 2005; Alessandrini *et al.*, 2011; Pach & Podlaski, 2015) depending on the particular plot under scrutiny. Bimodal or rotated-sigmoid shapes were not reproduced. This discrepancy may be based on differences in the observation scale: this study observes distributions on a constant area of 0.5 ha, while empirical studies use larger areas for example 10 ha (Pach & Podlaski, 2015). Peck *et al.* (2015) suggest that even small research plots of 10 ha may lead to misconceptions about the forest structure because of their size and their unrepresentative placement. Thus, the simulation area in the experiment may contain a significant bias concerning forest structure characteristics. In fact, this small area may lead to a decreased possible variability of the spatial and temporal dynamics. A possible solution to correct this bias is the increase of the simulation area as well as the rotation of subsamples drawn from the simulated forest. In contrast to Peck *et al.* (2015), Lombardi *et al.* (2015) suggest a minimum plot size of 500 m^2 for the assessment of structural characteristics. These rather small-sized plots would agree with the finding that typical structural characteristics of

126

old-growth forests are evident even on small spatial scales of less than 1 ha (Piovesan *et al.*, 2005; Winter, 2005; Alessandrini *et al.*, 2011). From this point of view, the simulation area used in this study seems appropriate. Nevertheless, a final decision about the appropriateness of the simulation area can only be found in accordance with unambiguous empirical studies. The hypothesis that the BEEP model is able to reproduce a typical reversed-J-shaped diameter distribution can be confirmed.

8.1.4 Age ranges of canopy trees

Large age ranges of more than 100 years of canopy trees taller than 20 m are clearly reached in the simulation with plastic tree crowns. The simulated age ranges approach values between 200 and even 300 years, while maximum tree ages reach 500 years. Tree age in the BEEP model is a function of tree competition and tree senescence, the latter being based on the tree height as driving variable. Maximum simulated tree ages of up to 500 years are also reported from Trotsiuk *et al.* (2012), Piovesan *et al.* (2005), and Hobi *et al.* (2015a). The study of Hobi *et al.* (2015a) further revealed that those high tree ages may be driven by long periods in the forest understory. The suppressed trees increase their growth when canopy gaps open. If those trees reach the forest canopy, they may be already 200 years old, but not affected by decreasing vitality. The hypothesis that the BEEP model is able to reproduce large age ranges of canopy trees of more than 100 years can be confirmed.

8.1.5 Spatial patterns of stem foot positions and crown centroids

Clark-Evans indices for stem foot points and crown centroids vary from aggregated to regular, but neither crown centroids nor stem foot positions are regularly distributed in the long run. Levels of regular distributions for stem foots and crown centroids from Czech beech forest and Serrahn beech

forests are not reached (Bílek *et al.*, 2011; Schröter *et al.*, 2012; Bulušek *et al.*, 2016), which reveals restrictions in the ability of tree crowns for a plastic behavior, but also in the competition-driven tree mortality. The interplay of tree competition, regeneration, and mortality does not lead to a regular tree distribution in the simulation. However, observed Clark-Evans indices show considerable differences that may be caused by the study location (latitude, elevation), but also by differences in the forest inventory. For example, Bílek *et al.* (2011) investigated spatial tree distributions on plot areas of 1 ha, Bulušek *et al.* (2016) used plot sizes of 0.24 ha, respectively, and Schröter *et al.* (2012) calculated Clark-Evans indices on a area of 2.8 ha. These plot sizes may cause serious differences for the Clark-Evans-indices, if spatial distributions change on a smaller or greater plot area. However, varying plot sizes in the simulation experiment with plastic tree crowns has not been tested so far, although the sensitivity analysis suggest that spatial tree distributions are influenced by the simulation area. Improvements could be accomplished not only by increasing the simulation area but also by dynamically assessing Clark-Evans-indices on subsamples of varying sizes derived from the simulated plot. Another possible reason for the observed differences may be the slope terrain that characterizes the plots investigated by Bílek *et al.* (2011), which could lead to more regular stem foot distributions. However, the hypothesis that the BEEP model is able to reproduce regular distributions of stem foots and crown centroids in the long-term cannot be confirmed.

8.2 Effects of crown plasticity on forest structure and dynamics of near-natural beech forests

8.2.1 Enhanced regular distribution of crown centroids

Crown centroids are more regularly distributed than stem foot positions in simulations with plastic tree crowns without thinning. This pattern is caused by tree crown plasticity. The values for the average crown displacement in the first simulation with plastic tree crowns are smaller than the values reported from Schröter *et al.* (2012) and Bulušek *et al.* (2016), which indicates that the plasticity of tree crowns is still too constrained, which is likely caused by the regular crown point arrangement that decreases the flexibility of crown vectors to grow in different directions. On the other side, implausible maximum crown displacements of 11.5 m indicate a strong need to constrain the unhindered crown growth in terms of tree stability.

The enhanced regularity of crown centroids may be the reason for the stand productivity even in late successional stages in which leaf area losses from sudden deaths of individual trees can be rapidly compensated (Glatthorn *et al.*, 2017). The beech crown plasticity increases canopy space filling and stand productivity (Juchheim *et al.*, 2017a). Therefore, the simulation results are in accordance with empirical findings and support the importance of plastic tree crowns for forest dynamics and structure in beech forests. The hypothesis that crown plasticity leads to enhanced regular distribution of crown centroids compared to stem foot positions can be confirmed, but comparisons of simulated and empirical crown displacements call for a thorough revision of the crown growth submodel.

8.2.2 Above-ground competition for crown space and PAR

Conclusions about the effects of crown plasticity on aboveground competition can be drawn by comparing results of simulations with plastic and

rotation-symmetric tree crowns. As direct comparison by means of competition measures cannot be achieved as a result of altered model formulations, effects can be observed in the resulting forest structure. By comparing age and diameter ranges of canopy trees, those of simulations with geometric crowns are much lower, which is reflected by strong effect sizes. This leads to the conclusion that rotation-symmetric tree crowns lead to premature tree deaths, which is not caused by irregular mortality formulations, which remained unaltered, but by changes in the competition for crown space. Rotation-symmetric tree crowns do not allow trees to escape neighborhood crown pressure by crown plasticity, which intensifies competition for crown space and leads to premature tree death. This in turn decreases the observed diameter and age ranges. Thus, the hypothesis that crown plasticity decreases the aboveground competition for PAR and crown space can be confirmed.

8.2.3 Horizontal and vertical forest structure

Comparing the SI and SCI values between the first and second experiment reveals that tree crown plasticity do not lead to enhanced SI values reflected by a very small effect size, but to increased SCI values reflected by a strong effect size. This indicates that the vertical forest structure is unaffected by tree crown plasticity, whereas the horizontal and vertical structural complexity (SCI) may increase. This pattern may be caused by the reduction in crown competition due to crown plasticity, which also lead to higher age ranges of canopy trees. Thus, in the simulation with plastic tree crowns, trees are getting older and larger and may serve as parent trees for new tree regeneration in their proximity over longer time spans. This causes the horizontal forest structure to be more divers, while the vertical forest structural diversity remains almost unaffected. Therefore, tree crown plasticity enhances the horizontal, but not the vertical forest structure. The hypothesis

that crown plasticity enhances both horizontal and vertical forest structure can only be confirmed for the horizontal forest structure.

8.2.4 Effects on the small-scale heterogeneous forest structure

Rotation-symmetric crowns had a strong effect size on the number of detected development phases, which decreased to an average of 7 phases. Further, the index SCI decreased to an average value of 1.94 with an effect size of 0.86. Both results indicate that crown plasticity in turn enhances the forest heterogeneity by allowing more developmental phases to establish, which increases the overall structural complexity or forest rugosity assessed with the SCI. Thus, the hypothesis that crown plasticity enhances the small-scale heterogeneous forest structure can be confirmed.

8.3 Effects of selective thinning on forest structure and dynamics of near-natural beech forests

8.3.1 Horizontal and vertical forest structure

The comparison of the SCI development over the simulation period shows that selective thinning decreases the structural complexity with an effect size of 0.86. However, thinning had only a very small effect size of 0.04 on the vertical forest structure assessed with the SI. Thus, selective thinning does not affect the vertical, but the horizontal forest structure. The hypothesis that selective thinning decreases both horizontal and vertical forest structure can only be confirmed for the horizontal forest structure.

8.3.2 Above-ground competition for crown space and PAR

Similar to section 9.2.2, conclusions about thinning effects on aboveground competition for crown space and PAR cannot be directly drawn, but inferred from simulation results concerning calculated CSI as well as age and

diameter ranges. Selective thinning had a strong effect size of 0.6 on crown-shift-indices CSI indicating more enhanced regular distributions of crown centroids if thinning is applied. This is caused by tree removal and opening canopy gaps, which can be filled in with neighboring crowns extending into those canopy gaps and, thereby, increase their crown displacement and crown size which in turn leads to increased tree diameters. Because of the increased available crown space for canopy trees due to thinning, the effect size on diameter ranges of canopy trees is small (0.19), although the effect size on the age range is strong (0.75), because trees are removed prematurely. Based on those findings, a decreasing effect of selective thinning on the aboveground competition for crown space and PAR can be observed and the associated hypothesis confirmed. This finding is in accordance with empirical research (Fichtner *et al.*, 2013).

8.3.3 Effects on the small-scale heterogeneous forest structure

Selective thinning had only a small effect size of 0.19 on the number of development phases, which is on average not different to simulations with plastic tree crowns without thinning application. However, the above mentioned effect on the structural complexity or forest rugosity assessed with the SCI indicates a decreasing effect on the horizontal forest structure, while vertical forest structure assessed with the SI was unaffected. Based on those findings, no clear decreasing effect on the small-scale heterogeneous forest structure can be observed and the associated hypothesis cannot be confirmed. This is in contrast to empirical studies, which found a decreasing effect of shelterwood and selective thinning on forest stand heterogeneity (Nocentini, 2008; Bílek *et al.*, 2011; Pafetti *et al.*, 2012; Becagli *et al.*, 2013) and on both horizontal and vertical forest structure (Szmyt, 2012; Pafetti *et al.*, 2012). However, comparisons are difficult, as the studies used the SI for characterizing the vertical forest structure, but no study used the SCI

as a measure of forest rugosity or searched for forest development phases. Another index to assess the horizontal forest structure might have produced different results. Further, the selective thinning approach in this study reflect the low-thinning interference approach used in the forest district of Lübeck (Sturm, 1993; Westphal *et al.*, 2004), which was not applied in the mentioned studies. As this thinning approach is designed to increase the near-naturalness of forest management, the results in this study rather support the success of this approach.

8.3.4 Spatial patterns of stem foot positions and crown centroids

Selective thinning had only a very small effect size of 0.04 on spatial distributions of stem foot positions, but a medium effect of 0.53 on the distribution of crown centroids. Thus, selective thinning do not lead to more aggregated tree distributions. In contrast, thinning allows increased crown displacements and more effective resource use of canopy gaps through increased regular distributions of crown centroids (Glatthorn *et al.*, 2017; Juchheim *et al.*, 2017a). The tree establishment pattern of locations is unaffected, which implies that selective thinning only decreases the tree age and leads to premature deaths, but does not alter tree distributional patterns. The hypothesis that selective thinning leads to more aggregated patterns of stem foots and crown centroids cannot be confirmed. The unaltered stem foot distributions is in contrast to empirical findings (Boncina *et al.*, 2007; Nocentini, 2008; Szmyt, 2012; Becagli *et al.*, 2013) which revealed increased regular distributions of stem foot positions due to thinning. This discrepancy may indicate that the interplay of tree regeneration, competition and mortality in the BEEP model formulation cannot represent natural tree establishment processes to a sufficient degree, but slope terrains and varying plot size in the empirical studies may further complicate comparisons.

8.4 General discussion of the study results

The discussion above shows that almost all hypotheses could be confirmed. In particular, the first research question with its associated hypotheses can be confirmed, except for regular spatial patterns of stem foot positions and crown centroids that the model was not able to reproduce in the long run. Nevertheless, the BEEP model with its focus on the aboveground competition for crown space and PAR without any further descriptions of belowground processes suffices to reproduce the patterns observed in near-natural beech forests: a multi-layered vertical forest structure, a small-scale heterogeneous forest structure consisting of several developmental phases, a reversed-J-shaped diameter distribution as well as large age ranges of canopy trees of more than 100 years.

Concerning the second research question, tree crown plasticity increases the horizontal but not vertical forest structure, leads to more regularly distributed crown centroids, and decreases aboveground competition for PAR and crown space, which leads to a more heterogeneous forest structure on a a small scale and more coexisting developmental stages.

In terms of the third research question, selective thinning decreases the aboveground competition for PAR and crown space, decreases the horizontal forest structure and forest structural complexity, but has no effect on the vertical forest structure. Further, thinning does not lead to a decreased heterogeneity in terms of development phases and does not lead to more aggregated distribution patterns of stem foots. Rather, crown centroids are more regularly distributed.

8.5 Discussion of the applied methods

8.5.1 Individual-based forest modeling

As outlined in section 2.4, models describe certain aspects of real-life systems. They reduce the level of complexity to facilitate understanding and hypothesis testing. In particular, individual-based models assume that individual-level processes produce patterns at higher levels of complexity, for example at the level of the population or community (Huston *et al.*, 1988). This level of reductionism imposed on the model development and implementation contributes to the overall uncertainty (see section 2.4) against which the model results must be weighted. The BEEP model uses a 3D approximation and time steps that mimic vegetation periods in real-forest systems. The temporal scale upon which simulation steps are run is therefore one year. Tree growth is referred to that particular period. In short, the BEEP model describes the directed movement of points in an artificial 3D world, from which inferences about the space occupation behavior of trees are drawn. Thus, the level of reductionism in this phenomenological and partly process-based model is very high, but it allows studying tree growth on an individual basis.

The reason to opt for a modeling approach to answer the research question introduced above is the possibility to test hypothesis about real-world phenomena that could not be answered with other approaches. To base hypothesis testing on long-term effects of crown plasticity on beech forest structures with field research would outreach our current resources. First, we cannot yet study a forest system development under ceteris-paribus conditions for 1000 years. Second, we cannot yet alter natural system behavior with the level of detail we would possibly require to answer our questions, because we lack a deeper understanding. That is, we cannot force trees in a real forest to grow with rotation-symmetric crown shapes. These experi-

ments, which are indeed experiments of thought, can only be set within an artificial world which rules we control. From this point of view, computer models are a means of outsourcing information processes that our intellect cannot deal with, because of its complexity. In this regard, computer models are the only means for answering the research questions stated introductory.

Therefore, the modeling approach in this study seems appropriate. BEEP was established on a phenomenological and process-basis to address the questions of what effects do crown plasticity and selective thinning evoke on beech forest structure. A combination of the BEEP model with detailed descriptions on other ecological processes than PAR attenuation, such as soil hydrology and root water uptake by trees, could further enhance model predictions on tree growth.

8.5.2 Data material

As described in section 2.1, data availability was restricted to inventory data from the forest 'Schattiner Zuschlag' as well as to two additional sites at Langula and Fabrikschleichach. The BEEP model uses coarse assumptions about crown growth, because detailed long-term measurements were unavailable. A glimpse of the uncertainty that these assumptions produce shows the short model validation (see section 2.5). The BEEP model crowns are by far more regularly shaped than their empirical counterparts, which could be improved by independently growing crown vectors. In the current model version, the crown vector growth follows a systematic growth reduction caused by the available PAR expressed as percentage of above-canopy light (PACL). The modeled crown structure, however, imposes an artificial regularity on the crown shape that has an uncertain effect on tree crown interaction. As pointed out in section 4.2, long-term TLS-data from unmanaged beech forest would provide an excellent basis for model validation and formulating a revised version of the crown growth submodel depend-

ing on the available PACL. Unfortunately, the BEEP model development precedes sufficient data availability.

Further, tree height growth is based on a potential growth function derived from inventory measurements that may not include the correct maximum tree heights at the particular tree age, which bias crown growth predictions that rely on potential tree height growth. The approach to base crown growth predictions on height growth can be replaced if long-term crown data is available from which a new crown growth model can be developed and parameterized. This crown growth model could include influencing factors of climate, soil conditions, and available PAR that improve crown growth predictions.

8.5.3 Modeling tree mortality

The validity of the mortality submodel has been discussed earlier in terms of the gap patterns it produces. This submodel could be improved by an additional algorithm that mimics recurrent storm events that kill certain trees following a probability approach, in which neighbor trees to a tree that is selected as "killed by the storm event" are more likely to be killed as well either by a lack of their own stability or by receiving damage from neighbor trees. This probability could be inferred from the mortality patterns in beech forests after storm events (Nagel & Diaci, 2006).

8.5.4 Modeling tree regeneration

The regeneration submodel focuses on the establishment of new trees according to the available PACL, which excludes other important factors like competition to grasses, micro-relief differences or even the water-availability at forest gap edges (Gálhidy *et al.*, 2006; Wagner *et al.*, 2010). This submodel routine could be improved by introducing an underlying patch structure that transfers site characteristics to the tree being established. This

means, a tree establishing at the south-exposing gap edge receives more PACL but may be exposed to less water availability, which would reduce tree growth. These important ecological factors could change the structural outcomes of the BEEP model, especially regarding the horizontal forest structure. However, introducing such environmental variables would link BEEP with a more process-based approach. This would actually require an ecophysiological submodel that influences tree growth.

8.5.4 Modeling belowground interactions

Another important aspect that could influence the outcome of the BEEP model is the deliberately excluded belowground interaction of trees. Referring to the tree establishment above, new tree seedlings are influenced by root competition to their neighboring parent trees (Wagner, 1999), while other studies suggest a possible facilitation mechanism that enhances seedling growth in the proximity of parent trees (Simard *et al.*, 2012). The effect that the inclusion of belowground processes would have on the model outcome cannot be estimated, as the process as such is barely understood. A possible approach to improve the BEEP model in this respect would be an additional submodel that describes rooting zones of trees. These zones could follow the approach of Zone-of-Influences (ZOI, Lin *et al.* (2012)) or ecological field-theory (Wu *et al.*, 1985) that describe the resource uptake of an individual within a field which size is dependent on allometric relationships to tree height or tree diameter. However, those submodels would be difficult to parameterize and to calibrate if the aboveground tree growth is described in a completely different way.

8.5.4 BEEP simulation setting

As mentioned earlier, the actual restriction to the simulation area of 0.5 ha and number of simulation runs to 10 is not only influenced by findings on the

size of development phases by Tabaku (2000), but also by the computation time for simulations. If the latter would pose no restriction on the simulation experiments, best would be to enlarge the simulation area for example to 1000 ha. Structural indices could then be calculated on subsamples of the simulation area. Additionally, the edge-bias could be better reduced, which was originally introduced with the computation of competition indices in single-tree growth simulators (Monserud & Ek, 1974). In the current BEEP model version, a reduction of edge effects is achieved by simply cutting off 10 m borders from the simulated area and excluding the border trees from further analysis, which is referred to as buffer zone correction (Diggle *et al.*, 2003; Gadow *et al.*, 2003). The 10 m buffer zone equals the largest observed crown radii of canopy trees (see section 4.1.1). Other approaches would be a translation (torus) (Radke & Burkhart, 1998; Torquato, 2002) or reflection (Radke & Burkhart, 1998; Pretzsch *et al.*, 2002). Both reflection and translation extrapolate the spatial structure within a particular simulation plot to an infinite plane. As these methods are rather speculative and join point patterns that usually do not occur in nature in such proximity (Pommerening & Stoyan, 2006), the improvement achieved by applying such methods compared to a buffer zone is questionable. The radiation submodel already makes this buffer zone correction by assuming the simulated area being placed within a closed forest and all rays a tree receives are absorbed if they pass through outer ranges of the simulation area. Similar corrections could be achieved for tree crown growth, because it can be reasonably assumed that a 10 m border width may be too small. Thus, the boundary consist of only one tree row in the worst case. This biases the model outcome, as restrictions of crown growth towards the plot boundary, such as enhanced competition for PACL, transfers into the plot center which impacts tree crown growth.

The approach to place the simulated area into a closed surrounded for-

139

est enables a more realistic forest development, because beech re-grows in naturally occurring gaps of varying size (Wagner *et al.*, 2010; Hobi *et al.*, 2015b). However, the notion that the surrounding virtual forest is always closed is a strong approximation and restricts forests successional dynamics. This restriction might overemphasize structural attributes artificially. This problem again could be solved by enlarging the simulation area (see above).

Various indices were applied to describe forest structural attributes. The choices for the Clark-Evans-Index, the Stand-Structural-Complexity-Index (SCI), and the Shannon-Index (SI) were made because of their wide application and the possibility to compare the simulated indices with those calculated on empirical data. The Crown-Shift-Index (CSI) was developed to describe the temporal variation of spatial point patterns and specifically the enhanced regularity of crown centroids compared to stem foot points. Other measures that could have been used to describe the temporal variation of spatial point patterns is the Contagion index (Gadow *et al.*, 1998), which produces similar outcomes as the Clark-Evans-index. An alternative to the newly introduced CSI would have been to calculate the difference between the Clark-Evans-indices of crown centroids and stem foot points.

It is important to note that the CSI is sometimes negative, which indicates that stem foot points are more regularly distributed. These observations seem rather unlikely, as no empirical study has mentioned this possibility. This deviation may be an artifact from the BEEP crown model itself and shows that crown space occupation in the simulation is not always ideal. The model validation results support this assumption.

Due to numerous model assumptions on which sensitive model outcomes as the forest structure rely on, the research questions cannot be completely verified. Additional tests with revised versions of the submodel routines may produce different results, which renders the outcome of this study questionable in terms of their transferability to real-life situations.

8.6 Discussion of the contribution to beech forest and forest ecosystem research

This study contributes to basic research on tree interactions and the emergence of patterns and structures in near-natural beech forests. The results presented confirm empirical findings that crown plasticity is an important mechanism driving beech forest dynamics, but the results clearly demonstrate the importance for long-term research in near-natural beech forests in order to unravel the exact interactions in such forest ecosystems. This may open up new opportunities to improve forest management practices, because of the enhanced efficiency with which silvicultural goals are met. For example, if we understand the role of belowground facilitation on tree growth more deeply, we can make inferences about the climate-sensitivity of beech forests and even their adaptability to weather extremes (Mausolf *et al.*, 2018). Although it was possible to reproduce a wide range of patterns observed in near-natural beech forest by simply focusing on the aboveground competition for PAR, the results cannot undermine the importance of belowground interactions, the biodiversity or legacy effects. Thus, the BEEP model stresses important aspects of beech forest ecosystems, but was not designed to replace existing theories. If one extrapolates from the study results, one may question the overall implicitness with which interactions in beech forests are interpreted. For example, forest ecosystems could be seen as holobionts or super-organisms (see introduction) that show a new level of complexity in forest ecosystem research.

The study is further a contribution to the field of individual-based modeling and forest modeling. So far, beech forests have not been modeled on an individual basis (Rademacher *et al.*, 2004; Beyer *et al.*, 2017). This is the first model that describes plastic beech crowns in a spatially-explicit and individual-based model. The BEEP model is further written in R, which is an open platform usually used for statistics. The merits of the modelling

environment R enhance further model development because of the ease with which new packages can be incorporated and through this gaps to other programming languages as C++ can be bridged. Last, this study contributes to the field of system analysis, as the BEEP model enables the investigation of forest ecosystem behavior.

9. Summary

A new individual-based forest model for the species beech (*Fagus sylvatica* L.) was developed and implemented. The model called BEEch Plasticity (BEEP) describes tree crown plasticity phenomenologically and is able to model aboveground competition for PAR on a process basis. The current debate about the tree interactions in near-natural beech forests and their role in emergent forest structures and dynamics led to the research questions if (1) observed patterns can be modeled and reproduced by only describing the aboveground tree interactions, (2) what effects tree crown plasticity has on the structure and dynamics of near-natural beech forests, and (3) what effects selective thinning has on the structure and dynamics of near-natural beech forests. The BEEP model was developed, parameterized, calibrated, and validated according to data from the unmanaged forest 'Schattiner Zuschlag' near Lübeck, North-Germany, while additional data from the sites Langula (Thuringia) and Fabrikschleichach (Bavaria) was used for model parameterization and calibration. Three simulation experiments were conducted. In the first experiment, the BEEP model was run 10 times for 2000 time steps with plastic tree crowns and the emergent forest structure was analyzed using structural indices. In the second experiment, the BEEP model was run again 10 times for 2000 time steps but with a modified crown model that only uses rotation-symmetric tree crowns. In the third experiment, the BEEP model was enhanced with a selective thinning procedure that uses target trees with specific diameter and heights as thinning objects. Forest structure was analyzed through the application of structural indices that capture different aspects of forest structure and by means of characterization of forest development phases. Analysis was accomplished only for the time steps 1000-2000 in order to allow transient oscillation in forest dynamics to develop. The results showed that the focus on aboveground competition and tree interactions sufficed to model beech

forests and reproduced a wide range of patterns observed in near-natural and old-growth beech forest. In particular, the BEEP model was able to simulate a multi-layered forest structure with a mosaic structure of several developmental stages on a relatively small area of 0.5 ha. The simulated forest had wide diameter and age distributions. The diameter distribution was reversed-J-shaped. The age range of canopy trees exceeded 200 years. The comparison between simulations with plastic and rotation-symmetric tree crowns revealed that crown plasticity reduced tree competition for crown space and PAR and enhanced the forest structure and heterogeneity in the long term by allowing more tree cohorts of different developmental stages to coexist. This supports the notion that crown plasticity drives beech forest dynamics in near-natural forests. The comparison between simulations with plastic tree crowns and with additional selective thinning showed that thinning does not affect the forest structural heterogeneity and reduces tree crown competition, while spatial patterns of tree positions remained unaltered. However, crown centroids were more regularly distributed. Model assumptions in the submodel routines, especially in the radiation and mortality submodel, question the reliability of the model results, because of the high sensitivity that these routines evoke on model outcomes. Therefore, revised versions of the submodels and a thoroughly validated crown growth model, may produce different results. Thus, the results presented in this study should be treated with care and cannot be used for generalizations about tree interactions in near-natural beech forests.

References

Adler, D., Murdoch, D., 2018. rgl: 3D Visualization Using OpenGL. R package version 0.99.16. https://CRAN.R-project.org/package=rgl

Akhavan, R., Sagheb-Talebi, Kh., Zenner, E.K., Safavimanesh, F., 2012. Spatial patterns in different forest development stages of an intact old-growth Oriental beech forest in the Caspian region of Iran. Eur. J. For. Res. **131**: 1355–1366.

Alessandrini, A., Biondi, F., Di Filippo, A., Ziaco, E., Piovesan, G., 2011. Tree size distribution at increasing spatial scales converges to the rotated sigmoid curve in two old-growth beech stands of the Italian Apennines. For. Ecol. Manage. **262**: 1950-1962.

Ammer, C., 2000. Untersuchungen zum Einfluss von Fichtenbeständen auf die Entwicklung junger Buchen. Aachen, Shaker Verlag. 185 p.

Ammer, C., Kateb, H.E., 2007. Buchensaat oder -pflanzung: Vergleich zweier Optionen zum Umbau von Fichtenreinbeständen. LWF Wissen **58**: 38–41.

Ammer, C., Stimm, B., Mosandl, R., 2008. Ontogenetic variation in the relative influence of light and belowground resources on European beech seedling growth. Tree physiology **28**: 721–728.

Amoroso, M.M., Turnblom, E.C., 2006. Comparing productivity of pure and mixed Douglas-fir and western hemlock plantations in the Pacific Northwest. Can. J. For. Res. **36**: 1484–1496.

Annighöfer, P., 2018. Stress relief through gap creation? Growth response of a shade tolerant species (Fagus sylvatica L.) to a changed light environment. For. Ecol. Manage. **415-416**: 139–147.

Assmann, E., Franz, F., 1963. Vorläufige Fichten-Ertragstafel für Bayern. Institut für Ertragskunde der Forstlichen Versuchsanstalt, München, 104 p.

Baddeley, A., Rubak, E., Turner, R., 2018. Spatial Point Patterns: Methodology and Applications with R. London: Chapman and Hall/CRC Press, 2015. URL http://www.crcpress.com/Spatial-Point-Patterns-Methodology-and-Applications-with-R/Baddeley-Rubak-Turner/9781482210200/.

Balandier, P., Collet, C., Miller, J.H., Reynolds, P.E., Zedaker, S.M., 2006. Designing forest vegetation management strategies based on the mechanisms and dynamics of crop tree competition by neighboring vegetation. Forestry **79(1)**: 3–27.

Balandier, P., Sinoquet, H., Frak, E., Guiliani, R., Vandame, M., Descamps, S., Coll, L., Adam, B., Prevesto, B., Curt, T., 2007. Six-year time course of light-use efficiency, carbon gain and growth of beech saplings (Fagus sylvatica) planted under a Scots pine (Pinus sylvestris) shelterwood. Tree Physiol. **27(8)**: 1073–1082.

Beaudet, M., Messier, C., 1998. Growth and morphological responses of yellow birch, sugar maple, and beech seedlings growing under a natural light gradient. Can. J. For. Res. **28**: 1007–1015.

Becagli, C., Puletti, N., Chiavetta, U., Cantiani, P., Salvati, L., Fabbio, G., 2013. Early impact of alternative thinning approaches on structure diversity and complexity at stand level in two beech forests in Italy. Ann. Silv. Res. **37(1)**: 655–63.

Beiler, K.J., Simard, S.W., Durall, D.M., 2015. Topology of tree-mycorrhizal fungus interaction networks in xeric and mesic Douglas-fir forests. Ecology **103**: 616–628.

Besag, J., 1977. Discussion of Dr Ripley's paper. Journal of the Royal Statistical Society Series B **39**: 193–195.

Berger, U., Piou, C., Schiffers, K., Grimm, V., 2008. Competition among plants: Concepts, individual-based modeling approaches, and a proposal for a future research strategy. Perspect. Plant Ecol. **9**: 121–135.

Bertness, M.D., Callaway, R., 1994. Positive interactions in communities. Trends Ecol. Evol. **9**: 191–193.

Beyer, F., Hertel, D., Jung, K., Fender, A.-C., Leuschner, C., 2013. Competition effects on fine root survival of Fagus sylvatica L. and Fraxinus excelsior L. For. Ecol. Manage. **302**: 14–22.

Beyer, R., Letort, V., Cournède, P.-H., 2014. Modeling tree crown dynamics with 3D partial differential equations. Front. Plant Sci. **5**: 1–8.

Beyer, R., Etard, O., Cournède, P.-H., Laurent-Gengoux, P., 2015. Modeling spatial competition for light in plant populations with the porous medium equation. J. Math. Biol. **70**: 533–547.

Beyer, R., Letort, V., Bayer, D., Pretzsch, H., Cournède, P.-H., 2017. Leaf density-based modelling of phototropic crown dynamics and long-term predictive application to European beech. Ecol. Model. **347**: 63–71.

Bílek, L. Remeš, J., Zahradník, D., 2009. Natural regeneration of senescent even-aged beech (Fagus sylvatica L.) stands under the conditions of Central Bohemia. J. For. Sci. **55**: 145–155.

Bílek, L. Remeš, J., Zahradník, D., 2011. Managed vs. unmanaged structure of beech forest stands (Fagus sylvatica L.) after 50 years of development, Central Bohemia. For. Syst. **20**: 122–138.

Bílek, L., Remeš, J., Podráský, V., Rozenbergar, D., Diaci, J., Zahradník, D., 2014. Gap regeneration in near-natural European beech forest stands

147

in Central Bohemia – the role of heterogeneity and micro-habitat factors. Dendrobiology **71**: 59–71.

Bingham, M.A., Simard, S.W., 2013. Seedling genetics and life history outweigh mycorrhizal networks potential to improve conifer regeneration under drought. For. Ecol. Manage. **287**: 132–139.

Biovin, F., Paquette, A., Racine, P.B., Messier, C., 2011. A fast and reliable method for the delineation of tree crown outlines for the computation of crown openness values and other crown parameters. Can. J. For. Res. **41(9)**: 1827–1835.

Bivand, R., Rundel, C., 2017. Interface to Geometry Engine - Open Source ('GEOS'). R package version 0.3-26. R package version 0.3-26. https://CRAN.R-project.org/package=rgeos.

Boncina, A., Kadunc, A., Robic, D., 2007. Effects of selective thinning on growth and devlopment of beech (*Fagus sylvatica* L.) forest stands in south-eastern Slovenia. Ann. For. Sci. **64**: 47–57.

Boeck, A., Dieler, J., Biber, P., Pretzsch, H., Ankerst, D.P., 2014. Predicting tree mortality for European beech in southern Germany using spatially explicit competition indices. For. Sci. **60**: 613–622.

Booth, M.G., Hoeksema, J.D., 2010. Mycorrhizal networks counteract effects of canopy trees on seedling survival. Ecol. Lett. **91**: 2294–2302.

Botkin, D.B., Janak, J.F., Wallis, J.R., 1972. Some ecological consequences of a computer model of forest growth. J. Ecol. **60**: 849–872.

Box, E.O., Meentenmeyer, V., 1991. Geographic modeling and modern ecology. In: Modern Ecology. Basic and applied aspects. Esser, G., Overdieck, D. (eds.). Elsevier, Amsterdam, p. 773–804.

Brinkmann, N., Seeger, S., Weiler, M., Buchmann, N., Eugster, W., Kahmen, A., 2018. Employing stable isotopes to determine the residence times of soil water and the temporal origin of water uptake by Fagus sylvatica and Picea abies in a temperate forest. New Phytol. **219**: 1300–1313.

Brock, T.D., 1981. Calculating solar radiation for ecological studies. Ecol. Model. **14**: 1–19.

Bronstein, J.L., 2009. The evolution of facilitation and mutualism. Ecology **97**: 1160–1170.

Brooker, R.W., Maestre, F.T., Callaway, R.M., Lortie, C.L., Cavieres, L.A., Kunstler, G., Liancourt, P., Tielbörger, K., Travis, J.M.J., Anthelme, F., Armas, C., Coll, L., Corcket, E., Delzon, S., Forey, E., Kikvidze, Z., Olofssn, J., Pugnaire, F., Quiroz, C.L., Saccone, P., Schiffers, K., Seifan, M., Touzard, B., Michalet, R., 2008. Facilitation in plant communities: the past, the present, and the future. Ecology **96**: 18–34.

Brunner, A., 1998. A light model for spatially explicit forest stand models. For. Ecol. Manage. **107**: 19–46.

Bugmann, H., 2001. A review of forest gap models. Climatic Change **51**: 259–305.

Bulušek, D., Vacek, Z., Vacek, S., Král, J., Bílek. L., Králíček, I., 2016. Spatial pattern of relict beech (Fagus sylvatica L.) forests in the Sudetes of the Czech Republic and Poland. J. For. Sci. **62**: 293–305.

Burkhart, H.E., Farrar, R.L., Amateis, R.L., Daniels, R.F., 1987. Simulation of individual tree growth and stand development in loblolly pine plantations on cutover, site-prepared areas. Publication Number FWS-1-87. Virginia Polytechnic Institute and State University, School of Forestry and Wildlife Resources, Blacksburg, VA.

Burschel, H., Schmaltz, J., 1965a. Untersuchungen über die Bedeutung von Unkraut- und Altholzkonkurrenz für junge Buchen. Forstwiss. Centralbl. **84**: 230–243.

Burschel, H., Schmaltz, J., 1965b. Die Bedeutung des Lichts für die Entwicklung junger Buchen. AFZ **136**: 193–210.

Cahill, J.F.J., Casper, B.B., 2000. Investigating the relationship between neighbor root biomass and belowground competition: field evidence for symmetric competition belowground. Oikos **90**: 311–320.

Caldwell, M.M., Dawson, T.E., Richards, J.H., 1998. Hydraulic Lift: consequences of water efflux from the roots of plants. Oecologia **113**: 151–161.

Callaway, R.M., 2007. Positive Interactions and Interdependence in Plant Communities. Springer, Dordrecht. 404 p.

Callaway, R.M., Walker, I.R., 1997. Competition and facilitation: a synthetic approach to interactions in plant communities. Ecology **78**: 1958–1965.

Campolongo, F., Saltelli, A., Cariboni, J., 2011. From screening to quantitative sensitivity analysis. A unified approach. Comput. Phys. Commmun. **182**: 978–988.

Canham, C.D., Denslow, J.S., Platt, W.J., Runkle, J.R., Spies, T.A., White, P.S., 1990. Light regimes beneath closed canopies and tree-fall gaps in temperate and tropical forests. Can. J. For. Res. **20**: 620–631.

Canham, C.D., Coates, K.D., Bartemucci, P., Quaglia, S., 1999. Measurement and modeling of spatially explicit variation in light transmission through interior cedar-hemlock forests of British Columbia. Can. J. For. Res. **29(11)**: 1775–1783.

Čater, M., Diaci, J., Roženbergar, D., 2014. Gap size and position influence variable response of Fagus sylvatica L. and Abies alba Mill. For. Ecol. Manage. **325**: 128–135.

Čater, M., Kobler, A., 2017. Light response of Fagus sylvatica L. and Abies alba Mill. in different categories of forest edge. Vertical abundance in two silvicultural systems. For. Ecol. Manage. **391**: 417–426.

Cermak, L., 1910. Einiges über den Urwald von waldbaulichen Gesichtspunkten. Cbl. Ges. Forstwes. **36**: 340–370.

Cesarz, S., Fender, A.-C., Beyer, F., Valtanen, K., Pfeiffer, B., Gansert, D., Hertel, D., Polle, A., Daniel, R., Leuschner, C., Scheu, S., 2013. Roots from beech (Fagus sylvatica L.) and ash (Fraxinus excelsior L.) differentially affect soil microorganisms and carbon dynamics. Soil Biol. Biochem. **61**: 23–32.

Chave, J., 1999. Study of structural, successional and spatial patterns in tropical rain forests using TROLL, a spatially explicit forest model. Ecol. Model. **124**: 233–254.

Clark, P.J., Evans, F.C., 1954. Distance to nearest neighbor as a measure of spatial relationships in populations. Ecology **35**: 23–30.

Coomes, D.A., Grubb, P.J., 2000. Impacts of root competition in forests and woodlands: a theoretical framework and review of experiments. Ecol. Monogr. **70**: 171–207.

Chu, C.J., Maestre, F.T., Xiao, S., Weiner, J., Wang, Y.S., Duan, Z.H., Wang, G., 2008. Balance between facilitation and resource competition determines biomass-density relationships in plant populations. Ecol. Lett. **11**: 1189–1197.

Chu, C.J., Weiner, J., Maestre, F.T., Xiao, S., Wang, Y.S., Li, Q., Yuan, J.-L., Zhao, L.-Q., Ren, Z.-W., Wang, G., 2009. Positive interactions can increase size inequality in plant populations. Ecology **97**: 1401–1407.

Chu, C. J., J. Weiner, F. T. Maestre, Y. S. Wang, C. Morris, S. Xiao, J. L. Yuan, G. Z. Du, Wang, G., 2010. Effects of positive interactions, size symmetry of competition and abiotic stress on self-thinning in simulated plant populations. Ann. Bot. - London **106**: 647–652.

Cohen, J., 1988. Statistical power analysis for the behavioral sciences. (2nd ed.). Hillsdale, NJ: Erlbaum. 567 p.

Commarmot, B., Bachofen, H., Bundziak, Y., Bürgi, A., Ramp, B., Shparyk, Y., Sukhariuk, D., Viter, R., Zingg, A., 2005. Structures of virgin and managed beech forests in Uholka (Ukraine) and Sihlwald (Switzerland): a comparative study. For. Snow Landsc. Res. **79**: 45–56.

Condés, S., Vallet, P., Bielak, K., Bravo-Oviedo, A., Coll, L., Ducey, M.J., Pach, M., Pretzsch, H., Sterba, H., Vayreda, J., del Rio, M., 2017. Climate influences on the maximum size-density relationship in Scots pine (Pinus sylvestris L.) and European beech (Fagus sylvatica L.) stands. For. Ecol. Mange. **385**: 295–307.

DaSilva, D., Balandier, P., Boudon, F., Marquier, A., Godin, C., 2012. Modeling of light transmission under heterogeneous forest canopy: an appraisal of the effect of the precision level of crown description. Ann. For. Sci. **69(2)**: 191–193.

Dawson, T.E., 1993. Hydraulic Lift and water use by plants: implications for water balance, performance and plant-plant interactions. Oecologia **95**: 565–574.

Dieler, J., Pretzsch, H., 2013. Morphological plasticity of European beech (Fagus sylvatica L.) in pure and mixed-species stands. For. Ecol. Manage. **295**: 97–108.

Dietze, M.C., Moorcroft, P.R., 2011. Tree mortality in the eastern and central United States: patterns and drivers. Global Change Biol. **17**: 3312–3326.

Diggle, P.J., 2003. Statistical analysis of spatial point patterns. 2nd ed. Arnold, London. 288 p.

Dobbertin, M., Brang, P. 2001. Crown defoliation improves tree mortality models. For. Ecol. Manage. **141**: 271–284.

Donnelly, K., 1978. Simulations to determine the variance and edge-effect of total nearest neighbour distance. In: I. Hodder (ed.) Simulation studies in archaeology, Cambridge/New York: Cambridge University Press, pp 91–95.

Dolnik, C., Ellenberg, H., Fähser, L., Fichtner, A., Hampicke, U., Heeschen, G., Irmler, U., Lüderitz, M., Lütt, S., Rasran, L., Schäfer, A., Schrautzer, J., Sturm, K., Vahder, S., Vogt, K., Wagner, J., 2008. Nutzung ökologischer Potenziale von Buchenwäldern für eine multifunktionale Bewirtschaftung. Flintbek: Landesamt für Natur und Umwelt Schleswig Holstein.

Drößer, L., von Lüpke, B., 2005. Canopy gaps in two virgin beech forest reserves in Slovakia. J. For. Sci. **51**: 446–457.

Dupuy, L., Gregory, P.J., Bengough, A.G., 2010. Root growth models: towards a new generation of continuous approaches. J. Exp. Bot. **61(8)**: 2131–2143.

Ek, A.R., Monserud, R.A., 1974. Trials with program FOREST: Growth and reproduction simulation for mixed species even- or uneven-aged forest

stands. In: Growth models for tree and stand simulation. Fries. J. (ed.). Royal College of Forestry, Stockholm, Sweden, research Notes, No. 30, p. 56-73.

Ekblad, A., Wallander, H., Gofbold, D.L., Cruz, C., Johnson, D., Baldrian, P., Björk, R.C., Epron, D., Kieliszewska-Rokicka, B., Kjøller, R., Kraigher, H., Matzner, E., Neumann, J., Plassard, C., 2013. The production and turnover of extrametrical mycelium of ectomychorrhizal fungi in forest soils: role in carbon cycling. Plant Soil **366**: 1–27.

Emborg, J., 1998. Understory light conditions and regeneration with respect to the structural dynamics of a near-natural temperate deciduous forest in Denmark. For. Ecol. Manage. **106**: 83–95.

Enquist, B.J., Brown, J.H., West, G.B., 1998. Allometric scaling of plant energetics and population density. Nature **395**: 163–165.

Erskine, P.D., Lamb, D., Bristow, M., 2006. Tree species diversity and ecosystem function: can multi-species plantations generate greater productivity? For. Ecol. Manage. **223**: 205–210.

Eränen, J.K., Kozlov, M.V., 2008. Tree species diversity and ecosystem function: can multi-species plantations generate greater productivity? Oikos **117**: 1569–1577.

Facelli, E., Facelli, J.M., 2002. Soil phosphorous heterogeneity and mycorrhizal symbiosis regulate plant intra-specific competition and size distribution. Oecologia **133**: 54–61.

Fellbaum, C.R., Mensah, J.A., Cloos, A.J., Strahan, G.E., Pfeffer, P.E., Kiers, T., Bücking, H., 2014. Fungal nutrient allocation in common mycorrhizal networks is regulated by the carbon source strength of individual host plants. New Phytol. **203**: 646–656.

154

Feldmann, E., Drößler, L., Hauck, M., Kucbel, S., Pichler, S., Leuschner, C., 2018. Canopy gap dynamics and tree understory release in a virgin beech forest, Slovakian Carpathians. For. Ecol. Manage. **415–416**: 38–46.

Fichtner, A., Sturm, K., Rickert, C., von Oheimb, G., Härdtle, W., 2013. Crown size-growth relationships of European beech (Fagus sylvatica L.) are driven by the interplay of disturbance intensity and inter-specific competition. For. Ecol. Manage. **302**: 178–184.

Fichtner, A., Forrester, D.I., Härdtle, W., Sturm, K., von Oheimb, G., 2015. Facilitative-competitive interactions in an old-growth forest: The importance of large-diameter trees as benefactors and stimulators for forest community assembly. PLoS ONE **10(3)**: e0120335.

Fölster, H. Degenhardt, M., Flor, T., Lux, M., 1991. Untersuchungen zur Tiefendurchwurzelung und Durchwurzelungsintensität auf Braunerde-Pseudogleyen im Vorderen Hundsrück in Abhängigkeit von Baumart und Bestandesstrukturparametern. Mitteilungen aus der Forstlichen Versuchsanstalt Rheinland-Pfalz **19(91)**: 91–106.

Forrester, D.I., 2014a. The spatial and temporal dynamics of species interactions in mixed-species forests: From pattern to process. For. Ecol. Manage. **312**: 282-292.

Forrester, D.I., 2014b. A stand-level light interception model for horizontally and vertically heterogeneous canopies. Ecol. Model. **276**: 14–22.

Franklin, J.F., Shugart, H.H., Harmon, M.E., 1987. Tree death as an ecological process: the causes, consequences and variability of tree mortality. BioScience **37**: 550–556.

Frölich, J., 1925. Aus dem südosteuropäischem Urwalde. Forstwiss. Centralbl. **47**: 199–220.

Fritz, C.O., Morris, P.E., 2012. Effect size estimates: current use, calculations, and interpretation. J. Exp.. Psychol. **141(1)**: 2–18.

Gadow, K.v., Hui, G.Y., Albert, M., 1998. Das Winkelmaß – ein Strukturparameter zur Beschreibung der Individualverteilung in Waldbeständen. (The neighborhood pattern – a new parameter for describing forest structures). Centralbl. Gesamte Forstwes. **115**: 1–10.

Gadow, K.v., Hui, G.Y., Chen, B.W., Albert, M., 2003. Beziehungen zwischen Winkelmaß und Baumabständen. Forstwiss. Centralbl. **122**: 127–137.

Galen, C., Rabenold, J.J., Liscum, E., 2007. Functional ecology of a blue light photoreceptor: effects of phototropin-I on root growth enhance drought tolerance in arabidopsis thaliana. New Phytol. **173(1)**: 91–99.

Gauer, J., Aldinger, E., 2005. Waldökologische Naturräume Deutschlands. Mitteilungen Verein für Forstliche Standortskunde und Forstpflanzenzüchtung **43**, Henkel, Stuttgart.

Gayler, S., Grams, T.E.E., Kozovits, A.R., Winkler, J.B., Luedermann, G., Priesack, E. 2006. Analysis of competition effects in mono- and mixed cultures of juvenile beech and spruce by means of the plant growth simulation model PLATHO. Plant Biol. **8**: 503–514.

Gálhidy, Mihók, B., Hagyó, A., Rajkai, K., Standovár, T., 2006. Effects of gap size and associated changes in light and soil moisture on the understory vegetation of a Hungarian beech forest. Plant Ecol. **183**: 133–145.

Gemmel, P., Nilsson, U., Welander, T., 1996. Development of oak and beech seedlings planted under varying shelterwood densities and with different site preparation methods in southern Sweden. New For. **12**: 141–161.

Georgi, L., Kunz, M., Fichtner, A., Härdtle, W., Reich, K.F., Sturm, K., Welle, T., von Oheimb, G., 2018. Long-term abandonment of forest management has a strong impact on tree morphology and wood volume allocation pattern of European beech (*Fagus sylvatica* L.). Forests **9**: 704.

Gerold, D., Biehl, R., 1992. Der Buchenwald von Langula. AFZ **2**: 91–94.

Gilbert, N., Troitzsch, K., 2005. Simulation for the Social Scientist. 2nd ed. Open University Press, Milton Keynes. 312 p.

Glatthorn, J., Pichler, V., Hauck, M., Leuschner, C., 2017. Effects of forest management on stand leaf area: Comparing beech production and primeval forests in Slovakia. For. Ecol. Manage. **389**: 76–85.

Godin, C., 2000. Representing and encoding plant architecture: A review. Ann. For. Sci. **57**: 413–438.

Goldmann, K., Schoening, I., Buscot, F., Wubet, T., 2015. Forest management type influences diversity and community composition of soil fungi across temperate forest ecosystems. Front. Microbiol. **6**: 1300.

Gorzelak, M.A., Asay, A.K., Pickles, B.J., Simard, S.W., 2015. Inter-plant communication through mycorrhizal networks mediates complex adaptive behaviour in plant communities. AoB PLANTS **7**: plv050.

Gralher, B., Herbstritt, B., Weiler, M., Wassenaar, L.I., Stumpp, C., 2018. Correcting for biogenic gas matrix effects on laser-based porewater-vapor stable isotope measurements. Vadose Zone J. **17**: 170168.

Grimm, V., Frank, K., Jeltsch, F., Brandl, R., Uchmanski, J., Wissel, C., 1996. Pattern-oriented modelling in population ecology. Sci. Total Evinron. **183**: 151–166.

Grimm, V., 1999. Ten years of individual-based modelling in ecology: What have we learned, and what could we learn in the future? Ecol. Model. **115**: 129–148.

Grimm, V., Revilla, E., Berger, U., Jeltsch, F., Mooji, W.M., Railsback, S.F., Thulke, H.-H., Weiner, J., Wiegand, T., DeAngelis, D.L., 2005. Pattern-oriented modeling of agent-based complex systems: lessons from ecology. Science **310(5750)**: 987–991.

Grimm, V., Berger, U., DeAngelis, D.L., Polhill, J.G., Giske, J., Railsback, S.F., 2010. The ODD protocol: A review and first update. Ecol. Model. **221**: 2760-2768.

Grimm,V., Berger, U., 2016. Robustness analysis: Deconstructing computational models for ecological theory and applications. Ecol. Model. **326**: 162–167.

Gruber, F., 2003. Steuerung und Vorhersage der Fruchtbildung bei der Rotbuche (Fagus sylvatica L.) durch die Witterung. Schr. Forstl. Fak. Univ. Gött. Niedersächs. forstl. Vers., Sauerländer's Verlag. 141 p.

Grueters, U., Seltmann, T., Schmidt, H., Horn, H., Pranchai, A., Vovides, A.G., Peters, R., Vogt, J., 2014. The mangrove forest dynamics model mesoFON. Ecol. Model. **291**: 28–41.

Habel, K., Grasman, R., Gramacy, R.B., Stahel, A., Sterratt, D.C., 2015. geometry: Mesh Generation and Surface Tesselation. R package version 0.3-6. https://CRAN.R-project.org/package=geometry.

Hacquard, S., Schadt, C.W., 2015. Towards a holistic understanding of the beneficial interactions across the Populus microbiome. New Phytol. **205**: 1424–1430.

Hahn, K., Madsen, P., Lindholt, S., 2007. Gap regeneration in four natural gaps in Suserup Skov — a mixed deciduous forest reserve in Denmark. Ecol. Bull. **52**: 133–145.

Hafner, B.D., Tomasella, M., Häberle, K.-H., Goebel, M., Matyssek, R., Grams, T.E.E., 2007. Hydraulic redistribution under moderate drought among English oak, European beech and Norway spruce determined by deuterium isotopes in a split-root experiment. Tree Physiol. **37**: 950–960.

Hann, D.W., Ritchie, M.W., 1988. Height growth rate of Douglas-fir: A comparison of model forms. For. Sci. **34**: 165–175.

Hasenauer, H., 1994. Ein Einzelbaumwachstumssimulator für ungleichaltrige Fichten-, Kiefern- und Buchen-Fichtenmischbestände. Forstliche Schriftenreihe Universiät für Bodenkultur Wien. Österreichische Gesellschaft für Waldökosystemforschung und experimentelle Baumforschung. Wien. 152 p.

Hasenauer, H., 1997. Biased predictions for tree height increment models developed from smoothed data. Ecol. Model. **98**: 13–22.

Hawkes, C., 2000. Woody plant mortality algorithms: description, problems and progress. Ecol. Model. **126**: 225–248.

He, Q., Bertness, M.D., Altieri, A.H., 2013. Global shifts towards positive species interactions with increasing environmental stress. Ecol. Lett. **16**: 695–706.

Hegyi, F., 1974. A simulation model for manageing jack-pine stands. In: Growth models for tree and stand simulation. Fries, J. (ed). Royal College for Forest Research. Notes 30, Stockholm. pp. 74–90.

Heiri, C., Wolf, A., Rohrer, L., Bugmann, H., 2009. Forty years of natural dynamics in Swiss beech forests: structure, composition, and the influence of former management. Ecol. Appl. **19**: 1920–1934.

Hobi, M.L., Commarmot, B., Bugmann, H., 2015a. Pattern and process in the largest primeval beech forest of Europe (Ukrainian Carpathians). J. Veg. Sc. **26**: 323–336.

Hobi, M.L., Ginzler, C., Commarmot, B., Bugmann, H., 2015b. Gap pattern of the largest primeval beech forest of Europe revealed by remote sensing. Ecosphere **6(5)**: 76.

Hoeksema, J.D., 2015. Experimentally testing effects of mycorrhizal networks on plant-plant interactions and distinguishing among mechanisms. In: Horton, T.R. (ed.) Mycorrhizal Networks. Springer, pp. 255-279.

Holland, J.H., 1996. Studying complex adaptive systems. J. Syst. Sci. Compl. **19**: 1–8.

Holmgren, M., Scheffer, M., Huston, M.A., 1997. The interplay of facilitation and competition in plant communities. Ecol. Lett. **78(7)**: 1966–1975.

Holmgren, M., Scheffer, M., 2010. Strong facilitation in mild environments: the stress gradient hypothesis revisited. Ecology **98**: 1269–1275.

Holmgren, M., Gómez-Aparicio, L., Quero, J.L., Valladares, F., 2012. Non-linear effects of drought under shade: reconciling physiological and ecological models in plant communities. Oecologia **169**: 293–305.

Holzwarth, F., Kahl, A., Bauhus, J., Wirth, C., 2013. Many ways to die: partitioning tree mortality dynamics in a near-natural mixed deciduous forest. Ecology **101**: 220–230.

Huckfeldt, R., Johnson, P.E., Sprague, J.D., 2004. Political Disagreement: The Survival of Diverse Opinions within Communication Networks. Cambridge University Press, Cambridge, UK. 274 p.

Hunter, A.F., Aarssen, L.W., 1988. Plants helping plants. BioScience **38**: 34–40.

Hülsmann, L., Bugmann, H.K.M., Commarmot, B., Meyer, P., Zimmermann, S., Brang, P., 2016. Does one model fit all? Patterns of beech mortality in natural forests of three European regions. Ecol. Appl. **26**: 2465–2479.

Huston, M., DeAngelis, D., Post, W., 1988. New computer models unify ecological theory. BioScience **38**: 682–691.

Itoo, Z.A., Reshi, Z.A., 2013. The multifunctional role of ectomycorrhizal associations in forest ecosystem processes. Bot. Rev. **79**: 371–400.

Jacob, A., Hertel, D., Leuschner, C., 2013. On the significance of belowground overyielding in temperate mixed forests: separating species identity and species diversity effects. Oikos **122**: 463–473.

Jansen, M.J.W., 1999. Analysis of variance designs for model output. Comput. Phys. Commun. **117**: 35–43.

Jeltsch, F., Moloney, K.A., Milton, S.J., 1999. Detecting process from snapshot pattern: lessons from tree spacing in the southern Kalahari. Oikos **85**: 451–467.

Jucker, T., Bouriaud, O., Coomes, D.A., 2015. Crown plasticity enables trees to optimize canopy packing in mixed-species forests. Funct. Ecol. **29**: 1078–1086.

Juchheim, J., Ammer, C., Schall, P., Seidel, D., 2017a. Canopy space filling rather than conventional measures of structural diversity explains productivity of beech stands. For. Ecol. Manage. **395**: 19–26.

Juchheim, J., Annighöfer, P., Ammer, C., Calders, K., Raumonen, P., Seidel, D., 2017b. How management intensity and neighborhood composition affect the structure of beech (Fagus sylvatica L.) trees. Trees **31**: 1723–1735.

Kim, Y., Maroulis, S., 2018. Rethinking social welfare fraud from a complex adaptive systems perspective. Admin. Soc. **50(1)**: 78–100.

Koop, H., Hilgen, P., 1987. Forest dynamics and regeneration mosaic shifts in unexploited beech (Fagus sylvatica) stands at Fontainebleau (France). For. Ecol. Manage. **20**: 135–150.

Korpel, S., 1995. Die Urwälder der Westkarpaten. Fischer, Stuttgart Jena, NY. 310 p.

Klein, T., Siegwolf, R.T.W., Körner, C., 2016. Belowground carbon trade among tall trees in a temperate forest. Science **352**: 342–344.

Kucbel, S., Saniga, M., Jaloviar, P., Vencurik, J., 2012. Stand structure and temporal variability in old-growth beech-dominated forests of the northwestern Carpathians: A 40-years perspective. For. Ecol. Manage. **264**: 125–133.

Kunstler, G., Curt, T., Bouchaud, M., Lepart, J., 2005. Growth, mortality, and morphological response of European beech and downy oak along a light gradient in sub-Mediterranean forest. Can. J. For. Res. **35**: 1657–1668.

Kunstler, G., Albert, C.H., Courbaud, B., Lavergne, S., Thuiller, W., Vieilledent, G., Zimmermann, N.E., Coomes, D.A., 2011. Effects of

162

competition on tree radial-growth vary in importance but not in intensity along climatic gradients. Ecology **99**: 300–312.

Kunstler, G., Lavergne, S., Courbaud, B., Thuiller, W., Vieilledent, G., Zimmermann, N.E., Kattge, J., Coomes, D.A., 2012. Competitive interactions between forest trees are driven by species' trait hierarchy, not phylogenetic or functional similarity: implications for forest community assembly. Ecology Lett. **15**: 831–840.

Kunstler, G., Falster, D., Coomes, D.A., Hui, F., Kooyman, R.M., Laughlin, D.C., Poorter, L., Vanderwel, M., Vieilledent, G., Wright, S.J., Aiba, M., Baraloto, C., Caspersen, J., Cornelissen, J.H.C., Gourlet-Fleury, S. Hanewinkel, M., Nerault, B., Kattge, J., Kurokawa, H., Onoda, Y., Peñuelas, J., Poorter, H., Uriarte, M., Richardson, S., Ruiz-Benito, P., Sun, I.-F., Ståhl, G., Swenson, N.G., Thompson, J., Westerlund, B., Wirth, C., Zavala, M.A., Zeng, H., Zimmermann, J.K., Zimmermann, N.E., Westoby, M., 2016. Plant functional traits have globally consistent effects on competition. Nature **529**: 204–207.

Kytöviita, M.-M., Vestberg, M., Tuomi, J., 2003. A test of mutual aid in common mycorrhizal networks: established vegetation negates benefit in seedlings. Ecology **84**: 898–906.

Landsberg, J.J., Waring, R.H., Coops, N.C., 2003. Performance of the forest productivity model 3-PG applied to a wide range of forest types. For. Ecol. Manage. **172**: 199–214.

Lang, C., Dolynska, A., Finkeldey, R., Polle, A., 2010. Are beech (Fagus sylvatica L.) roots territorial? For. Ecol. Manage. **260**: 1212–1217.

Lang, C., Seven, J., Polle, A., 2011. Host preferences and differential contributions of deciduous tree species shape mycorrhizal species richness in a mixed Central European forest. Mycorrhiza **21**: 297–308.

Lei, P., Scherer-Lorenzen, M., Bauhus, J., 2012. Belowground facilitation and competition in young tree species mixtures. For. Ecol. Manage. **265**: 191–200.

Leibundgut, H., 1959. Über Zweck und Methodik der Struktur- und Zuwachsanalysen von Urwäldern. SZF **110**: 111–124.

Leibundgut, H., 1993. Europäische Urwälder. Haupt Bern, Stuttgart. 350 p.

Lemée., G., 1987. Dynamique de fermeture par régénération et évolutin morphométrique du hêtre dans les vides d'une forêt non exploiteé (Réserves biologuques de la fôret de Fontainebleau). Bull. Ecol. **18**: 1–11.

Leroy, C. Sabatier, S., Wahyuni, N., Barczi, J.-F., Dauzat, J., Laurans, M., Auclair, D., 2009. Virtual trees and light capture: a method for optimizing agroforestry stand design. Agroforest. Syst. **77(1)**: 37–47.

Leuschner, C., Hertel, D., Coners, H., Büttner, V., 2001. Root competition between beech and oak: a hypothesis. Oecologia **126**: 267–284.

Leuschner, C., Ellenberg, H., 2017. Ecology of Central European Forests. Vegetation Ecology of Central Europe, vol. I, Springer nature, Cham. 971 p.

Levin, S.A., 1998. Ecosystems and the biosphere as complex adaptive systems. Ecosystems **1**: 431–436.

Levin, S.A., 2002. Complex adaptive systems: exploring the known, the unknown and the unknowable. B. Am. Math. Soc. **40(1)**: 3–19.

Liénard, J., Strigul, N., 2016. An individual-based forest model links canopy dynamics and shade tolerances along a soil moisture gradient. R. Soc. Open sci. **3**: 150589.

164

Ligot, G., Balandier, P., Courbaud, B., Claessens, H., 2014. Forest radiative transfer models: which approach for which application? Can. J. For. Res. **44**: 385–397.

Lin, Y., Berger, U., Grimm, V., Ji, Q.-R., 2012. Differences between symmetric and asymmetric facilitation matter: exploring the interplay between modes of positive and negative plant interactions. Ecology **100**: 1482–1491.

Lombardi, F., Marchetti, M., Corona, P., Merlini, P., Chirici, G., Tognetti, R., Burrascano, S., Alivernini, A., Puletti, N., 2015. Quantifying the effect of sampling plot size on the estimation of structural indicators in old-growth forest stands. For. Ecol. Manage. **346**: 89–97.

Longuetaud, F., Piboule, A., Wernsdörfer, H., Collet, C., 2013. Crown plasticity reduces inter-tree competition in a mixed broadleaved forest. Eur. J. For. Res. **132**: 621–634.

Madsen, P., Hahn, K., 2008. Natural regeneration in a beech-dominated forest managed by close-to-nature principles–a gap cutting based experiment. Can. J. For. Res. **38**: 1716–1729.

Maestre, F.T., Valladares, F. Reynolds, J.F., 2005. Is the change of plant-plant interactions with abiotic stress predictable? A meta-analysis of field results in arid environments. Ecology **93**: 748–757.

Maestre, F.T., Callaway, R.W., Valladares, F. Lortie, C.J., 2009. Refining the stress-gradient hypothesis for competition and facilitation in plant communities. Ecology **97**: 199–205.

Markgraf, F., 1931. Aus den südosteuropäischen Urwäldern. I. Die Wälder Albaniens. Zeitschrift f. Forst- u. Jagdwesen 310–319.

Mausolf, K., Wilm, P., Härdtle, W., Jansen, K., Schuldt, B., Sturm, K., von Oheimb, G., Hertel, D., Leuschner, C., Fichtner, A., 2018. Higher drought sensitivity of radial growth of European beech in managed than in unmanaged forests. Sci. Total Environ. **642**: 1201–1208.

Mayer, H., 1978. Über die Bedeutung der Urwaldforschung für den Gebirgswaldbau. AFZ **33(24)**: 691–693.

McArthur, R.H., MacArthur, J.W., 1961. On birds species diversity. Ecology **42**: 594–598.

McIntire, E.J., Fajardo, A., 2011. Facilitation within species: a possible origin of group-selected superorganisms. Am. Nat. **178**: 88–97.

McIntire, E.J., Fajardo, A., 2013. Facilitation as a ubiquitous driver of biodiversity. New Phytol. **201**: 403–416.

Merrild, M.P., Ambus, P., Rosendahl, S., Jakobsen, I., 2013. Common arbuscular mycorrhizal networks amplify competition for phosphorus between seedlings and established plants. New Phytol. **200**: 229–240.

Messier, C., Puettmann, K., Chazdon, R., Andersson, K.P., Angers, V.A., Brotone, L., Filotas, E., Tittler, R., Parrott, L., Levin, S.A., 2014. From management to stewardship: viewing forests as complex adaptive systems in an uncertain world. Conserv. Lett. **8(5)**: 368–377.

Messier, C., Nikinmaa, E., 2000. Effects of light availability and sapling size on the growth, biomass allocation, and crown morphology of understory sugar maple, yellow birch, and beech. Ecoscience **7**: 345–356.

Metz, J., Seidel, D., Schall, P., Scheffer, D., Schulze, E.D., Ammer, C., 2013. Crown modelling by terrestrial laser scanning as an approach to assess the effect on aboveground intra- and interspecific competition on tree growth. For. Ecol. Manage. **310**: 275–288.

Meyer, P., 1995. Untersuchungen waldkundlicher Entwicklungstendenzen und methodischer Fragestellungen in Buchen- und Buchenmischwaldbeständen niedersächsischer Naturwaldreservate (NWR). Diss. Forstl. Fak. Universität Göttingen.

Meyer, P., Tabaku, V., v. Lüpke, B., 2003. Die Struktur albanischer Rotbuchen-Urwälder – Ableitungen für eine naturnahe Buchenwirtschaft. Forstw. Centralbl. **122**: 47–58.

Michalet, R., Le Bagousse-Pinguet, Y., Maalouf, J.-P., Lortie, C., 2014. Two alternatives to the stress gradient hypothesis at the edge of life: the collapse of facilitation and the switch from facilitation to competition. J.Veg. Sci. **25**: 609–613.

Mitleton-Kelly, E., 1997. Organisations as co-evolving complex adaptive systems. British Academy of Management Conference.

Mitchell, K.J., 1975. Dynamics and simulated yield of douglas-fir. For. Sci. Monogr. **17**: 39 p.

Modrý, M., Hubený, D., Rejšek, K., 2004. Differential response of naturally regenerated European shade tolerant tree species to soil type and light availability. For. Ecol. Manage. **188**: 185–195.

Monserud, R.A., Ek, A.R., 1974. Plot edge bias in forest growth simulation models. Can. J. For. Res. **4**: 419–423.

Monserud, R.A., Sterba, H., 1996. A basal area increment model for individual trees growing in even- and unevenaged stands in Austria. For. Ecol. Manage. **80**: 57–80.

Monserud, R.A., Sterba, H., 1999. Modeling individual tree mortality for Austrian forest species. For. Ecol. Manage. **113**: 109–123.

Morris, M.D., 1991. Factorial sampling plans for preliminary computational experiments. Technometrics **21**: 239–245.

Muck, P., Borchert, H., Hahn, J., Immler, T., Joos, A., Konnert, M., Walentowski, H., Walter, A., 2009. Die Rotbuche – Mutter des Waldes. LWF aktuell **69**: 54–57.

Münch, D., 1993. Bestandesdynamik von Naturwaldreservaten. Eine Dauerbeobachtung in Luftbildzeitreihen. Diss. Universität Freiburg.

Muth, C.C., Bazzaz, F.A., 2002. Tree canopy displacements at forest gap edges. Can. J. For. Res. **32**: 247–254.

Muth, C.C., Bazzaz, F.A., 2003. Tree canopy displacement and neighborhood interactions. Can. J. For. Res. **33**:1323–1330.

Nagel, J., 1999. Konzeptionelle Überlegungen zum schrittweisen Aufbau eines waldwachstumskundlichen Simulationssystems für Norddeutschland. Schriften aus der forstlichen Fakultät der Universität Göttingen 128, Paul Parey. Frankfurt. 122 p.

Nagel, T.A., Diaci, J., 2006. Intermediate wind disturbance in an old-growth beech-fir forest in southeastern Slovenia. Can. J. For. Res. **36**: 629–638.

Nair, A., Reed-Tsochas, F., 2019. Revisiting the complex adaptive systems paradigm: Leading perspectives for researching operations and supply chain management basis. J. Oper. Manag. **65**: 80–92.

Nelson, W.A., Bjørnstad, O.N., Yamanaka, T., 2013. Recurrent insect outbreaks caused by temperature-driven changes in system stability. Science **341**: 796–799.

Neuner, S. Albrecht, A., Cullmann, D., Engels, F., Griess, V.C., Hahn, A., Hanewinkel, M., Härtl, F., Kölling, C., Staupendahl, K., Knoke, T., 2015.

Survival of Norway spruce remains higher in mixed stands under a dryer and warmer climate. Global Change Biol. **21**: 935–946.

Niinemets, Ü, 2010. A review of light interception in plant stands from leaf to canopy in different plant functional types and in species with varying shade tolerance. Ecol. Res. **25(4)**: 693–714.

Nocentini, A., 2008. Structure and management of beech (*Fagus sylvatica* L.) forests in Italy. iForest **2**: 105–113.

Nothdurft, A., 2013. Spatio-temporal prediction of tree mortality based on long–term sample plots, climate change scenarios and parametric frailty modeling. For. Ecol. Manage. **291**: 43–54.

von Oheimb, Westphal, C., Tempel, H., Härdtle, W., 2005. Structural pattern of a near-natural beech forest (Fagus sylvatica) (Serrahn, Northeast Germany). For. Ecol. Manage. **212**: 253–263.

von Oheimb, G., Härdtle, W., Eckstein, D., Engelke, H.-H., Hehnke, T., Wagner, B., Fichtner, A., 2014. Does forest continuity enhance the resilience of trees to environmental change? PLoS ONE **9**: e113507.

Pacala, S.W., Canham, C.D., Saponara, J., Silander, J.A., Kobe, R.K., Ribbens, E., 1996. Forest models defined by field measurements: estimation, error analysis and dynamics. Ecol. Monogr. **66(1)**: 1–43.

Pach, M., Podlaski, R., 2015. Tree diameter structural diversity in Central European forests with Abies alba and Fagus sylvatica: managed versus unmanaged forest stands. Ecol. Res. **30**: 367–384.

Pafetti, D., Travaglini, D., Buonamici, A., Necentini, S., Vendramin, G.G., Giannini, R., Vettori, C., 2012. The influence of forest management on beech (*Fagus sylvatica* L.) stand structure and genetic diversity. For. Ecol. Manage. **284**: 34–44.

Paquette, A., Messier, C., Perinet, P., Cogliastro, A., 2008. Simulating light availability under different hybrid poplar clones in a mixed intensive plantation system. For. Sci. **54(5)**: 481–489.

Paluch, J.G., Kolodziej, Z., Pach, M., Jastrzębski, R., 2015. Spatial variability of close-to-primeval Fagus-Abies-Picea forests in the Western Carpathians (Central Europe): a step towards a generalised pattern. Eur. J. For. Res. **134**: 235–246.

Parker, D.C., Manson, S.M., Janssen, M.A., Hoffmann, M.J., Deadman, P., 2003. Multi-agent systems for the simulation of land-use and land-cover change: a review. Ann. Assoc. Am. Geogr. **93**: 314–337.

Pebesma, E.J., Bivand, R.S., 2005. Classes and methods for spatial data in R. R News **5(2)** https://cran.r-project.org/doc/Rnews/.

Peck, J.E., Commarmot, B., Hobi, M.L., Zenner, E.K., 2015. Should reference conditions be drawn from a single 10 ha plot? Assessing representativeness in a 10,000 ha old-growth European beech forest. Restor. Ecol. **23**: 927–935.

Pelissier, R., Goreaud, F., 2015. A Fast Unbiased Implementation of the K-function Family for Studying Spatial Point Patterns in Irregular-Shaped Sampling Windows. J. Stat. Softw. **63(6)**: 1–18. http://www.jstatsoft.org/v63/i06/.

Peterken, G., 1996. Natural Woodland. Cambridge University Press, Cambridge. 522 p.

Peters, R., Olagoke, A., Berger, U., 2019. A new mechanistic theory of self-thinning: Adaptive behaviour of plants explains the shape and slope of self-thinning trajectories. Ecol. Model. **390**: 1–9.

Petriţan, A.M., von Lüpke, Burghard, Petriţan, I.C., 2009. Influence of light availability on growth, leaf morphology and plant architecture of beech (Fagus sylvatica L.), maple (Acer pseudplatanus L.), and ash (Fraxinus excelsior L.) saplings. Eur. J. For. Res. **128**: 61–74.

Pianosi, F., Beven, K., Freer, J., Hall, J.W., Rougier, J., Stephenson, D.B., Wagener, T., 2016. Sensitivity analysis of environmental models: A systematic review with practical workflow. Environ. Modell. Softw. **79**: 214e232.

Piccolroaz, S., Calamita, E., Majone, B., Gallice, A., Siviglita, A., Toffolon, M., 2016. Prediction of river water temperature: a comparison between a new family of hybrid models and statistical approaches. Hydrol. Proc. **30**: 3901–3917.

Piovesan, A., Di Filippo, A., Alessandrini, A., Biondi, F., Schirone, B., 2005. Structure, dyanmics and dendroecology of an old-growth Fagus forest in the Apennines. J. Veg. Sci. **16**: 13–28.

Piovesan, G., Alessandrini, A., Baliva, M., Chiti, T., D'Andrea, L., De Cinti, B., Di Filippo, A., Hermanin, L., Lauteri, M., Mugnozza, G.S., Schirone, B., Ziaco, E., Matteuci, G., 2010. Structural patterns, growth processes, carbon stocks in an Italian network of old-growth beech forests. L'Italia Forestale e Montana **65**: 557–590.

Pommerening, A., Stoyan, D., 2006. Edge-correction needs in estimation indices of spatial forest structure. Can. J. For. Res. **36**: 1723–1739.

Prescott, C.E., Grayston, S.J., 2013. Tree species influence on microbial communities in litter and soil: current knowledge and research needs. For. Ecol. Manage. **309**: 19–27.

Pretzsch, H., 1992. Konzeption und Konstruktion von Wuchsmodellen für Rein- und Mischbestände. Forstliche Forschungsberichte München 115.

Forstwissenschaftliche Fakultät der Universität München und Bayerische Forstliche Versuchs- und Forschungsanstalt. 332 p.

Pretzsch, H., 2001. Modellierung des Waldwachstums. Verlag Eugen Ulmer. 357 p.

Pretzsch, H., Biber, P., Dursky, J., 2002. The single tree-based stand simulator SILVA: construction, application and evaluation. For. Ecol. Manage. **162**: 3–21.

Pretzsch, H., 2003. The elasticity of growth in pure and mixed stands of Norway spruce (*Picea abies* (L.) Karst.) and common beech (*Fagus sylvatica* L.). J. For. Sci. **49**: 491–501.

Pretzsch, H., 2005. Stand density and growth of Norway spruce (*Picea abies* (L.) Karst.) and European beech (*Fagus sylvatica* L.): evidence from long-term experimental plots. Eur. J. For. Res. **124**: 193–205.

Pretzsch, H., 2006. Species-specific allometric scaling under self-thinning: evidence from long-term plots in forest stands. Oecologia **146**: 572–583.

Pretzsch, H., Schütze, G., 2005. Crown allometry and growing space efficiency of Norway spruce (*Picea abies* (L.) Karst.) and European beech (*Fagus sylvatica* L.) in pure and mixed stands. Plant Biol. **7**: 628–639.

Pretzsch, H., Schütze, G., 2009. Transgressive overyielding in mixed compared with pure stands of Norway spruce and European beech in Central Europe: evidence on stand level and explanation on individual tree level. Eur. J. For. Res. **128**: 183–204.

Pretzsch, H., Mette, T., 2008. Linking stand-level self-thinning allometry to the tree-level leaf biomass allometry. Trees **22**: 611–622.

Pretzsch, H., 2009. Forest Dynamics, Growth and Yield. From Measurement to model. Springer, Berlin. 664 p.

172

Pretzsch, H., Block, J., Dieler, J., Dong, P.H., Kohnle, U., Nagel, J., Spellmann, H., Zingg, A., 2010. Comparison between the productivity of pure and mixed stands of Norway spruce and European beech along an ecological gradient. Ann. For. Sci. **67**: 712.

Pretzsch, H., Schütze, G., Uhl, E., 2012. Resistance of European tree species to drought stress in mixed versus pure forests: evidence of stress release by interspecific facilitation. Plant Biol. **15**: 483–495.

Pretzsch, H., Bielak, K., Block, J., Bruchwald, A., Dieler,J., Ehrhart, H.-P., Kohnle, U., Nagel, J., Spellmann, H., Zasada, M., Zingg, A., 2013. Productivity of mixed versus pure stands of oak (Quercus pertrea (Matt.) Liebl. and Quercus robur L.) and European beech (Fagus sylvatica L.) along an ecological gradient. Eur. J. For. Res. **132**: 263–280.

Pugnaire, F.I., Armas, C., Maestre, F.T., 2011. Positive plant interactions in the Iberian Southeast: Mechanisms, environmental gradients, and ecosystem function. J. Arid Environ. **75**: 1310–1320.

Puettmann, K.J., Messier, C., Coates, K.D., 2013. Managing forests as complex adaptive systems. Introductory concepts and applications. In: Managing Forests as Complex Adaptive Systems. Messier, C., Puettmann, K.J., Coates, K.D. (eds.). pp 4–16.

R Development Core Team, 2017. R: A language and environment for statistical computing. R Foundation for Statistical Computing. Vienna, Austria. http://www.R-project.org.

Rademacher, C., Neuert, C., Grundmann, V., Wissel, C., Grimm, V., 2004. Reconstructing spatiotemporal dynamics of Central European natural beech forests: the rule-based forest model BEFORE. For. Ecol. Manage. **194**: 349–368.

Radke, P.J., Burkhart, H.W., 1998. A comparison of methods for edge-bias compensation. Can. J. For. Res. **28**: 942–945.

Railsback, S.F., 2001. Concepts from complex adaptive systems as a framework for individual-based modelling. Ecol. Model. **139**: 47–62.

Rajaniemi, T. K., 2003. Evidence for size asymmetry of belowground competition. Basic Appl. Ecol. **4**: 239–247.

Reineke, L.H., 1933. Perfecting a stand density index for even-aged forests. J. Agr. Res. **46**: 627-638.

Rewald, B., Leuschner, C., 2009a. Belowground competition in a broad-leaved temperate mixed forest: pattern analysis and experiments in a four-species stand. Eur. J. For. Res. **128**: 387–398.

Rewald, B., Leuschner, C., 2009b. Does root competition asymmetry increase with water availability? Plant Ecol. Divers. **2**: 255–264.

del Rio, M., Condés, S., Pretzsch, H., 2014. Analyzing size-symmetric vs. size-asymmetric and intra- vs. interspecific competition in beech (Fagus sylvatica L.) mixed stands. For. Ecol. Manage. **325**: 90–98.

Ringler, P., Keles, D., Fichtner, W., 2016. Agent-based modelling and simulation of smart electricity grids and markets - A literature review. Renew. Sust. Energ. Rev. **57**: 205–215.

Ripley, B.D., 1976. The second-order analysis of stationary point process. J. Appl. Probab. **13**: 255–266.

Ritter, E., Dalsgaard, L., Einhorn., K.S., 2005. Light, temperature and soil moisture regimes following gap formation in a semi-natural beech-dominated forest in Denmark. For. Ecol. Manage. **206**: 15–33.

174

Ritter, E., Vesterdal, L., 2006. Gap formation in Danish beech (Fagus sylvatica) forests of low management intensity: soil moisture and nitrate in soil solution. Eur. J. For. Res. **125**: 139–150.

Rugani, T., Diaci, J., Hladnik, D., 2013. Gap dynamics and structure of two old-growth beech forest remnants in Slovenia. PLoS ONE **8(1)**: e52641.

Sachs, L., 2004. Angewandte Statistik. Springer Heidelberg Berlin. 889 p.

Sabatini, F.M., Burrascano, S., Keeton, W.S., Leverls, C., Lindner, M., Pötschner, F., Verkerk, P.J., Bauhus, J., Buchwald, E., Chaskovsky, O., Debaive, N., Horváth, F., Garbarino, M., Grigoriadis, N., Lombardi, F., Duarte, I.M., Meyer, P., Midteng, R., Mikac, S., Mikoláš, M., Motta, R., Mozgeris, G., Nunes, L., Panayotov, M., Ódor, P., Ruete, A., Simovski, B., Stillhard, J., Svoboda, M., Szwagrzyk, J., Tikkanen, O.-P., Volosyanchuk, R., Vrska, T., Zlatanov, T., Kuemmerle, T., 2017. Where are Europe's last primary forests? Divers. Distrib. **24**: 1426–1439.

Saltelli, P., Annoni, P., Azzini, I., Campolongo, F., Ratto, M., Tarantola, S., 2010. Variance-based sensitivity analysis of model output. Design and estimator for the total sensitivity index. Comput. Phys. Commun. **181**: 259–270.

Schmolke, A., Thorbek, P., DeAngelis, D.L., Grimm, V., 2010. Ecological models supporting environmental decision making: a strategy for the future. Trends Ecol. Evol. **25**: 479–486.

Schröter, M., Härdtle, W., von Oheimb, G., 2012. Crown plasticity and neighborhood interactions of European beech (Fagus sylvatica L.) in an old-growth forest. Eur. J. For. Res. **131**: 787–798.

Schwinning, S., Fox, G.A., 1995. Population dynamic consequences of competitive symmetry in annual plants. Oikos **72**: 422–432.

175

Schwinning, S., Weiner, J., 1998. Mechanisms determining the degree of size- asymmetry in competition among plants. Oecologia **113**: 447–455.

Šebková, B., Šamonil, P., Janík, D., Adam, D., Krål, K., Vrška, T., Libor, H., Unar, P., 2011. Spatial and volume patterns of an unmanaged submontane mixed forest in Central Europe: 160 years of spontaneous dynamics. For. Ecol. Manage. **262**: 873–885.

Sefidi, K., Mohadjer, M.R.M., Mosandl, R., Copenheaver, C.A., 2011. Canopy gaps and regeneration in old-growth Oriental beech (Fagus orientalis Lipsky) stands, northern Iran. For. Ecol. Manage. **262**: 1094–1099.

Seidl, R., Fernandes, P.M., Fonseca, T.F., Gillet, F., Jönsson, A.M., Merganičová, K., Netherer, S., Arpaci, A., Bontemps, J.-D., Bugmann, H., Ganzález-Olabarria, J.R., Lasch, P., Meredieu, C., Moreira, F., Schelhaas, M.-J., Mohren, F., 2011. Modelling natural disturbances in forest ecosystems: a review. Ecol. Model. **222**: 903–924.

Seven, J., Polle, A., 2014. Subcellular nutrient element localization and enrichment in ecto- and arbuscular mycorrhizas of field-grown beech and ash trees indicate functional differences. PLoS ONE **9**: e114672.

Shugart, H.H., West, D.C., 1977. Development of an Appalachian deciduous forest succession model and its application to assessment of the impact of the chestnut blight. J. Environ. Manage. **5**: 161–179.

Simard, S.W., Beiler, K.J., Bingham, M.A., Deslippe, J.R., Philip, L.J., Teste, F.P., 2012. Mycorrhizal networks: Mechanisms, ecology and modelling. Fungal Biol. Rev. **26**: 39–60.

Simard, S.W.,Martin, K., Vyse, A., Larson, B., 2013. Meta-networks of fungi, fauna and flora as agents of complex adaptive systems. In: Managing Forests as Complex Adaptive Systems. Messier, C., Puettmann, K.J., Coates, K.D. (eds.). pp 133–164.

Smejkal, G.M., Bindiu, C., Visoiu-Smejkal, D., 1997. Banater Urwälder. Ökologische Untersuchungen in Rumänien. Mirton Verlag, Temeswar. 198 p.

Szmyt, J., 2012. Spatial structure of managed beech-dominated forest: applicability of nearest neighbors indices. Dendrobiology **68**: 69–76.

Schütz, J.-P., Zingg, A., 2010. Improving estimations of maximal stand density by combining Reineke's size-density rule and the yield level, using the example of spruce (Picea abies (L.) Karst.) and European Beech (Fagus sylvatica L.). Ann. For. Sci. **67**: 507.

Sobol, I.M., 1976. Uniformly distributed sequences with an addition uniform property. USSR Computational Mathematics and Mathematical Physics **16**: 236–242.

Soliveres, S., Eldridge, D.J., Maestre, F.T., Bowker, M.A., Tighe, M., Escudero, A., 2011. Microhabitat amelioration and reduced competition among understory plants as drivers of facilitation across environmental gradients: Towards a unifying framework. Perspect. Plant Ecol. **13**: 247–258.

Stillmann, J., Thorarinsdottir, T., Keenlyside, N., Schaller, N., Alexander, L.V., Hegeri, G., Seneviratne, S.I., Vautard, R., Zhang, X., Zwiers, F.W., 2011. Understanding, modeling and predicting weather and climate extremes: challenges and opportunities. Weather Clim. Extremes **18**: 65–74.

Stoll, P., Weiner, J., 2000. Neighbourhood view of interactions among plants. In: Dieckmann, U., Law, R., Metz, J.A.J. (Eds.), The Geometry of Ecological Interactions. Cambridge University Press, Cambridge, p. 11-27.

Sturm, K., 1993. Prozessschutz - ein Konzept für naturschutzgerechte Waldwirtschaft. Zeitschrift für Ökologie und Naturschutz **2**: 181–192.

Tabaku, V., 2000. Struktur von Buchen-Urwäldern in Albanien im Vergleich mit deutschen Buchen-Naturwaldreservaten und Wirtschaftswäldern. Cuvillier Verlag, Göttingen. 220 p.

Taylor, A.R., Chen, H.Y.H., VanDamme, L., 2009. A review of forest succession models and their suitability for forest management planning. For. Sci. **55(1)**: 22–36.

Tesfatsion, L., 2002. Agent-based computational economics: growing economies from the bottom up. Artif. Life **8**: 55–82.

Tielbörger, K., Kadmon, R., 2000. Temporal environmental variation tips the balance between facilitation and interference in desert plants. Ecology **81**: 1544–1533.

Torquato, S., 2002. Random heterogeneous materials. Microstructure and macroscopic porperties. Interdisciplinary Applied Mathematics 16. Springer, New York. 703 p.

Trotsiuk, V. Hobi, M., Commarmot, B., 2012. Age structure and disturbance dynamics of the relic virgin beech forest Uholka (Ukrainian Carpathians). For. Ecol. Manage. **265**: 181–190.

Turner, R., 2018. deldir: Delaunay Triangulation and Dirichlet (Voronoi) Tessellation. R package version 0.1-14. https://CRAN.R-project.org/package=deldir.

Uria-Diez, J., Pommerening, A., 2017. Crown plasticity in Scots Pine (Pinus sylvestris L.) as a strategy of adaption to competition and environmental factors. Ecol. Model. **356**: 117–126.

Valtanen, K., Eissfeller, V., Beyer, F., Hertel, D., Scheu, S., Polle, A., 2014. Carbon and nitrogen fluxes between beech and their ectomycorrhizal assemblage. Mycorrhiza **24**: 645–650.

Vilà, M., Carrillo-Gavilán, A., Vayreda, J., Bugmann, H., Fridman, J., Grodzki, W., Haase, J., Kunstler, G., Schelhaas, M., Trasobares, A., 2013. Disentangling biodiversity and climatic determinants of wood production. PLoS ONE **8**: e53530.

Vincent, G., Harja, D., 2008. Exploring ecological significance of tree crown plasticity through three-dimensional modelling. Ann. Bot. London **101**: 1221–1231.

Volkmann, T.H.M., Haberer, K., Gessler, A., Weiler, M., 2016. High-resolution isotope measurements resolve rapid ecohydrological dynamics at the soil-plant interface. New. Phytol. **210**: 839–849.

Vološčuk, I., 2014. Joint Slovak-Ukraine-Germany beech ecosystems as the World Natural Heritage. Ekológia Bratislava **33(3)**: 286–300.

Wang, W., Peng, C., Kneeshaw, D.D., Larocque, G.R., Luo, Z., 2012. Drought–induced tree mortality: ecological consequences, causes, and modeling. Env. Rev. **20**: 2109–121.

Wagner, S., 1999. Ökologische Untersuchungen zur Initialphase der Naturverjüngung in Eschen-Buchen-Mischbeständen. Sauerländer Verlag, Frankfurt am Main. 262 p.

Wagner, S., Collet, C., Madsen, P., Nakashizuka, T., Nyland, R.D., Sagheb-Talebi, K., 2010. Beech regeneration research: From ecological to silvicultural aspects. For. Ecol. Manage. **259**: 2172–2182.

Watt, A.S., 1925. On the ecology of British beechwoods with special references to their regeneration. J. Ecol. **13**: 27–73.

Weiner, J., Stoll, P., Muller-Landau, H., Jasentuliyana, A., 2001. The effects of density, spatial pattern and competitive symmetry on size variation in simulated plant population. Am. Nat. **158**: 438–450.

Weiner J., Damgaard C., 2006. Size-asymmetric competition and size-asymmetric growth in a spatially-explicit zone-of-influence model. Ecol. Res. **21**: 707–712.

Weiskittel, A.R., Hann, D.W., Kershaw, J.A., Vanclay, J.K., 2011. Forest growth and yield modeling. John Wiley & Sons, Ltd, West Sussex, UK., 415 p.

Werner, G.D.A., Kiers, E.T., 2015. Partner selection in the mycorrhizal mutualism. New Phytol. **205**: 1437–1442.

Westphal, C., Härdtle, W., von Oheimb, G., 2004. Forest History, Continuity and Dynamic Naturalness. In: Forest Biodiversity: Lessons from History for Conservation (eds. Honnay, O., Verheyen, B., Bossuyt, B., Hermy, M.), CAB International, Wallingford, UK, pp. 205–220.

Wiedemann, E., 1936. Die Fichte 1936. Erweiterte Fortführung der Berichte von Geheimrat Schwappach über die preußischen Versuchsflächen. Schaper, Hannover, 248 p.

White, P.S., Jentsch, A., 2001. The search for generality in studies of disturbance and ecosystem dynamics. Prog. Bot. **62**: 399–449.

White, J.W., Rassweiler, A., Samhouri, J.F., Stier, A.C., White, C., 2013. Ecologists should not use statistical significance tests to interpret simulation model results. Oikos **123**: 385–388.

Wiegand, T., Jeltsch, F., Hanski, I., Grimm, V., 2003. Using pattern-oriented modeling for revealing hidden information: a key for reconciling ecological theory and application. Oikos **100**: 209–222.

Wickham, H., 2011. The Split-Apply-Combine Strategy for Data Analysis. J. Stat. Softw. **40**: 1–29.

Winter, S., 2005. Ermittlung von Struktur-Indikatoren zur Abschätzung des Einflusses forstlicher Bewirtschaftung auf die Biozönosen von Tiefland-Buchenwäldern. Dissertation. Technische Universität Dresden. 321 p.

Wissel, C., 1992. Modeling the mosaic cycle of a Middle-European beech forest.. Ecol. Model. **63**: 29–43.

Wood, S.N., 2017. Generalized Additive Models: An Introduction with R. 2nd edition. Chapman and Hall/CRC, 476 p.

Wu, H., Sharpe, P.J.H., Walker, J., Penridge, L.K., 1985. Ecological field theory: A spatial analysis of resource interference among plants. Ecol. Model. **29**: 215–243.

Wubet, T., Christ, S., Schöning, I., Boch, S., Gawlich, M., Schnabel, B., Fischer, M., Buscot, F., 2012. Differences in soil fungal communities between European beech (Fagus sylvatica L.) dominated forests are related to soil and understory vegetation. PLoS ONE **7(10)**: e47500.

Wunder, J.B., Brzeziecki, B., Zybura, H., Reineking, B., Bigler, C., Bugmann, H., 2008. Growth–mortality relationships as indicators of life-history strategies: a comparison of nine tree species in unmanaged European forests. Oikos **117**: 815–828.

Wykoff, W.R., Crookston, N.L., Stage, A.R., 1982. User's guide to the stand prognosis model. U.S. For. Serv. Gen. Techn. Rep. INT-133, Ogden, Utah, 112 p.

Yoda, K., T., Ogawa, H., Hozumi, K., 1963. Self-thinning in overcrowded pure stands under cultivated and natural conditions. J. Biol. Osaka City Univ. **14**: 107–129.

Zeibig, A., Diaci, J., Wagner, S., 2005. Gap disturbance patterns of a Fagus sylvatica virgin forest remnant in the mountain vegetation belt of Slovenia. For. Snow Landsc. Res. **79(1/2)**: 69–80.

Zenner, E.K., Hibbs, D.E., 2000. A new method for modeling the heterogeneity of forest structure. For. Ecol. Manage. **129**: 75–87.